Stony Brook University

Domain Formation in Asymmetric Model Membranes

A Dissertation Presented

by

Hui-Ting Cheng

to

The Graduate School

in Partial Fulfillment of the

Requirements

for the Degree of

Doctor of Philosophy

in

Molecular and Cellular Biology

Stony Brook University

December 2010

Stony Brook University

The Graduate School

Hui-Ting Cheng

We, the dissertation committee for the above candidate for the
Doctor in Philosophy degree,
hereby recommend acceptance of this dissertation.

Erwin London, Ph.D. – Dissertation Advisor

Professor, Department of Biochemistry and Cell Biology

Deborah A. Brown, Ph.D. – Chairperson of Defense

Professor, Department of Biochemistry and Cell Biology

James Konopka, Ph.D.

Professor, Department of Molecular Genetics and Microbiology

Suzanne Scarlata, Ph.D.

Professor, Department of Physiology and Biophysics

Nicole S. Sampson, Ph.D.

Professor, Department of Chemistry

This dissertation is accepted by the Graduate School

Lawrence Martin

Dean of the Graduate School

Abstract of the Dissertation

Domain Formation in Asymmetric Model Membranes

by

Hui-Ting Cheng

Doctor in Philosophy

in

Molecular and Cellular Biology

Stony Brook University

2010

The plasma membrane of eukaryotic cells contains a lipid bilayer which acts as a physical barrier and is the site for many cellular signaling events. The lipid molecules in the plasma membrane are non-randomly distributed within the bilayer. Both their lateral organization (lipid domains) and transverse distribution (lipid asymmetry) are important in membrane function. Since the function and structure of the plasma membrane are difficult to study due to its complex and dynamic nature, a good model membrane is needed. However, commonly used procedures for liposome preparation cannot truly mimic plasma membranes because they do not provide control over lipid asymmetry, i.e. differences between lipid composition in the inner and outer leaflets. To prepare biological-like asymmetric vesicles with a sphingolipid-rich outer leaflet and an unsaturated phospholipid-rich inner leaflet, a methyl-beta-cyclodextrin (MβCD)-induced lipid exchange technique was devised. Moreover, cholesterol can be introduced into the vesicles without destroying lipid asymmetry (by a second exchange step). Lipid asymmetry was confirmed by several assays.

Lipid domain formation behavior in asymmetrical small unilamellar vesicles (SUVs) were characterized and compared to those in symmetric SUVs. Model membrane studies using symmetric model membranes have demonstrated that sphingolipids and

cholesterol can form ordered domains that co-exist with liquid disordered domains formed by unsaturated phospholipids. Results from asymmetric SUVs showed that the sphingomyelin-rich outer leaflet formed ordered domains that were not affected by the presence of inner leaflet unsaturated phospholipids. This indicates that asymmetric lipid distribution can be conducive to ordered domain formation and thus support the possible existence of raft in eukaryotic plasma membranes. It was also found that the ordered domains in the outer leaflet can induce a certain amount of ordered domain formation in the inner leaflet, implying the existence of leaflets coupling behavior. Furthermore, it was discovered that asymmetric SUVs containing about 25mol% cholesterol formed ordered domains more thermally stable than those in asymmetric vesicles lacking cholesterol, showing that the crucial ability of cholesterol to stabilize ordered domain formation is likely to contribute to ordered domain formation in cell membranes.

To mimic plasma membrane more closely, it is necessary to avoid use of SUVs which have very high curvature. To do this, the MβCD-induced lipid exchange method was extended to prepare asymmetric large unilamellar vesicles (LUVs). Domain-forming properties in asymmetric LUVs are analogous to those in asymmetric SUVs, exhibiting that ordered domain formation and leaflet-coupling behavior observed in asymmetric SUVs did not result from membrane curvature. The ability to prepare asymmetric vesicles represents an important improvement in model membrane preparation, and should aid in many future studies of lipid asymmetry in membrane structure and functions.

To my family,

with love and gratitude

Table of Contents

Chapter 4: Preparation of asymmetric large unilamellar vesicles

Chapter 5: Summary and future directions

List of Tables

List of Figures

List of Abbreviations

ABC: ATP-binding cassette

APT: adenosine triphosphate

CD: cyclodextrin

CL: cardiolipin

DLS: dynamic light scattering

DRM: detergent resistant membrane

DOPE: 1,2-dioleoylphosphatidylethanolamine

GSL: glycosphingolipid

ILS: inositol sphingolipid

LB technique: Langmuir-Blodgett technique

LB/LS technique: Langmuir-Blodgett/Langmuir-Schafer technique

LB/VF technique: Langmuir-Blodgett/vesicle fusion

LPG: lysyl- phosphatidylglycerol

LPS: lipopolysacchride

LUV: large unilamellar vesicle

MβCD: methyl-β-cyclodextrin

MLV: multi-lamellar vesicle

PC: phosphatidylcholine

PE: phosphatidylethanolamine

PG: phosphatidylglycerol

PI: phosphatidylinositol

POPC: 1-palmitoyl-2-oleoyl-phosphatidylcholine

PS: phosphatidylserine

SM: sphingomyelin

SUV: small unilamellar vesicle

Tm: melting temperature

TM: transmembrane

Acknowledgements

To my advisor Dr. Erwin London – I would like to express my sincere appreciation for the guidance and support you provided me during my Ph.D. training. I am very fortunate to have learned from you one of the most important skill in research, which is how to approach a scientific question and dissect the hints from complicate data. Your commitment to research, love for science, passion to teach, and intelligence for solving problems have motivated me to be a better student and inspired me to become a better scientist. You will always be my career role model as I continue my trainings. I thank you for being my teacher.

To my committee members, Dr. Deborah Brown, Dr. James Konopka, Dr. Nicole Sampson, and Dr. Susanne Scarlata – I thank you for your valuable comments and insightful discussions. The diverse suggestions and questions allowed me to look at my project in a broader sense and design my experiments accordingly. Thank you all for seating through my committee meetings and examine each step of my training so I can be confidence of earning this degree.

To the past and present members in the London laboratory, Megha and Omar – thank you for teaching me how to handle lipid samples from the very beginning. Jie and Bing – thank you for welcoming me to the laboratory. Shyam, Khurshida, Lindsay, Priya, Qingqing, Diya, and James – thank you for making my days here fun and pleasant.

To my dear friends, Nu-Chu, Su-Yi, Hui-Jun, Limei, Hui-Ju, and Pei-Jeng – you were my best remedy for the lonely and endless research life. Thank you for always listening patiently to my complaints and cheering me up when I feel down.

To Ellen and Frank, thank you for teaching me English and accepting me as one of your family. With your kindness, you have shown me the beauty and compassion of Americans.

To my family, my mom and dad, sister, and brothers – coming to the United States and being separated from you for these many years has been one of the most difficult aspects of my Ph.D. You have provided me with endless love and support.

To my family in law, I feel lucky to become a member of the family. Thank you for understanding the life of a research student and helping for the daily chores. Without you I cannot work late.

To my dear husband, Tony – thank you for being extremely encouraging and supportive. To my darling daughter, Ileene – thank you for bringing me a lot of joy and always behaving well. You both are the happiness of my life. Without you as my strong support, my achievement would not have been possible.

Chapter 1

Introduction

Lipid Composition of Plasma Membranes

The lipid molecules in the plasma membrane form a lipid bilayer, providing the basic structure of the membrane and the location for many cellular events. Eukaryotic membranes are mainly formed by three types of lipids: glycerophospholipids, sphingolipids and sterols (Fig. 1.1). They together form the lipid bilayer of the membranes, with their polar head groups interfacing with the aqueous environment and their hydrophobic tails sandwiched in between.

Glycerophospholipids are the major structural lipids in plasma membranes. They consist of a polar head group connected to two fatty acid tails (acyl chains) by glycerol. Based on the modification of their head groups, there are various kinds of glycerophospholipids commonly found in plasma membrane, such as phosphatidylcholine (PC), phosphatidylethanolamine (PE), phosphatidylserine (PS) and phosphatidylinositol (PI). Their fatty acyl chains can also vary in degree of unsaturation (i.e. number of double bonds) and length (in terms of number of carbon atoms), thus creating a diverse variety of glycerophospholipids.

Sphingolipids are another major type of structural lipids. They contain a polar head group and two mainly saturated hydrocarbon chains (a long sphingoid chain and a long fatty acid tail). In mammalian cells, the most abundant sphingolipids are sphingomyelin (SM) and glycosphingolipids (GSL) (containing phosphocholine and sugar headgroups, respectively). In yeast, inositol sphingolipids (ISL) are the commonly found sphingolipids.

The third major lipid component of plasma membranes is sterol. Cholesterol predominates in mammals, whereas ergosterol predominates in yeasts. The content of cholesterol in mammalian plasma membrane is high — up to one molecule for every phospholipid molecule (*1*-*2*). Sterols consist of a small polar head group, rigid steroid rings and hydrocarbon tail. Since their head groups are too small to shield their bulky steroid groups, they prefer to mix with glycerophospholipids and sphingolipids and hide their hydrophobic portion under the large head groups of those lipids (the umbrella model) (*3*-*4*).

The lipid composition in prokaryotes is simpler than that in eukaryotes (*5*). Bacterial plasma membranes usually consist of one or two major type(s) of phospholipids and no cholesterol (*6*-*7*). The phospholipid compositions of several biological membranes are compared in Fig. 1.2. It has to be noted that the composition of bacterial membranes are very flexible. They can respond to their environments by varying their phospholipid composition both in changing lipid headgroup species and by altering hydrocarbon chain structure (*5, 8*).

Lipid Domains in Model and Plasma Membranes

Depending on their structures and temperature, the lipids in a membrane bilayer can exist in several phase states which differ in lipid packing (Fig. 1.3). The variation in their headgroups and hydrocarbon chains leads different lipid species to have different abilities to pack against one another, and thus different melting temperatures (Tm). Lipids can exist in an ordered, solid-like gel phase (Lβ state) with a low lateral motion when their acyl chains are tightly packed at low temperature. However, at temperatures above their Tm, lipid acyl chains become loosely packed and the lipids take on a disordered fluid phase (Lα or Ld state) with a high degree of lateral motion.

Saturated lipids, such as sphingolipids, which have no double bonds in their hydrocarbon tails generally have high Tm and can pack tightly in membrane bilayers at a physiologically relevant temperature. On the other hand, unsaturated lipids, such as most natural glycerophospholipids, which contain one or more double bonds in their acyl chains, usually have low Tm and are loosely packed in membrane bilayers. Therefore, sphingolipids have a higher tendency to form ordered domains than glycerophospholipids. The differential packing ability of sphingolipids and glycerophospholipids may result in phase separation in membranes that contain these types of lipids (*9*). Indeed, model membrane studies showed that in mixtures of sphingolipids and glyerophospholipids the sphingolipids form gel phase and are separated from the fluid Ld domains formed by glycerophospholipids (*10-11*).

In the presence of cholesterol, lipids with saturated acyl chains (e.g. sphingolipids) are tightly packed (like gel state), but have high lateral mobility (similar to disordered fluid phase). This cholesterol-containing ordered state is called the liquid ordered (Lo) state (*12*). It is now known from model membrane studies that cholesterol promotes separation of lipid mixtures into co-existing sphingolipid/cholesterol-rich Lo domains and unsaturated glycerophospholipids-rich Ld domains (*11, 13*).

The discovery of selective sorting of glycosphingolipids to the apical membrane in polarized epithelial cells (*14-16*) and the differential membrane solubility in Triton X-100 (*17*) raised the idea that lipid domains may exist in cell membranes. Studies on detergent resistant membranes (DRMs) isolated from cells have shown that they are cholesterol and sphingolipid rich membranes and are in Lo state (*18*). Moreover, detergent insolubility appeared when model membrane samples contained Lo domains (*19*). The co-relationship between DRMs and Lo phase domains lead to the postulate that DRMs might derive from Lo phase bilayers in cell membranes (*20*) and thereby indirectly indicating the existence of lipid domains in cell membranes. The conceptual

cellular Lo phase domains were named ”lipid rafts” referring to their presumed function in transporting apically-directed proteins from Golgi to specific sites of plasma membrane(*21*). Since then, the lipid raft concept has become a general principle for membrane organization rather than just a mechanism for apical sorting in epithelial cells (*22*).

Lipid rafts have been implied in many cellular processes, such as endocytosis, signal transduction, and viral/bacterial pathogenesis (*23-27*). This is primarily based on the results obtained from DRM isolation, cholesterol removal or co-localization of raft markers (such as the ganglioside GM1 or glycophosphatidylinositol (GPI)-anchored proteins) with a potential raft associated-protein. However, the existence of lipid rafts in resting cells remains controversial because, unlike Lo domains in model membranes could be visualized by microscopy, the direct observation of lipid rafts in resting cells is still lacking in most cases (*28-29*).

One explanation for this is that the Lo domains might exist in the resting condition but could be too small to detect their co-existence with Ld domains (*30*). They can only be seen after clustering into larger domains upon the occurrence of some cellular events, such as the addition of raft binding proteins (*29, 31*). Another possibility is that, although domains might not be regularly present, the lipid molecules in plasma membranes might be sufficient to form transient clusters. The lipid molecules within the same phase can form transient clusters of up to ~100 molecules, which appear and disappear based on diffusion (*1*). In this case, large scale phase separation can be induced by some biological events, like temperature changes or lipid composition changes during cellular signaling (*1*). Thus, although the exact nature of lipid rafts in cells is still under debate, the most likely model is as described in 2006 Keystone Symposium on Lipid Rafts and Cell Function, “ they are small (10 to 200nm), heterogeneous, and highly dynamic sterol/sphingolipid-riched domains which compartmentalize cellular processes” (*32*).

Lipid Asymmetry in Cell Membranes

Besides lateral heterogeneity, the different species of membrane lipids are non-randomly distributed over the outer and inner leaflets of the cellular membranes. This transbilayer asymmetry can be found in most of eukaryotic membranes (*1, 33*) and some prokaryotic membranes (*6-7, 34-35*). Lipid asymmetry creates a difference of biophysical properties of the bilayer and is likely to couple to many cellular events, such as structural functions or signal transduction.

In eukaryotic cells, an asymmetrical lipid distribution has been found in Golgi, plasma and endosomal membranes with aminophospholipids (PE and PS) in the cytosolic leaflet and choline-containing phospholipids (PC and sphingolipids) in the non-cytosolic leaflet (*36*). Fig. 1.4*A* shows the asymmetric distribution of phospholipids in the plasma membrane of human erythrocytes. In bacteria, an asymmetric lipid distribution has found in the outer membrane of Gram-negative bacteria with lipopolysacchrides (LPS) in the outer leaflet and phospholipids in the inner leaflet. The LPS in the outer leaflet serves as a barrier for hydrophobic components to prevent the de-stabilization of the cells (*6*). To our knowledge, the transbilayer asymmetry of phospholipid in prokaryotic plasma membrane remains uncertain due to various approaches yielding different results (*6, 8*). However, recent studies from *Staphylococcus aureus* showed that lysyl-phosphatidylglycerol (lysyl-PG) is asymmetrically distributed with more in the outer leaflet than in the inner leaflet (*7, 35*).

Lipid asymmetry is maintained by several factors, including the physical properties of the membrane lipid molecules and the presence of transporters to actively transport lipid molecules across the bilayer (*1, 33*). In model membranes, without the help of proteins, the transbilayer movement of a lipid is slow since it has to transfer its polar head group across the hydrophobic core of the bilayer. The ability of phospholipids to spontaneously flip-flop between the leaflets is governed by the size, charge and polarity of the head group of the lipid molecules (*37-38*) as well as the physical phases that the lipid molecules exist (*39-40*). The neutral lipids (such as diacylglycerol) and protonated form of charged lipids (such as free fatty acid, phosphatidic acid and phosphatidylglycerol) can move between bilayer in seconds to minutes. In contrast, PC, PS, PE, SM, and a glycolipid have polar head groups cross model membranes slowly, with a half-time from hours to days (*37-38, 41-42*).

In biological membranes, the discovery of the adenosine triphosphate (ATP)-dependent aminophospholipid translocation between inner and outer leaflets of erythrocytes revealed the existence of mechanisms which generate and maintain membrane asymmetry (*43-44*). Three classes of proteins have been found to function in the regulation of lipid asymmetry (Fig. 1.4*B*). Aminophospholipid translocases (belonging to the P4 subfamily of P-type ATPase) are flippases which catalyze ATP-dependent movement of PE and PS from the non-cytosolic leaflet to cytosolic leaflet (*45*), whereas ATP-binding cassette (ABC) transporters work in the opposite direction. Unlike the well characterized substrates of aminophospholipid translocases, the specific substrates of ABC transporters remain disputed (*1, 33*). Plasma membrane scramblases are the third type of enzymes that determine lipid asymmetry. In contrast to lipid transporters consuming ATP to generate and maintain asymmetry, scramblases function

in an ATP-independent manner to non-specifically and bi-directionally randomize the phospholipid distribution across the plasma membranes (*1*, *33*).

It is interesting to note that although the lipid movement stops when one inhibits the activities of aminophospholipid translocases and ABC transporters, membrane asymmetry does not disappear at least for several days *in vitro* (*44*). Activation of scramblases by apoptotic stimuli or the influx of Ca^{2+} in cytoplasm, on the other hand, results in rapid transbilayer phospholipid mixing and the collapse of lipid asymmetry (*44*, *46-47*). The well known consequence is the exposure of PS to the outer leaflet of the plasma membrane, which induces phagocytosis of apoptotic cells.

Cyclodextrin

One of the common methods used for relating a specific cellular event to lipid rafts is its sensitivity to cholesterol removal by cyclodextrin (CD). Cyclodextrins are α-1,4 linked cyclic oligosaccharides consisting of six (αCD), seven (βCD), or eight (γCD) glucopyranose units. These compounds form a truncated cone-shaped structure with a hydrophilic outer surface and a hydrophobic inner cavity (Fig. 1.5) (*48-49*). This unique structure allows these compounds to be potent carriers for cholesterol or lipophilic drug molecules. The cavity size is different between each type of cyclodextrin depending upon how many glucose units they possess. The cavity size is the major decisive factor when choosing a cyclodextrin for a guest molecule to properly fit (*49*). For instance, βCD has the cavity size that is well-suited for cholesterol.

The compound that is most widely used in manipulating cholesterol content is methyl-β-cyclodextrin (MβCD), a βCD derivative with random methylated modification(s) on the exterior hydroxyl group(s). Numerous studies have shown MβCD is efficient in extracting or delivering cholesterol in both cellular and model membranes (*50*). Accordingly, it has become a common tool for studying lipid rafts. However, the effects of MβCD on lipid membranes are not yet well-characterized. First, different experimental conditions yield different degrees of change in cholesterol levels. The degree of cholesterol depletion or enrichment (if cholesterol-loaded MβCD is added to cells) is related to the MβCD concentration, incubation time, temperature, and cell types used in the experiments (*50*). Second, some reports showed that MβCD seems to alter cholesterol distribution between different cellular compartments (*51-52*) and to deplete both raft and non-raft cholesterol (*53-55*). Last but not least, MβCD may not only interact with cholesterol but also with membrane phospholipids (*54*, *56-59*). In addition, there is a difference between cholesterol-dependent and lipid raft-dependent cellular processes (*50*,

60). All of these suggest that one should use caution when interpreting MβCD effects on cell and model membranes.

By using right-angle light scattering and isothermal titration calorimetry, Anderson et al. found that, at high concentrations (above 20 mM), MβCD can bind to 1-palmitoyl-2-oleoyl-phosphatidylcholine (POPC) and solubilize POPC membranes (*56*). Furthermore, by considering the dimensions of MβCD cavity (0.8 nm) and POPC acyl chains (about 2 nm in length), they suggested that each acyl chain needs two MβCD molecules to form a POPC/MβCD inclusion complex with a 1:4 (POPC:MβCD) stoichiometry. Accordingly, they proposed the stepwise model for POPC- MβCD interaction. In their model, a single MβCD molecule first comes to contact with the lipid bilayer and extract a phospholipid molecule to form a 1:1 complex. After that, additional three cyclodextrin molecules then attach to the complex and form a larger complex. Since the formation of MβCD inclusion complexes is reversible, it is likely that MβCD can function as a carrier to transfer POPC monomers from one vesicle to another. This finding extends the possible applications of CD in membrane biology beyond its well-known function in cholesterol manipulation. In fact, γCD has been used to deliver fluorescent-labeled phospholipids between vesicles or from vesicles to cultured cells (*61*).

Model membranes

Due to their complex and dynamic nature, the function and structure of cell membranes are often difficult to study. In this regard, model membranes, which mimic natural cell membranes in their arrangement of lipid molecules, are widely used. Since they are easy to prepare and their lipid composition can be well controlled, they have become a powerful tool in understanding many membrane-related events. Two types of model membrane systems have been widely used: supported planar lipid bilayers and liposomes.

Supported lipid bilayers are lipid bilayers formed on smooth solid supports (such as silicon or quartz) or on polymers linked-solid supports. They can be prepared by vesicle adsorption to the surface of these supports, by Langmuir-Blodgett (LB) technique, by Langmuir-Blodgett/Langmuir-Schafer (LB/LS) technique, or by Langmuir-Blodgett/vesicle fusion (LB/VF). When using the last three methods, a Langmuir monolayer has to be prepared by lifting a chip (the solid support, immersed in water initially) vertically through the Langmuir monolayer formed at air/water interface (prepared by spreading the lipid molecules at the air-water interface) to allow the Langmuir monolayer coating onto the chip. In LB technique, the other monolayer can be

added onto the chip by vertically passing the chip through (downward) the air/water interface again (*62*). In LB/LS technique, the LB monolayer-coated chip horizontally contacts the air/water interface to form the bilayer (*63*). For the LB/VF method, the lipid bilayer is formed by incubating vesicles with the LB monolayer-coated chip. The planar bilayers so-prepared are suitable for characterizing the lateral lipid heterogeneities or observing membrane integrity during different treatments (*64-65*).

Liposomes are spherical vesicles with a small aqueous solution enclosed within a lipid bilayer. They can vary in size from about 30 nm to several μm in diameter, depending on how they are prepared. Multi-lamellar vesicles (MLV; size of tens of nanometers to several micrometers) are formed when dried lipid films are rehydrated in a desired buffer while simultaneously shaking. MLVs can be sonicated to create small unilamellar vesicles (SUV; below 50 nm). To prepare large unilamellar vesicles (LUV; size around 100 nm), MLVs are subjected to 3-5 cycles of freeze/thawing to make the sizes of vesicles uniform and then the samples are passed through extruders containing filters with a defined pore size to create vesicles with the desired size. Another commonly used method to prepare LUVs is octyl glucoside dialysis (*66*). By combining with fluorescence spectrometry or differential scanning calorimetry, these type of liposomes are frequently used to study the properties of lipid bilayers, such as phase separation or phase transitions (*67-72*). However, because of their small size, it is difficult to do imaging using SUVs or LUVs. To overcome this problem, methods to prepare giant unilamellar vesicles (GUV), which are cell-sized vesicles (1-100 μm), have been developed. They are prepared by slow and gentle re-hydration of dried lipid films. Since they can be directly seen by traditional fluorescence microscopy and their lipid compositions can be controlled, they are particularly helpful in determining compositional phase diagrams (*37*, *73-74*) and lipid diffusion (*75*).

Each type of model membrane has its own advantages and disadvantages. GUVs represent a self-closed lipid matrix similar to the plasma membrane (*76*) and are in a more "natural" environment compared to supported lipid bilayers (since there is no solid surface to stabilize or disturb membrane bilayers) or smaller vesicles. Nevertheless, they are relatively unstable, time consuming to make and can only be prepared in small yield. On the other hand, MLVs, SUVs and LUVs are easy to make and can be made in large quantities more suitable for many spectroscopic experiments. Although MLVs have multiple layers that limit some of their applications, they are an easy tool when one needs to separate membrane bound and un-bound components by centrifugation. There are other applications for model membranes, for example LUVs have been used for drug delivery (*77*).

Pautot *et al*. published a method to prepare asymmetric vesicles with PC and PS in each monolayer using a similar concept to LB techniques (*78*). To prepare such

vesicles, three components were placed in a centrifuge tube. The upper layer contained inner leaflet lipid-saturated oil in which small amount of aqueous solution was added to produce an inverted emulsion with the acyl chains of lipids facing outside and the headgroups interacting with water molecules. The intermediate layer consisted of another kind of oil solution saturated with the lipid molecules for the outer leaflet and the bottom layer composed of aqueous solution to allow the formation of a lipid monolayer containing outer leaflet lipids at the oil/water interface. After centrifugation to transfer the water droplets through the outer leaflet lipid monolayer, the asymmetric vesicles were created and collected to the aqueous solution. However, it is not clear how widely this method can be used, or to what extent oil remains in the final vesicles.

Domain formation in the outer and inner leaflet

Model membrane studies showed that Lo domains co-exist with Ld domains in a symmetric lipid composition crudely mimicking plasma membrane outer leaflet (*11, 19*). However, the lipid composition of the plasma membrane is asymmetrical as described above. The outer leaflet contains sufficient components (saturated SM, unsaturated PC and cholesterol) for lipid raft formation, whereas the sphingolipid-poor/ PE-PS-rich inner leaflet does not. Nevertheless, the recovery of PE (an inner leaflet lipid) (*17*) and inner leaflet-associated proteins in DRMs (*79-80*) seems to suggest that rafts are present in the inner leaflet.

Forming Lo domains with inner leaflet type lipids in model membranes has not been successful (*81*). Additional factors, such as the rafts in outer leaflet or saturated acyl chain-linked proteins, may be needed to induce the domain formations in the inner leaflet. The abilities of PE and PS to form ordered domains in the presence of cholesterol are moderate, i.e., not good as sphingomyelin but better than corresponding PC. This suggests that the lipid composition of inner leaflets (PE, PS, and cholesterol) maybe close to the borderline of forming ordered domains (*68*). Thus, the inter-leaflet interaction or changes in lipid composition due to some cellular response (such as the generation of ceramide upon Fas ligand-induced cell death) may be sufficient for the domain formation in the inner leaflet.

By observing planar supported lipid bilayers with asymmetric transbilayer lipid distributions, Tamm's group found the existence of transbilayer lipid domain coupling behavior. From their results, Lo phase domains in one monolayer can induce domain formation in an opposite leaflet composed of at least one high Tm lipid, one low Tm lipid, and cholesterol (*64-65, 82*). By tuning lipid composition of one leaflet, Collins and Keller further showed that domains either induced or suppressed across asymmetric un-

supported planar bilayers (*83*). Therefore, the domain formation in one leaflet can be induced by form in registration with that in the opposite leaflet in planar bilayer.

Goal of this work: prepare asymmetric model membranes that mimic plasma membranes

Since many cellular signaling events occur in the plasma membrane, a good model plasma membrane is needed. Current studies on liposomes have yielded many important insights into the architecture of cell membranes. However, commonly used procedures for liposome preparation cannot truly mimic plasma membranes since they do not provide lipid asymmetry. To mimic plasma membrane more closely, a MβCD-induced lipid exchange method was devised to create biological-like asymmetric vesicles having a sphingomyelin-riched outer leaflet and an unsaturated phospholipid-riched inner leaflet. Moreover, cholesterol was introduced into the vesicles (by a second exchange step) without destroying lipid asymmetry. Lipid asymmetry was confirmed by several assays and domain formation behavior in asymmetric membranes was characterized.

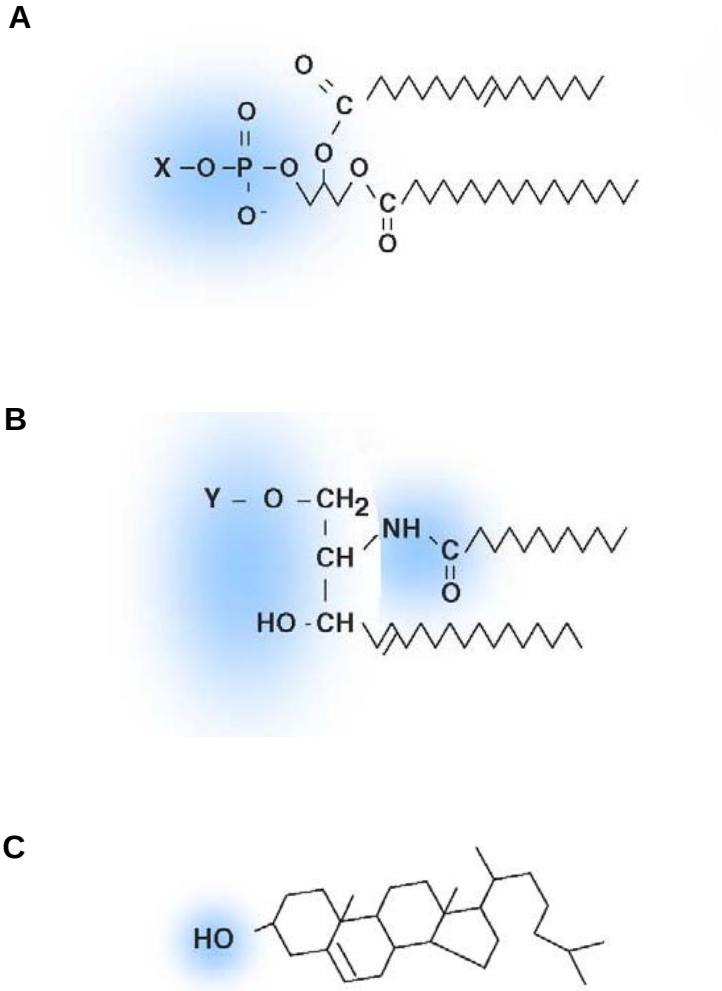

Figure 1.1. Three major types of plasma membrane lipids in mammalian cells. (A) glycerophospholipid; (B) spingolipid; (C) sterol. Moiety X can be choline in PC, ethanolamine in PE, serine in PS, and inositol in PI. Moiety Y can be hydrogen in ceramide, phosphorylcholine in SM, and sugars in glycolipids. Cholesterol is shown as an example of a sterol. Hydrophilic parts are indicated by blue clouds. This figure is taken and modified from Pohl *et al*. (*84*), with permission from Elsevier.

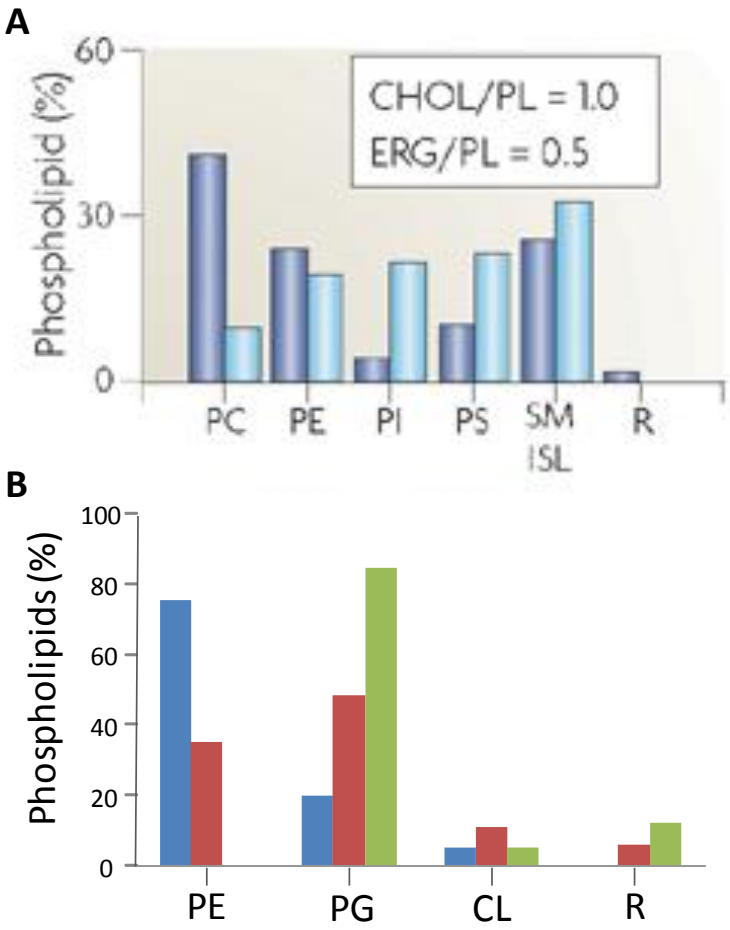

Figure 1.2. The phospholipid composition of cell membranes. (A) The lipid composition of mammals (blue) and yeast (light blue) are shown as a percentage of total phospholipids. The insert shows sterol content as the molar ratio of cholesterol (CHOL; in mammals) and ergosterol (ERG; in yeast) to phospholipid. This figure was adapted by permission from Macmillan Publishers Ltd: [*Nat. Rev. Mol. Cell. Biol.*] (*1*). (B) The phospholipid composition in one typical Gram-negative bacterium (*Eschericha coli*; blue) and two Gram-positive bacteria (*Bacillus meggaterium*; red and *Staphylococcus aureus*; green). PG: phosphatidylglycerol; CL: cardiolipin; R: remaining lipids.

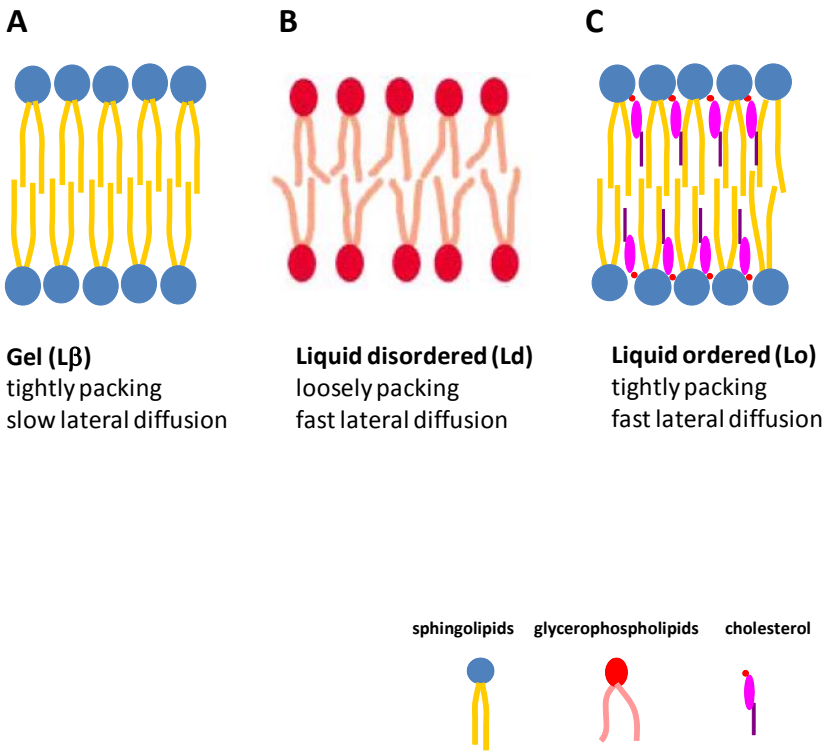

Figure 1.3. Lipid phases in membrane bilayers. (A) Gel (Lβ) phase is a solid-like phase in which the lipid molecules are tightly packed and the lateral movement is slow. (B) Liquid disordered (Ld) phase is a loosely packed state with a fast lateral movement. (C) Liquid ordered (Lo) phase exists in the presence of cholesterol. The lipid molecules are packed in a high order like Lβ phase, but their lateral mobility is almost as fast as in the Ld phase.

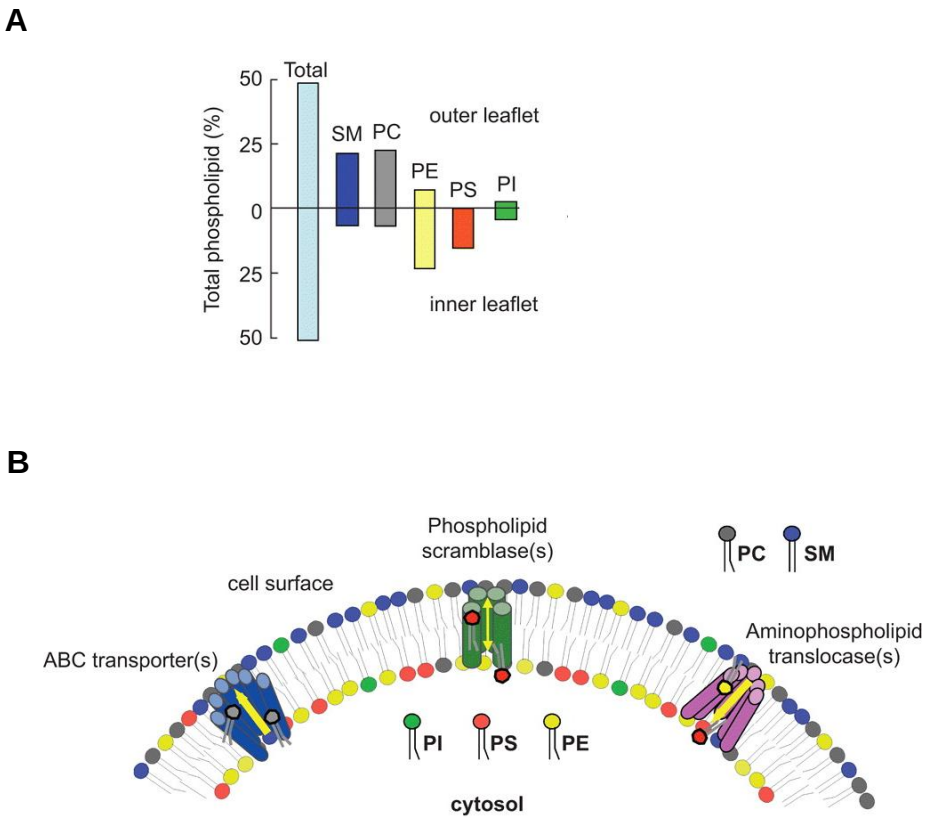

Figure 1.4. Phospholipid asymmetry and related lipid-translocating enzymes. (A) The transbilayer distribution of phospholipids in human erythrocyte membrane. The majority of the SM and PC exists in the outer leaflets, while most of PE and PI are in the inner leaflet. PS is almost confined exclusively in the inner leaflet. (B) Three types of lipid transporters that regulate membrane asymmetry. This figure is taken and adapted by permission from Informa Healthcare: [Critical Reviews in Biochemistry and Molecular Biology] (*33*), copyright 2009.

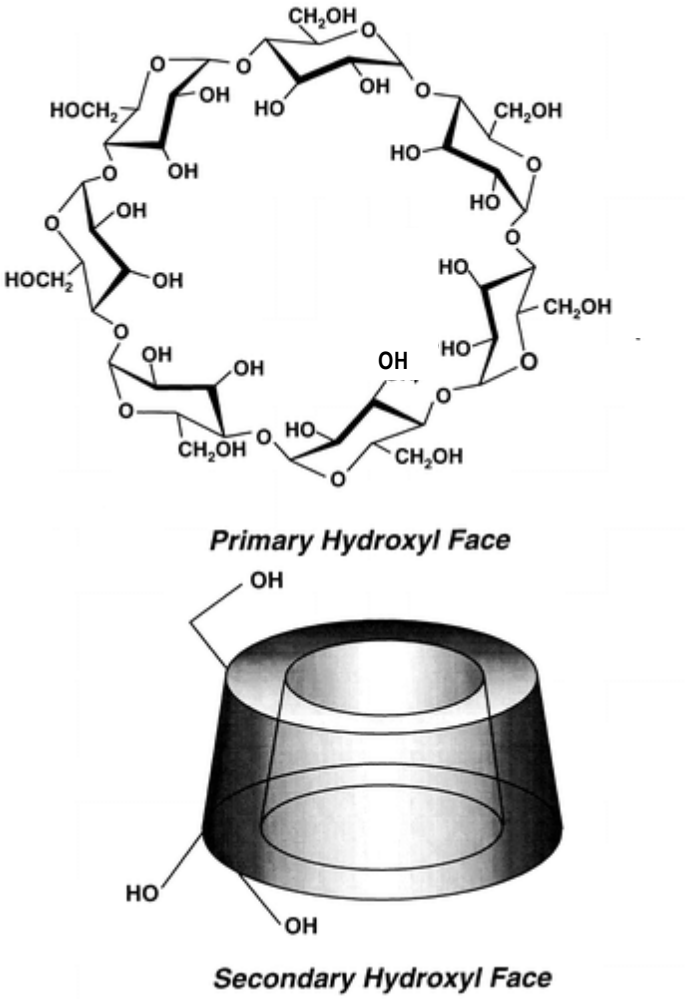

Figure 1.5. The structure of β-cyclodextrin. Upper panel: βCD contains 7 glucopyranose units linked by 1-4 glycosidic bonds into a macrocycle. Lower panel: schematic structure of cyclodextrin to show the truncated cone-shape. This figure is taken and adapted with permission from ref (*49*), copyright 1998 American Chemical Society.

Chapter 2

Materials and Methods

Materials: 1,2-Dipalmitoylphosphatidylcholine (DPPC), porcine brain SM, 1,2-dioleoylphosphatidylcholine (DOPC), 1-palmitoyl-2-oleoyl-phosphatidylcholine (POPC), 1-palmitoyl-2-oleoyl-phosphatidylethanolamine (POPE), 1,2-dioleoylphosphatidylethanolamine (DOPE), 1-palmitoyl-2-oleoyl-phosphatidyl-L-serine (POPS), 1,2-[9,10-dibromo] stearoylphosphatidylcholine (BrPC), and cholesterol were purchased from Avanti Polar Lipids (Alabaster, AL). 1,6-Diphenyl-1,3,5-hexatriene (DPH), MβCD, and alamethicin were purchased from Sigma-Aldrich. 1-(4-Trimethylammoniumphenyl)-6-phenyl-1,3,5-hexatriene *p*-toluenesulfonate (TMADPH), *N*-(Rhodamine Red-X)-1,2-dihexadecanoyl-*sn*-glycero-3-phosphoethanolamine (rhodamine-PE), and *N*-(7-nitrobenz-2-oxa-1,3-diazol-4-yl)-1,2-dihexadecanoyl-*sn*-glycero-3-phosphoethanolamine (NBD-PE) were purchased from the Molecular Probes division of Invitrogen. [^{3}H]cholesterol was purchased from PerkinElmer Life Sciences. Lipids were dissolved in chloroform and stored at –20 °C. DPH and TMADPH were dissolved in ethanol. Concentrations were determined by dry weight or, in the case of DPH and TMADPH, by absorbance using $\epsilon = 84{,}800\ cm^{-1}\ M^{-1}$ at 353 nm in ethanol (*85*). LW peptide (acetyl-$K_2W_2L_8AL_8W_2K_2$-amide) and pL4A18 peptide (acetyl-$K_2LA_9LWLA_9LK_2$-amide) were purchased from Anaspec (San Jose, CA). LW peptide was used without further purification, and pL4A18 was purified via reverse-phase HPLC (see below). Sephacryl S-200 and Sepharose CL-4B were purchased from Amersham Biosciences. High performance thin layer chromatography (HP-TLC) plates (Silica Gel 60) were purchased from VWR International. (Batavia, IL).

Ordinary Vesicle Preparation Procedures: All steps in this and the following procedures were carried out at room temperature except where otherwise noted. Multilamellar vesicles (MLVs), small unilamellar vesicles (SUVs) and large unilamellar vesicles (LUVs) were prepared in glass tubes as described previously (*86-87*).

For MLVs, lipid mixtures were mixed and dried under nitrogen followed by high vacuum for at least 1 h, dispersed at 70 °C in PBS (1.8 mM KH_2PO_4, 10 mM Na_2HPO_4, 137 mM NaCl, and 2.7 mM KCl at pH 7.4), and vortexed in a multitube vortexer (VWR International) at 55 °C for 15 min. In the case of SM MLVs, to remove any small vesicles present prior to lipid exchange, the preparation was centrifuged at 11,000 × *g* for 5 min at room temperature. The supernatant was discarded, and the pellet obtained was resuspended to the original volume with PBS and used for further experiments. In some cases, MLVs were prepared with 0.01 mol % rhodamine-PE.

To prepare sonicated SUVs, MLVs containing 8 or 16 mM unsaturated glycerophospholipids dispersed in PBS (unless otherwise noted) were sonicated in a bath sonicator (Special Ultrasonic Cleaner Model G1112SP1, Laboratory Supplies Co., Hicksville, NY) at room temperature for at least 45 min (until the solution became nearly transparent) and then diluted to the desired concentration with PBS. As judged by their elution position on Sepharose CL-4B chromatography (see below) we found that the small size of the sonicated vesicles was stable for days. In some cases, the sonicated SUVs contained 0.5 mol % LW peptide and/or 0.01 mol % NBD-PE. For pL4A18-containing samples, the peptide was added to the lipid mixtures (at 1 mol % of total lipid concentration) and dried under nitrogen. The lipid films were re-resuspended in chloroform and dried under nitrogen followed by high vacuum for at least 1 h, dispersed at 70 °C in PBS, and then sonicated to SUVs as described above. For SUVs prepared by ethanol dilution, the desired lipid mixtures were dried, dissolved in 20 μl of ethanol, dispersed in 980 μl of PBS at 70 °C, and then cooled to room temperature.

For LUVs preparation, MLVs containing 8mM lipids were prepared in 1 ml of 25 w/v % sucrose solution. MLVs were freeze/thawed for 5 cycles and then passed through a 100nm or 200 nm polycarbonate filter 11 times to obtain LUV of a uniform vesicle size. To wash away the un-trapped sucrose molecules, the resulting LUV solution were mixed with 3ml PBS and subjected to ultracentrifugation at 190,000 x g for 45 min using a Beckman L8-55M ultracentrifuge. After discarding the supernatant, the LUV pellet was resuspended to the original volume with PBS. LUV suspensions were diluted to the desired concentration by PBS for further experiments.

Cholesterol-loaded MβCD (CLC) Preparation: Generally 100 μmol of MβCD were dissolved in 600 μl of methanol and mixed with 30.8 μmol of cholesterol while vortexing at room temperature. The mixture was dried by nitrogen followed by high vacuum for at least 1 h and then dispersed in 2 ml of PBS. The resulting solution (which is turbid due to excess cholesterol) was sonicated in the bath sonicator for 3 min and then incubated in a shaker at 37 °C overnight. The CLC-containing solution was then filtered with a 0.22-μm-pore size syringe filter, and the filtrate was used in subsequent experiments.

Exchange (Asymmetric) SUVs Preparation: First 500 μl of the resuspended pellet from a 16 mM SM MLV preparation (see above) and 95 μl of 625 mM MβCD dissolved in PBS were vortexed in the multitube vortexer at 55 °C for 2 h. Then 500 μl of 4 mM sonicated SUVs containing unsaturated glycerophospholipid were added to the MLV-MβCD mixture and vortexed at 55 °C for 30 min. After cooling for 5 min, samples were

centrifuged at 11,000 × *g* for 5 min, and the resulting supernatant was centrifuged at 49,000 × *g* for another 5 min using an air-driven microultracentrifuge (Beckman Airfuge). For asymmetric SUV preparations without cholesterol, the supernatant was chromatographed on a Sepharose CL-4B column (dimensions, 25-cm length and 1-cm diameter). Fractions of 1 ml were collected with asymmetric SUVs mainly eluting in fractions 10–14. Unless otherwise noted, fraction 12 was used for further analysis. Generally the approximate lipid concentration in the peak SUV fractions was about or somewhat greater than 200 μM as estimated by the recovery of peptide using fluorescence (by comparing it with that in the vesicles prior to exchange) or the recovery of lipid using HP-TLC. In cases in which lipid concentration was not explicitly measured, 200 μM was assumed unless otherwise noted.

To prepare SM/POPC outside and POPE/POPS inside SUVs (SM:POPCo/POPE:POPSi SUVs), exchange vesicles were prepared using mixed MLVs. First 300 μl of 16 mM SM MLVs were mixed with 57 μl of 625 mM MβCD and 200 μl of 16 mM POPC MLVs were mixed with 38 μl of 625 mM MβCD. Each was vortexed using a multitube vortexer at 55 °C for 2 h, and then the two MLV-MβCD mixtures were combined in one glass tube. Next 500 μl of 4 mM 1:1 POPE: POPS SUVs containing 1 mol % pL4A18 peptide were added to the tube with the MLV-MβCD mixtures and vortexed at 55 °C for 30 min. The exchange SUVs were then isolated as described above.

For asymmetric SUVs containing about 25 mol % cholesterol, the supernatant from the centrifugation at 49,000 × *g* was chromatographed on a Sephacryl S-200 column (dimensions, 7-cm length and 1-cm diameter), and 1-ml fractions were collected (although we later realized 0.5 ml fractions would be better to avoid dilution of lipid). To prepare cholesterol-containing SM outside, DOPC inside SUVs (SMo/DOPCi/CHOL SUVs), 950 μl of fraction 4 from this column were transferred to a new glass tube and mixed with 50 μl of a CLC preparation at 55 °C for 30 min. To prepare SMo/2:1 POPE:POPSi/CHOL SUVs, 850 μl of fraction 4 were transferred to a new glass tube and mixed with 150 μl of the CLC preparation at 55 °C for 30 min. The samples were then chromatographed on Sepharose CL-4B as described above. Fractions 12 and 13 from the Sepharose CL-4B column were used for further analysis of cholesterol-containing asymmetric vesicles. Because of losses during this procedure, lipid concentration in the Sepharose CL-4B fractions was lower than that without cholesterol with fractions 12 and 13 each having about 100 μM lipid as estimated by the recovery of peptide using fluorescence or lipid using HP-TLC. Although lipid recovery was occasionally even lower a 100 μM concentration in these fractions was assumed when the lipid concentration was not explicitly measured.

Asymmetric LUVs preparation: First 500 µl of the resuspended pellet from a 16 mM SM MLV preparation (see above) and 95 µl of 625 mM MβCD were mixed and vortexed in the multitube vortexer at 55 °C for 2 h. Then 500 µl of 4 mM 2:1 DOPE:POPS LUVs (with trapped 25% sucrose, see above) were added to the MLV-MβCD mixture. After vortexing at 55 °C for 30 min. and then cooling for 10 min, the mixture was overlaid onto 3ml of 10 w/v % sucrose solution and subjected to ultracentrifugation at 190,000 x g for 45 min. After the removal of the supernatant, the resulting pellet was resuspended with 1ml of 10% sucrose solution, overlaid onto a 3ml of 10% sucrose solution and subjected to ultracentrifugation again. The final pellet was resuspended in 1ml PBS and ready for further experiments.

Fluorescence Measurements: Fluorescence was measured by a SPEX FluoroLog 3 spectrofluorometer (Jobin-Yvon, Edison, NJ) using quartz semimicrocuvettes (excitation pathlength, 10 mm; emission, 4 mm). DPH and TMADPH fluorescence was measured at an excitation wavelength of 364 nm and emission wavelength of 426 nm. Trp fluorescence was measured at an excitation wavelength of 280 nm and emission wavelength of 340 nm. Rhodamine-PE fluorescence was measured at an excitation wavelength of 560 nm and emission wavelength of 580 nm. NBD-PE fluorescence was measured at an excitation wavelength of 465 nm and emission wavelength of 534 nm. The slit bandwidths for fluorescence measurements were generally set to 4.2 nm (2-mm physical size) for excitation and 4.2 nm (2-mm physical size) for emission. Background intensities in samples lacking fluorescent probe were negligible (<1–2%) and were generally not subtracted from the reported values. An exception to this was for measurements of TMADPH fluorescence anisotropy (see below).

Steady-state Fluorescence Anisotropy Measurements: Anisotropy measurements, unless otherwise noted, were made at room temperature using a SPEX automated Glan-Thompson polarizer accessory. DPH and TMADPH anisotropy values were calculated from the fluorescence intensities with polarizing filters set at all combinations of horizontal and vertical orientations. For TMADPH experiments anisotropy was calculated after subtraction of fluorescence intensity in background samples lacking fluorophore. Anisotropy was calculated from the following equation: $A = [((Ivv \times Ihh)/(Ivh \times Ihv)) - 1]/[((Ivv \times Ihh)/(Ivh \times Ihv)) + 2]$ where A is anisotropy and Ivv, Ihh, Ivh, and Ihv are the fluorescence intensities with the excitation and emission polarization filters, respectively, set in the vertical (v) and horizontal (h) orientations (*88*). For these and all the following experiments in which DPH and TMADPH were used, the fluorescence probe was added (from an about 100 µM stock solution dissolved in

ethanol) to preformed ordinary or preformed exchange vesicles to a concentration of about 0.1 mol % of the total lipid concentration, and the samples were incubated for at least 5 min before fluorescence was measured. This was sufficient time for the fluorescence of the probe, which increases upon binding to lipid vesicles, to reach nearly maximal intensity (Ref. (*89*)and data not shown). For samples containing alamethicin, vesicles were incubated with alamethicin for 15 min at room temperature before the addition of DPH or TMADPH.

Measurement of the Temperature Dependence of Fluorescence Anisotropy: To measure the temperature dependence of DPH anisotropy, samples containing (unless otherwise noted) about 50 μM lipid and 0.1 mol % DPH added as described above were cooled to about 16 °C, and anisotropy was measured. Samples were then heated in steps of about 4 °C, measuring anisotropy at each step once temperature stabilized (as measured with a probe thermometer placed in the cuvette (Fisherbrand traceable digital thermometer with a YSI microprobe, Fisher Scientific)). This process was repeated up to 60–70 °C. For samples containing alamethicin, vesicles were incubated with alamethicin for 15 min at room temperature before measurements were made. The ordered domain melting temperature was defined by the midpoint of a sigmoid fit to the anisotropy *versus* temperature curve using SlideWrite Plus software (Advanced Graphics Software, Inc., Encinitas, CA).

Re-reconstitution Experiments: Fraction 12 of a preparation of SMo/DOPCi SUVs, SMo/2:1 POPE:POPSi SUVs, or DPPCo/DOPCi SUVs was divided into four tubes (250 μl/tube), and then 750 μl of PBS were added to each aliquot. To two aliquots, either DPH (0.5 μl of 100 μM dissolved in ethanol) or TMADPH (0.57 μl of 87.7 μM dissolved in ethanol) was added to give a final membrane composition containing about 0.1 mol % fluorescent probe. The other two aliquots were subjected to re-reconstitution. They were dried by a N_2 stream, dissolved in 20 μl of ethanol, and then dispersed at 70 °C in 980 μl of distilled water (which should reconstitute the PBS as well as the lipid vesicles). After cooling to room temperature, DPH or TMADPH was added as described above. Ordinary vesicles were dried and then re-reconstituted by an analogous procedure.

For cholesterol-containing asymmetric SUVs fractions 12 and 13 were combined, and then the same procedure was used except that 500 μl of the combined fractions were used per tube so that the lipid concentration would be similar to that in the samples lacking cholesterol.

For asymmetric LUV samples, the LUV suspension was divided into 4 tubes (250 μl/tube), and then 750 μl of PBS were added to each aliquot. Two aliquots were used to measure DPH and TMADPH anisotropy as described above and the other two aliquots were subjected to re-reconstitution. To do this, the samples were first dried by a N_2 stream. Next 500 μl of ethanol was added to each tube to dissolve the dried lipids. After drying ethanol by a N_2 stream and 1 h of high vacuum, 1 ml of 70 °C pre-warmed distilled water was added to rehydrate the dried lipids. Samples were mixed by vortexing for at least 15 min in a 55 °C shaker, followed by freeze/thawing for 5 cycles. Samples were then allowed to reach room temperature and DPH or TMADPH was added as described above. In control experiments, ordinary (symmetric) vesicles were dried and then re-reconstituted in the same manner.

Extraction of TMADPH from vesicles by MβCD: To measure the MβCD concentration dependence of TMADPH extraction from the outer leaflet of vesicles at room temperature, TMADPH was added to preformed vesicles at a concentration of about 0.1 mol % of the lipid concentration. After a 5-min incubation, the initial TMADPH fluorescence of each sample was measured. Next an aliquot of MβCD from a 625 mM stock solution dissolved in PBS was added, and after incubation for 5 min TMADPH fluorescence intensity was remeasured. This was repeated for a series of aliquots of MβCD. Controls at both 0.5 and 1 mM MβCD showed that extraction by MβCD reached equilibrium within 3 min for vesicles of various lipid compositions.

Extraction of TMADPH from SM MLV by MβCD: TMADPH (0.05mol% of total lipid concentration) was added to each of 2 tubes of 200μM SM MLV. After incubating at room temperature for 5 min, the initial TMADPH fluorescence of each sample was measured. Then, 10mM MβCD (16μl from 625mM stock solution dissolved in PBS) was added into one of the SM MLV tubes. In the control sample, an equivalent volume of PBS was added. After 5 min incubation at room temperature TMADPH fluorescence intensity was re-measured. Both samples were then centrifuged at 49,000 x g for 5 min using an air-driven microultracentrifuge. For each sample, the supernatant was transferred to a new glass tube and the pellet was then re-suspended with PBS. Optical density at 450nm and TMADPH fluorescence of the supernatants and pellets were measured as described above.

Ca^{2+}-induced vesicle aggregation: To measure Ca^{2+}-induced vesicle aggregation ordinary SUV and exchange SUV were made as described above except that 137 mM NaCl, 20 mM Tris-Cl pH 7.4 (Tris buffer) was substituted for PBS. Optical density at 450 nm was measured and then the samples were titrated with aliquots from a 200 mM solution of $CaCl_2$ dissolved in water. Samples were mixed by pipetting immediately after adding $CaCl_2$ and (to avoid vesicle settling) again immediately before optical density measurements. One minute after the addition of each aliquot optical density was measured on a Beckman 640 spectrophotometer. The change in optical density was calculated after correcting for the Tris buffer background by subtracting the value of optical density in the absence of $CaCl_2$. Ordinary vesicles containing SM and/or cholesterol were prepared by ethanol dilution, while ordinary vesicles lacking both SM and cholesterol were prepared by sonication. Control experiments in which ethanol was added to sonicated preparations showed ethanol had no significant effect upon Ca^{2+}-induced aggregation (data not shown).

High Performance Thin Layer Chromatography: HP-TLC plates were preheated at 100 °C for 30 min and cooled to room temperature, and samples were then loaded. For asymmetric SUV samples, 200–500 μl of fraction 12 from the Sepharose CL-4B column were dried by an N_2 stream and dissolved in 20 μl of 1:1 chloroform:methanol (v/v) (excess salt was present as a solid). Then 5 μl of the dissolved lipid were loaded onto the plate. For each lipid standard, the desired lipid was first dried by an N_2 stream, dissolved in 20 μl of ethanol, and then dispersed in the same volume of PBS as present in the asymmetric SUV sample (so that the stock solution of the standards would have the same concentration of salt as the vesicle samples). The lipid standards were redried in N_2 and dissolved in 50–100 μl of 1:1 chloroform:methanol, and then desired amounts of each lipid were spotted onto the plates (generally loading a total of 8–9 μl for each spot).

For asymmetric LUV samples, lipids were extracted with 2.5 ml of 2:2:1 (v/v) chloroform:methanol:(water + sample solution). After 5 min of low speed centrifugation the upper aqueous phase was discarded and the lower phase (containing the lipid extract) was dried with N_2. The dried lipid film was redissolved in 20 μl of 1:1 (v/v) chloroform:methanol. Five microliters were spotted on an HP-TLC plate. Lipid standards were prepared and extracted by analogous procedures before loading on HP-TLC.

For samples without cholesterol, 65:25:4 chloroform:methanol:water (v/v) was used to separate each lipid. Samples with cholesterol were generally chromatographed in two solvents. The first solvent system was 50:38:8:4 chloroform:methanol: water:acetic acid (v/v). After the solvent front migrated about halfway up the plate, the plate was air-dried for 5 min. Then the plate was rechromatographed in 1:1 hexane:ethyl acetate (v/v)

until the solvent front migrated to near the top of the plate. After air drying for 10 min, the plate was evenly sprayed with a 3% (w/v) cupric acetate, 8% (v/v) phosphoric acid solution, dried for 45 min, and charred at 180 °C for 2–5 min.

Charred HP-TLC plates were scanned using an Epson 1640XL scanner (Epson America Inc., Long Beach, CA), and charred band intensity was measured by Scion Image software (Scion Corp., Frederick, MD). Lipid in samples was quantitated by comparing band intensity with that of the standards fit to an exponential intensity *versus* concentration curve (SlideWrite Plus software).

Sucrose Density Gradient Centrifugation: Sucrose gradient centrifugation was carried out in a Beckman L8-55M ultracentrifuge using an SW-60 rotor. Gradients for samples lacking cholesterol were prepared by freeze-thawing 3.4 ml of 25% (w/v) sucrose overnight at –20 °C in the (Beckman ultraclear) tubes used for centrifugation. Gradients for samples containing cholesterol were prepared by freeze-thawing 3.4 ml of 20% (w/v) sucrose. Next 400 μl of vesicle samples were loaded on top of the gradients, and the gradients were then centrifuged for 17 h at 38,000 rpm (average *g*, 148,305). After centrifugation the gradients were fractionated by pipetting into 200-μl aliquots. (The bottom, highest density fraction (fraction 18) contained 200–400 μl.) Lipids were extracted from each fraction with 2.5 ml of 2:2:1 (v/v) chloroform:methanol:water. After 5 min of low speed centrifugation the upper aqueous phase was discarded. Comparison of a control sample before and after extraction indicated that lipid was nearly fully recovered in the lower phase. The extract in the lower phase was then dried with N_2 and redissolved in 15 μl of 1:1 (v/v) chloroform:methanol. Five microliters were spotted on an HP-TLC plate and chromatographed in 50:38:8:4 (v/v) chloroform:methanol:water:glacial acetic acid. The amount of SM or glycerophospholipid in the extracts was then quantified by HP-TLC as described above. For cholesterol-containing samples, cholesterol with trace [^{3}H]cholesterol was used, and the amount of cholesterol in one-fifth of each fraction was measured by scintillation counting. The amount of SM or phospholipid in the remainder of the fractions was quantified by analysis of lipid extracts using HP-TLC and charring as described above. (For cholesterol-containing samples the silica gel on the upper portion of the plate, which contained radiolabeled cholesterol, was scraped off and discarded prior to charring!) Sucrose concentrations in the fractions were estimated using a refractometer (Abbe Precision Refractometer, Bausch & Lomb, Rochester, NY).

Peptide Topography Experiments: pL4A18 peptide was purified via reverse-phase HPLC using a C_{18} column as described previously (*90*). Purified peptide was dried under a nitrogen stream, redissolved in 1:1 (v/v) water:2-propanol, and stored at 4 °C. Trp fluorescence emission spectra measurements were taken by a SPEX 2 FluoroLog spectrofluorometer (Jobin-Yvon) using quartz semimicrocuvettes (excitation pathlength, 10 mm; emission, 4 mm) at room temperature as described previously (*90*). The slit bandwidths for this measurement were set to 4.5 nm (2.5-mm physical size) for excitation and 9 nm (5 mm) for emission. Trp fluorescence emission spectra were measured at an excitation wavelength of 280 nm and emission wavelength over the range of 300–400 nm and subjected to 21-point Savitsky-Golay smoothing (*91*). Fluorescence from background samples (containing lipids but lacking peptide) was subtracted from reported values.

Dynamic Light Scattering (DLS) Measurement: The sizes of LUV were determined dynamic light scattering using a ProteinSolution DynaPro instrument (Wyatt Technology Corp., Santa Barbara, CA) at 20 ^{o}C. To avoid the interference from impurities in the buffer, 5 μM of symmetric LUV or 1000-fold diluted asymmetric LUV were prepared using 0.22 μm filter-filtered PBS. Vesicle sizes were estimated by the Dynamics V5.25.44 program. For samples containing alamethicin, vesicles were incubated with alamethicin for 15 min at room temperature before light scattering measurements were made.

Chapter 3

Preparation and properties of asymmetric vesicles that mimic cell membranes: effect upon lipid raft formation and transmembrane helix orientation

Introduction

Over the last few decades artificial lipid bilayers of various types have been successfully used as models for biological membranes, yielding many important insights into the architecture of cell membranes. Vesicle dispersions (liposomes) have perhaps been the most useful model membrane system. However, commonly used preparation procedures do not provide control over differences in lipid composition between inner and outer leaflets (lipid asymmetry). This is a troubling limitation because biological membranes are highly asymmetric. In mammalian cells the plasma membrane outer leaflet (exofacial monolayer) is enriched in sphingolipids and phosphatidylcholines (PC), while the inner leaflet (cytofacial monolayer) is enriched in phosphatidylethanolamine (PE) and phosphatidylserine (PS) (*92*).

The subject of lipid asymmetry has become all the more important because of its potential role in the structure and function of lipid rafts. Lipid rafts are defined as sphingolipid and sterol-rich lipid domains that exist in the liquid ordered (Lo) state. Rafts are thought to co-exist in many eukaryotic cell membranes with liquid disordered (Ld) state domains rich in lipids having unsaturated acyl chains (*11, 93*), and have been proposed to be important for numerous cellular processes.

The physical properties of Lo domains and the lipid structure dependence of domain formation have been extensively characterized in model membranes bilayers with a symmetric lipid distribution (*11, 18, 20, 30, 70-73, 81, 87, 94-110*). The ability to prepare asymmetric vesicles would allow more direct comparison of raft-forming model membranes to cell membranes. Some important progress has been made in preparing asymmetric planar bilayers (*64, 83, 111*). However, asymmetric lipid vesicles would be of wider utility. Ordinary vesicle preparation procedures (e.g. sonication) can yield some degree of asymmetry in some cases (*112-113*), but it can be hard to control. Using pH gradients, asymmetry of small amounts of anionic lipids has been achieved (*114-115*). The ability to exchange lipids in one leaflet of the bilayer can provide a method to prepare asymmetric vesicles with controlled asymmetry (*116-117*). In one study, a phospholipid exchange protein was used to effectively deliver labeled phosphatidylcholines to the outer leaflet of model membranes (*117*). In addition, a monolayer-by-monolayer assembly method for preparation of asymmetric vesicles has been reported (*78*). Gamma-cyclodextrins have been used to deliver small amounts of labeled phospholipids into the outer leaflet of membranes (*61*).

Nevertheless, a facile and widely applicable method to prepare asymmetric vesicles with a wide variety of lipid compositions, including compositions that mimic cell

membranes, has not been described. In this report, we introduce such a method. This procedure is based on the observation that methyl-beta-cyclodextrin (MβCD) binds phospholipids at very high MβCD concentrations (*54, 56*). Using this method asymmetric vesicles were prepared with an external leaflet rich in SM and an internal leaflet rich in PE and PS, similar to eukaryotic plasma membranes. Furthermore, cholesterol was introduced into the asymmetric vesicles by exposure of the asymmetric vesicles to cholesterol-loaded MβCD (using lower MβCD concentrations).

The physical properties of these vesicles reveal some important differences and similarities between symmetric and asymmetric bilayers. Overall, it appears that the type of asymmetry found in eukaryotic cell membranes is not a barrier to raft formation, and even more importantly, that the stabilizing effects of cholesterol upon raft formation are not restricted to symmetric membranes. Furthermore, we find lipid asymmetry influences hydrophobic helix topography. Asymmetric vesicles prepared by this method should aid many studies of the role of lipid asymmetry in membrane structure and function.

Results

Exchange (Asymmetric) vesicle preparation— Our aim was to prepare asymmetric vesicles with SM in the outer leaflet and glycerophospholipids containing at least one unsaturated acyl chain in the inner leaflet. To accomplish this, SM MLV were incubated with 100 mM MβCD to allow the formation of MβCD-SM complexes (Fig. 3.1 *A*). This high concentration of MβCD was necessary to load the SM onto the MβCD, and dissolved a significant fraction of the SM MLV (about 25% solubilization as judged by the decrease in optical density at 450 nm, not shown). An elevated temperature was used (55 ^{o}C) so that the SM would be in a disordered fluid state, and a high SM concentration was used (16 mM prior to centrifugation) in order to saturate the MβCD so that it would not dissolve the SUV added in the following step, and so that exchange would result in an SUV population with an outer leaflet predominantly composed of SM. SUV composed of unsaturated glycerophospholipids (4 mM of DOPC, POPC, POPS or a 1:1 or 2:1 POPS:POPE (mol:mol) mixture) was then added, and the MLV removed by centrifugation. To separate the exchanged SUV from both MβCD and residual MLV the supernatant was then chromatographed on Sepharose CL4B.

Fig. 3.2*A* shows the Sepharose 4BCL chromatographic profile for a control sample in which POPC SUV (labeled with NBD-PE and a transmembrane peptide, LW peptide) and SM MLV were mixed in the absence of MβCD. NBD and peptide fluorescence exhibited nearly identical profiles and recoveries (~85%), mainly eluting in fractions containing SUV, and a chromatography profile of the SUV characteristic of that

for SUV having a 250±30 Å diameter (*118*)**.** As judged by the fluorescence of rhodamine-PE incorporated into the MLV, a small amount (<1%) of residual MLV was present, and mainly eluted in void volume fractions, which contain vesicles too large to enter the beads. HP-TLC analysis detected only a trace SM (SM:POPC ratio 0.02) in SUV-containing fractions.

In contrast, when a SM MLV-MβCD mixture was co-incubated with POPC SUV, HP-TLC analysis showed considerable SM transfer into SUV fractions within minutes (Fig. 3.2 *B* and 3.*2 C*). The Sepharose 4BCL elution profile for fluorescence markers (Fig. 3.*2 B*) showed some of the NBD-PE was transferred to the fractions containing large vesicles, presumably indicative of partial exchange of NBD-PE into (residual) MLV present, while the elution profile of LW peptide, which should not be extracted from membranes by MβCD, was largely unaltered from that in the absence of MβCD, i.e. the peptide remained SUV-associated. Consistent with these observations ~68% of the NBD-PE was recovered in the eluted fractions (the decrease in recovery likely being due to NBD-PE transfer to MLV which were removed by pelleting), while ~80% of the non-exchangable LW peptide was recovered in the eluted fractions, an amount similar to that recovered in the absence of MβCD. Thus, it appears that the SUV remained intact during exchange. In the presence of MβCD there was also an increase in rhodamine-PE fluorescence in void volume fractions, to almost 5% of the original amount in the MLV (not shown). This may be due to the presence of some SM vesicles slightly too small to pellet, and which form either when MβCD is added to SM MLV or when the SM-MβCD mixture is diluted with SUV. Vesicles in these fractions are also observed when the SM MLV-MβCD mixtures by themselves (i.e. without incubation with SUV) are applied to the Sepharose 4BCL column.

Similar column profiles were observed in preparations in which SM was exchanged into DOPC SUV or 2:1 (mol:mol) POPE:POPS SUV.

We refer to the SUV present after the lipid exchange step as exchange vesicles. Based on HP-TLC the exchange of lipids results in SM:POPC ratios of 1-1.2:1 mol:mol. If 66% of the total lipid resides in the outer leaflet of SUV, this is equivalent to exchange of up to 82% of the outer leaflet.

Preparation of cholesterol-containing exchange vesicles— To more closely imitate eukaryotic membranes, cholesterol was introduced into the exchange vesicles. As illustrated in Fig. 3.1*B*, in the first step SM was exchanged into the SUV. Then samples were subjected to centrifugation to remove MLV, followed by chromatography on a Sephacryl S-200 column to remove MβCD with minimal dilution of the vesicles. Void

volume fractions contained the lipid vesicles (SUV and residual MLV) (not shown). To incorporate cholesterol the exchange vesicles were then incubated with cholesterol-loaded MβCD (CLC), using a lower MβCD concentration (generally 2.5 mM for PC SUV and 7.5 mM for POPE:POPS SUV) so that the MβCD would not bind phospholipid (*56*). In the final step, the cholesterol-containing asymmetric SUVs were separated from other components on a Sepharose CL4B column. HP-TLC analysis of lipid composition of SUV fractions showed incorporation of ~25% cholesterol (not shown) and that introduction of cholesterol did not appreciably alter vesicle phospholipid composition (Fig. 3.2 *D*).

Comparison of ordinary and exchange SUV using fluorescence anisotropy— To test for asymmetry, ordered domain formation by ordinary and exchange vesicles were compared by measuring the steady state fluorescence anisotropy of diphenylhexatriene (DPH) and trimethylaminodiphenylhexatriene (TMADPH) added to the vesicles. DPH dissolves throughout the lipid bilayer, while TMADPH, which anchors to the polar interface by a charged quaternary amino group and does not flip rapidly between inner and outer leaflets, was restricted to the outer leaflet (see below) (*119-120*). High anisotropy is observed for these probes in gel (Lβ) and liquid ordered (Lo) state bilayers (referred to collectively as ordered states), while low anisotropy is observed in the liquid disordered (called Ld or Lα) state. Thus, at room temperature both DPH and TMADPH exhibit much higher anisotropy in gel phase SM vesicles than in Ld phase vesicles containing unsaturated glycerophospholipids (DOPC, POPC, or POPE:POPS) (Table 3.1) (*121-122*). However, the anchoring of TMADPH restricts its motional range so its anisotropy is higher than that of DPH in Ld state vesicles.

Table 3.1 also shows that intermediate anisotropy values are observed in ordinary SUV containing a 2:1 mol:mol ratio of SM to total unsaturated glycerophospholipids. These values reflect the presence of co-existing SM-rich gel domains and glycerophospholipid rich Ld domains in such vesicles at room temperature (*123-124*). From DPH anisotropy, which should report the average of inner and outer leaflet fluidity, 43-54% of the DPH fluorescence originated from the (SM-rich) ordered state domains for SM mixtures with DOPC, POPC, or 2:1 mol:mol POPE:POPS. Because DPH usually partitions equally between ordered and disordered domains (*125-126*), this should be close to the % of the bilayer that is in the ordered (here gel) state. (Differences in DPH intensity when it is located within an ordered and disordered state environment have little influence upon this conclusion. For the lipids used in this study, both in the absence and presence of cholesterol, we found the intensity of DPH in ordered state vesicles was only 5-20% larger than in vesicles in the Ld state.) TMADPH anisotropy indicated a smaller

fraction of TMADPH fluorescence originating from the ordered domains (17-36% depending on the identity of the unsaturated glycerophospholipid), consistent with the tendency of TMADPH to partition somewhat more favorably into disordered domains (*127*).

The anisotropy of exchange SUV containing SM and either DOPC, POPC or 2:1 POPE:POPS exhibited a striking contrast with that of ordinary vesicles of similar overall lipid composition. The anisotropy and calculated % of DPH fluorescence originating from ordered domains (66-77% depending on the identity of the unsaturated glycerophospholipid) was higher than for ordinary vesicles. Furthermore, no matter what unsaturated glycerophospholipid was used, high anisotropy values were observed for TMADPH, indicating that the fluorescence of TMADPH incorporated into the outer leaflet arose almost totally from ordered domains. This means that the outer leaflet of these vesicles was more ordered than the bilayer as a whole, and thus much more ordered than the inner leaflet. This is the expectation if there is an asymmetric distribution of lipids such that the outer leaflet is predominantly composed of SM in the ordered gel state.

The difference between the % ordered domains sensed in the entire vesicle by DPH, and in the outer leaflet in TMADPH, can be used to estimate the % ordered domains in the inner leaflet.

Assuming that the DPH anisotropy reflects a combination of that in the inner and outer leaflet; 2/3 of the total lipid (and DPH) in the exchange SUV is in the outer leaflet (*128*); ~17-31% of the inner leaflet lipid in exchange vesicles would be in an ordered state (in samples lacking peptide). This is consistent with an inner leaflet composed predominantly of the unsaturated lipids, which tend to form disordered domains. In other words, the fluorescence data indicated that the exchange vesicles had a highly asymmetric lipid distribution with a SM-rich outer leaflet and unsaturated glycerophospholipid-rich inner leaflet. It also indicated that ordered domain formation in the outer leaflet did not require ordered domain formation in the inner leaflet.

Anisotropy in exchange vesicles containing LW peptide were similar to those in its absence, suggesting asymmetry of the exchange vesicles was maintained. However, there was a small decrease in TMADPH anisotropy hinting that peptide may alter domain organization (see Discussion).

The results above imply the vesicles made by the exchange procedure have an asymmetric lipid composition, as confirmed by the experiments described in the following sections. To describe the lipid composition and asymmetry of such vesicles we propose the designations **"**o" = outer leaflet lipid; "i" = inner leaflet lipid. We use "/" to

separate the names of lipids in different leaflets, ":" to separate lipid names when the lipids are in the same leaflet or in ordinary vesicles, and "-" to separate lipid names when referring to both asymmetric and ordinary vesicles. Thus, a vesicle composed of SM, PE, and PS, would be designated SMo/PE:PSi when the SM is in the outer leaflet and PE and PS are in the inner leaflet, designated SM:PE:PS in ordinary symmetric vesicles and SM-PE-PS when asymmetry is undefined when talking about symmetric and asymmetric vesicles at the same time.

Cholesterol-containing vesicles were also studied. Ordinary vesicles containing 2:1 SM:unsaturated glycerophospholipids plus 25mol% cholesterol gave DPH and TMADPH anisotropy values consistent with a mixture of ordered (Lo) and disordered fluid (Ld) domains, with a higher overall level of ordered domain formation than without cholesterol (Table 3.1). Indeed, ordered/disordered domain co-existence in these mixtures has been found previously using fluorescence quenching (*68*). The apparent % ordered domains forming in the presence of cholesterol was higher than in its absence as noted previously (*11, 87, 110*).

Exchange vesicles containing cholesterol showed a significant degree of ordered domain formation as judged by DPH anisotropy, and fully ordered outer leaflets as judged by TMADPH anisotropy. Again, this indicates an asymmetric lipid distribution with a SM-rich outer leaflet and unsaturated glycerophospholipid-rich inner leaflet. As in the case of ordinary vesicles, exchange vesicles containing cholesterol showed a higher overall level of ordered domain formation than exchange vesicles lacking cholesterol (80-83%). Based on comparison of DPH and TMADPH anisotropy, we estimate that ~40-50% of the inner leaflet was in an ordered state in cholesterol-containing exchange vesicles. (In SMo/2:1 POPE:POPSi/CHOL vesicle inner leaflet order may be as higher if ordinary POPE:POPS:CHOL vesicles are already partly in an ordered state (Table 3.1 and (*68*)). This suggests that the SM-rich outer leaflet induces a greater level of ordering within the inner leaflet in the presence of cholesterol than in its absence.

Asymmetry was relatively stable. Anisotropy of both DPH and TMADPH (added to exchange vesicles right before measuring anisotropy) did not change significantly for at least 1-2 days after sample preparation both for SMo/POPCi or for SMo/2:1 POPE:POPS/CHOL vesicles [in each case the vesicles also contained LW peptide] (data not shown). Additional controls confirmed TMADPH flips slowly from the outer to the inner leaflet. In exchange vesicles movement of TMADPH to the inner leaflet should have been accompanied by a decrease in anisotropy, but we found only a very small drop in anisotropy over a period of a few hours. In addition, accessibility of TMADPH to extraction by externally added MβCD (see below) only decreased slightly over several hours (not shown).

Comparison of the thermal stability of ordered domains in ordinary and exchange SUV— To further characterize differences between ordinary and exchange vesicles the thermal stability of ordered domains was determined via the temperature dependence of DPH fluorescence anisotropy. As temperature is increased ordered state lipids melt and anisotropy shows a distinct transition from high to low values. The melting temperature (Tm) can be defined as the midpoint of this transition, the temperature at which the decrease in anisotropy per ^{o}C is a maximum (*125*, *129*).

Fig. 3 shows the temperature dependence of DPH anisotropy and Tm values derived from these curves. SUV composed of SM showed high DPH anisotropy at low temperature (~16^{o}C) (Fig. 3.3 *A*) and a Tm slightly above 35 ^{o}C (Fig. 3.3 *B*), as expected (*130-131*). DOPC vesicles exhibited a low anisotropy that decreased slowly as temperature increased, characteristic of the Ld state. Ordinary vesicles composed of SM:DOPC mixtures exhibited intermediate anisotropy at low temperature due to the co-existence of Ld and gel domains (Fig. 3.3 *A*, left panel), as noted above. As expected, they exhibited a lower Tm than that of pure SM vesicles, 27^{o}C for 2:1 SM:DOPC and 24 ^{o}C for 1:1 SM:DOPC (Fig. 3.3 *B*, left panel). This behavior contrasts with that of SMo/DOPCi exchange vesicles with an overall lipid composition similar to that of the ordinary vesicles. As in the case of ordinary vesicles, these vesicles had an intermediate anisotropy at low temperature (Fig. 3.3 *A*), but their melting transition occurred at about as high a temperature as that of pure SM vesicles (Fig. 3.3 *B*), indicating that the unsaturated glycerophospholipid-rich, largely Ld state inner leaflet did not have a deleterious effect on the stability of ordered domain formation by the SM-rich outer leaflet.

Ordered domain thermal stability was also measured for vesicles containing ~25 mol% cholesterol (Fig. 3.3, *A* and *B*, right panels.). The pattern of Tm values vs. vesicle composition mirrored that in vesicles without cholesterol, with higher and nearly equivalent Tm observed for SM:CHOL and exchange vesicles, and lower Tm for ordinary vesicles with an overall lipid composition similar to that of the exchange vesicles.

A very similar anisotropy and Tm pattern was observed for SMo/POPE:POPSi, SMo/POPE:POPSi/CHOL exchange vesicles, and the corresponding ordinary vesicles (see Fig. 3.4). The Tm of DPPCo/DOPCi exchange vesicles was also higher (by ~5^{o}C) than that of ordinary 2:1 DPPC:DOPC vesicles, but not as high as in pure DPPC vesicles (Fig. 3.4). This may reflect a lower level of DPPC exchange into SUV (relative to that of SM). Nevertheless, the observation that ordered domains in DPPC-containing exchange vesicles had a higher Tm than in ordinary vesicles suggests that the higher stability of

ordered domains in asymmetric vesicles is not restricted to ordered domains composed of SM.

It should be noted that both ordinary and exchange vesicles exhibited significantly higher Tm values (by 5-10^{o}C) in the presence of cholesterol. This thermal stabilization of ordered domains by cholesterol has been observed previously in the case of ordinary vesicles, and is one of the key *in vitro* observations suggesting Lo-like ordered domains might form in cell membranes under physiological temperatures (*11, 20, 72*). The fact that stabilization of ordered domains by cholesterol was observed in exchange vesicles indicates that this crucial property of cholesterol can be retained in asymmetric bilayers (see Discussion).

Controls confirmed that the difference between the Tm values in ordinary and exchange vesicles was not due to residual ethanol in the ordinary vesicles. Addition of ethanol to exchange vesicles (or any vesicles containing ordered domains) only decreased Tm by 1-2^{o}C (not shown). Also, the asymmetric arrangement of lipids in the exchange vesicles was largely maintained after heating to above Tm. Tm values remeasured after heating exchange vesicles to 60-70^{o}C and cooling to 16^{o}C were only generally 1-2^{o}C lower than those of initial samples (not shown).

Confirmation of asymmetry using TMADPH binding to vesicles—An alternate explanation of the high Tm values in exchange vesicles is that they contain separate populations of SM vesicles and unexchanged unsaturated glycerophospholipid vesicles. To rule this out, and further confirm asymmetry, several methods were used. The first asymmetry test was based on the observation that POPS (an anionic lipid) renders MβCD-induced extraction of outer leaflet TMADPH (a cationic molecule) from vesicles more difficult. Fig. 3.5 shows that extraction of TMADPH from bilayers by MβCD could be detected by a decrease in TMADPH fluorescence upon addition of MβCD (Fig. 3.5 *A*). That this fluorescence decrease was due to extraction was confirmed by centrifugation experiments measuring the amount of TMADPH bound to the outermost leaflet of SM MLV in the absence and presence of MβCD. Most of the TMADPH appeared in the MLV-containing pellet without MβCD, but in the supernatant after addition of MβCD (Fig. 3.6).

Fig. 3.5 *B* quantifies the lipid composition-dependence of the ability of MβCD to extract TMADPH from the outer leaflet of vesicles via the parameter $C_{50\%}$, defined as the MβCD concentration resulting in half as much extraction as at 20 mM MβCD. Extraction of the cationic TMADPH molecules from 2:1 mol:mol POPS:POPE vesicles, which are anionic, was much more difficult ($C_{50\%}$ ~ 1.9 mM) than extraction from zwitterionic SM

vesicles ($C_{50\%}$ ~ 0.29 mM). Consistent with an asymmetric structure with little POPS in the outer leaflet, SMo/POPE:POPSi exchange vesicles exhibited a low $C_{50\%}$ value (~ 0.5 mM) close to that of pure SM vesicles, and less than that of ordinary vesicles containing 75% SM ($C_{50\%}$~ 0.7 mM) or of TMADPH bound to a 1:1 mixture of SM vesicles and 2:1 POPE:POPS vesicles ($C_{50\%}$~ 1.3 mM). It should be noted that the $C_{50\%}$ values were affected by lipid concentration, such that the lower the concentration of lipid, the lower the $C_{50\%}$ value (not shown). We confirmed that for the exchange vesicle preparations, the low $C_{50\%}$ value observed was not due to a lower lipid concentration than in the ordinary vesicle preparations (data not shown).

$C_{50\%}$ values also showed that it was more difficult to extract TMADPH from DOPC vesicles ($C_{50\%}$ ~ 0.64 mM) than from SM vesicles, as predicted by the slightly higher affinity of TMADPH for disordered domains than ordered domains (*127*). However, this difference was too small to use in evaluating lipid asymmetry in SMo/DOPCi vesicles. Complications arising from extraction of cholesterol by MβCD precluded meaningful TMADPH extraction experiments on cholesterol-containing preparations.

Confirming asymmetry using Ca^{2+}-induced vesicle aggregation— A second asymmetry assay involved detection of the amount of PS on the outside of exchange vesicles via Ca^{2+}-induced vesicle aggregation. Vesicles containing the anionic lipid PS in their outer leaflet aggregate and fuse extensively in the presence of externally added Ca^{2+} (*132*). This process can be detected by an increase in light scattering (optical density). If PS is restricted to the inner leaflet of vesicles should be inaccessible to Ca^{2+}, and should not contribute to Ca^{2+}-induced vesicle aggregation.

The behavior of ordinary and exchange vesicles containing POPS in the presence of Ca^{2+} was consistent with the predictions that the exchange vesicles were asymmetric. As shown in Fig. 3.7 *A*, SM vesicles did not aggregate in the presence of Ca^{2+}, while ordinary 1:1 mol:mol POPE:POPS vesicles extensively aggregated. POPE:POPS vesicles mixed with SM vesicles aggregated to a similar degree as POPE:POPS vesicles in the absence of SM vesicles, indicating that SM vesicles do not participate in, or interfere with, the aggregation of POPE:POPS vesicles. In contrast SMo/POPE:POPSi exchange vesicles with a POPE and POPS content comparable to that in the mixture of separate SM and POPE:POPS vesicle populations showed very little aggregation, inconsistent with the hypothesis that the exchange preparation consisted of separate POPE:POPS SUV and SM SUV populations, but consistent with an asymmetric lipid distribution with POPS being largely restricted to the inner leaflet. This conclusion was supported by the observation that ordinary vesicles composed of 2:1:1 or 6:1:1

SM:POPE:POPS aggregate to a greater degree (increase in optical density of 0.039 and 0.009, respectively at 18 mM $CaCl_2$, respectively) than the MβCD exchange vesicles (increase in optical density of 0.0008 at 18 mM $CaCl_2$) even though the ordinary vesicles contained a lower amount of POPS than the exchange vesicles.

The small degree of Ca^{2+}-induced aggregation in the ordinary vesicles presumably reflects a strong dependence of aggregation upon POPS density in the outer leaflet, but the presence of POPE complicates interpretation. To rule out complications due to POPE, analogous experiments were carried out upon SM-POPS vesicles (Fig. 3.7 *B*). Again, the level of aggregation in a mixture of SM and POPS vesicles was much higher than in SMo/POPSi exchange vesicles. Furthermore, the differences between ordinary SM:POPS and SMo/POPSi exchange vesicles were analogous to those observed in the SM-POPE-POPS vesicles, but larger (Fig. 3.7, *A* and *B*). This confirmed the exchange vesicles do not consist of a mixture of unexchanged vesicle populations and are asymmetric, with SM in the outer leaflet and the unsaturated glycerophospholipid in the inner leaflet.

Similar results were found for analogous ordinary and exchange vesicles containing cholesterol (Fig. 3.7 *C*), indicating that the introduction of cholesterol did not disrupt asymmetry.

Distinguishing asymmetric vesicles from mixtures of two types of ordinary vesicles using sucrose gradient centrifugation— The methods above were suitable for assaying asymmetry for vesicles containing anionic lipid. To confirm that separate SM and unsaturated lipid vesicles were not being formed by the exchange procedure in vesicles lacking anionic lipid, sucrose density gradient centrifugation was used. SMo/PCi exchange vesicles were prepared from SUV containing a 2:3 mol:mol mixture of DOPC with a tetrabrominated derivative of DOPC (BrPC). The latter lipid has a high density, allowing BrPC-containing SUV to be distinguished from vesicles formed from unlabeled lipids on density gradients (*133*). Fig. 3.8 shows the density profile for SMo/2:3DOPC:BrPCi exchange vesicles. As assayed by HP-TLC analysis SM and PC primarily both located in the fraction 4. [In a separate experiment both SM and BrPC in ordinary SUV composed of 5:2:3 SM:DOPC:BrPC were found to predominantly locate in fraction 5 (not shown).] In contrast, in the case of a mixture of SM vesicles and 3:2 DOPC:BrPC vesicles, the SM vesicles mainly located in the lowest density fraction, while the PC vesicles were mainly in the highest density fractions. These results confirm that exchange procedure does not result in the formation of separate SM and PC vesicles.

When centrifuged under conditions with a shallower sucrose gradient, SMo/~2:3 DOPC:BrPCi exchange vesicles containing ~25 mol% cholesterol located at a similar average sucrose density as vesicles without cholesterol, but with the lipids spread into a wider number of fractions (data not shown). There was a constant phospholipid/cholesterol ratio over these fractions, but some heterogeneity in SM/PC ratio such that the estimated SM content varied over the range 50%±15%(data not shown).

Re-reconstitution confirms exchange induces the formation of asymmetric vesicles— The exact lipid composition of asymmetric vesicles was difficult to measure with very high accuracy. To compare the physical properties of ordinary and exchanged vesicles with identical lipid compositions, a re-reconstitution procedure was developed. Ordinary and exchange vesicle samples were dried, destroyed by solubilization in ethanol, and then re-reconstituted in vesicles by dispersion into aqueous buffer.

Ideally, ordinary and exchange vesicles with identical lipid compositions should have different properties before re-reconstitution but identical properties after re-reconstitution. Fig. 3.9 shows that this was to a large degree true. Before re-reconstitution, SMo/POPE-POPSi vesicles (gray bars) showed an outer leaflet TMADPH anisotropy (panel *A*) and thermal melting temperature (panel *B*) similar to that of SM vesicles (black bars), and significantly higher than that of ordinary 6:2:1 SM:POPE:POPS vesicles (open bars). Overall ordered domain formation in the SMo/POPE-POPSi vesicles, as judged by DPH anisotropy (panel *C*), was intermediate between that of SM vesicles and 6:2:1 SM:POPE:POPS vesicles. After re-reconstitution the anisotropy and ordered domain melting temperatures of the exchange vesicles decreased, and reached levels almost identical to those of ordinary mixed lipid vesicles. (Notice, that there is a much smaller change in these properties for the ordinary vesicles, and that it is generally in the opposite direction of that in the exchange vesicles, which is inconsistent with the hypothesis that some property other than asymmetry explains the decrease in anisotropy and melting temperatures in the exchange vesicles.) Clearly, very little, if any, of the physical differences between the ordinary and exchange vesicles was due to a difference in lipid composition. Similar behavior upon re-reconstitution was observed for analogous vesicles containing cholesterol (Fig. 3.9, panels *D*-*F*). However, there was a small residual difference between ordinary and exchange vesicles after re-reconstitution, perhaps reflecting a small difference between their lipid composition.

Analogous decreases in the level of outer leaflet ordered domains and ordered domain thermal stability upon re-reconstitution were also observed for SMo/DOPCi, SMo/DOPCi/CHOL and DPPCo/DOPCi exchange vesicles and the corresponding

ordinary vesicles (Fig. 3.10). (Notice that for SMo/DOPCi and SMo/DOPCi/CHOL SUV, the ordinary vesicles were 1:1 SM:DOPC rather than 2:1, and thus still have lower anisotropy and Tm values than the exchange vesicles after re-reconstitution.)

To summarize, all of the methods described above show that the behavior and properties of the exchange vesicles are inconsistent with the hypothesis that they have a symmetric lipid distribution, or the hypothesis that they are composed of separate SM-containing and unsaturated glycerophospholipid-containing populations. Instead, the data all point to their having an asymmetric $SM_{outside}$/unsaturated $glycerophospholipid_{inside}$ lipid distribution.

Lipid asymmetry affects the extent of transmembane insertion by hydrophobic helices— A long standing question in membrane structure is whether lipid asymmetry affects the topography of the hydrophobic helices found in membrane proteins. To test the hypothesis that asymmetry can affect topography, a hydrophobic helix (pL4A18: acetyl-$K_2LA_9LWLA_9LK_2$-amide) with a topography that is sensitive to lipid composition was used (*134*). Previous studies have shown that pL4A18 forms a TM helix in PS vesicles, but can only form a non-TM helix associated with the surface of the bilayer in zwitterionic vesicles composed of PC (*134*). pL4A18 has a Trp residue in the center of its hydrophobic sequence, and these helix configurations can be distinguished by the wavelength of maximum Trp fluorescence emission (λmax) (Fig. 3.11 *A*). In the transmembrane (TM) state, our previous studies show pL4A18 Trp emission is significantly more blue shifted (λmax 325 nm) in PS vesicles than in the non-TM, surface bound state formed in PC vesicles (λmax 335 nm)(Fig. 3.11). [We have demonstrated a similar difference in Trp emission in TM and non-TM configurations for hydrophobic helices with many other sequences (*134-137*).] Therefore, fluorescence was used to define pL4A18 topography in symmetric and asymmetric vesicles composed of anionic and zwitterionic lipids. We found peptide behavior consistent with these results in ordinary vesicles (Fig. 3.11 *B*). In ordinary zwitterionic SM:POPC vesicles, λmax was 333 nm, close to that in DOPC, while in ordinary 1:1 POPE:POPS vesicles (which have 50% anionic lipid) , λmax was 329 nm, intermediate between that in fully zwitterionic (PC or SM:PC) and fully anionic (PS) vesicles. This indicates that in SM:POPC pL4A18 is mainly non-TM, while it is in a mixture of TM and non-TM configurations in 1:1 POPE:POPS. It should be noted that pL4A18 is membrane bound in both of these cases. When dissolved in aqueous solution pL4A18 had a much more red shifted fluorescence (λmax 359 nm) (Fig. 3.11 *B*).

The behavior of pL4A18 inserted into asymmetric ~3:2 SM:POPCo/1:1POPE:POPSi vesicles was distinctly different from that in ordinary

vesicles. As shown in Fig. 3.11, the Trp fluorescence of pL4A18 was about as highly blue shifted (λmax 326 nm) in asymmetric vesicles as in fully anionic PS vesicles. This blue shifted fluorescence indicates the formation of a fully TM topography in the asymmetric vesicles, even though they contain only a low % of PS (16 mol% based on HP-TLC). It is especially noteworthy that this λmax is more blue shifted than in either vesicles composed entirely of the outer leaflet (3:2 SM:POPC) or inner leaflet (1:1 POPE:POPS) lipids, rather than an average of these values. That this blue shift is due to lipid asymmetry was confirmed by remeasuring λmax after destroying asymmetry by reconstitution. After rereconstitution of the vesicles, pL4A18 fluorescence red shifted significantly (λmax 331 nm). This value is between that of the 3:2 SM:POPC and 1:1 POPE:POPS vesicles, as predicted if the vesicles become symmetric after rereconstitution. [It should be noted that in control TLC experiments we confirmed that there had been about the expected total amount of lipid exchanged into the asymmetric vesicles, although the amount of SM was slightly lower than expected, and that, as in the case of the other asymmetric vesicles studied, after exchange the ordered domains had a thermal stability higher than that measured after rereconstitution, confirming lipid asymmetry. Furthermore, sucrose gradient experiments confirmed that the PC and SM exchanged into the same set of vesicles (data not shown).]

Discussion

Preparation of asymmetric vesicles— This report introduces a MβCD-induced exchange method to prepare small unilamellar vesicles with a stable asymmetry in which the outer leaflets are composed largely of sphingomyelin or other lipids containing saturated acyl chains, and the inner leaflets contain various glycerophospholipids with unsaturated acyl chains. Cholesterol can be incorporated into these vesicles with maintenance of phospholipid asymmetry. In addition, mixtures of lipids can be introduced by exchange, which results in great flexibility in the lipid compositions that can be prepared. The procedure is relatively rapid, requires little special equipment or materials and produces ample amount of exchange vesicles. It works with many different lipids, can be used at elevated temperatures which might aid exchange for lipids with high Tm values. Introduction of cholesterol without disruption of the vesicles is possible because cholesterol-MβCD complexes can be prepared at MβCD concentrations too low to bind phospholipids (*56*), and is no doubt aided by rapid cholesterol equilibration between the inner and outer leaflets (*58*). Although the final cholesterol concentration in the inner and outer leaflets is unknown, the need to maintain mass balance between the leaflets requires a similar final mole fraction of cholesterol in the two leaflets.

The experimental conditions that give maximal lipid change are empirical and are likely affected by the concentration of MβCD, MLV and SUV, and the identity of the lipids used. As noted in the results, the first step in the process involves solubilization of some of the MLV by the MβCD. We choose an excess of MLV, i.e. an amount that is not totally dissolved by MβCD, so that the MβCD will be saturated with lipid and not dissolve the SUV. Since the amount of MLV that dissolves is not well defined, it is hard to say what the exact excess is present, but even if that were known it might not help define the best exchange conditions because the difference in the relative affinity of MβCD for different types of lipids in MLV and SUV could also affect exchange. MβCD affinity for lipids is complex to determine because of the cooperative nature of the MβCD-lipid interaction, which only becomes strong enough to allow lipid binding at high MβCD concentration (*56*). Both the affinity of MβCD for lipid and its binding stoichiometry may to be dependent upon its concentration. However, it is important to note that the exchange method is practical without a full study of all of these variables. We find we can define optimal conditions for exchange by varying these parameters slightly when different lipid compositions are used.

The lipid concentration of asymmetric vesicles obtained after chromatography can be variable. The final lipid concentration was determined explicitly when desired, but it is important to note that in many cases the exact vesicle concentration is not important. It is the composition of the membrane that controls vesicle properties, not the number of vesicles in solution.

It should be noted that the small decrease in anisotropy that was detected in exchange vesicles in the presence of the LW peptide might be significant. The LW peptide used has a structure that strongly disfavors its insertion into ordered domains in ordinary vesicles, and it appears to nucleate disordered domains in ordinary vesicles (*138*). Thus, the decrease in TMADPH anisotropy in the presence LW peptide may suggest it induces formation of a small amount of disordered domains in outer leaflet of the exchange vesicles, and this property might be shared by transmembrane proteins in cell membranes.

Further studies will be necessary to define conditions suitable to prepare additional types of exchange vesicles. Preliminary studies indicate that by changing experimental conditions unsaturated lipids can be exchanged into small unilamellar vesicles composed largely of SM (MiJin Son and Erwin London, unpublished observations). Other preliminary studies indicate the exchange procedure can be used to prepare asymmetric large unilamellar vesicles. Such vesicles would lack the curvature of SUV, and are more appropriate model membranes for many types of experiments. However, SUV themselves are likely to be very useful. It should be noted in this regard

that studies of membrane-inserted hydrophobic helices have found little difference between SUV and large unilamellar vesicles (*139*).

Insights into the lipid behavior in eukaryotic plasma membranes from the physical properties of plasma membrane-mimicking asymmetric vesicles— The asymmetric vesicles we prepared mimic plasma membranes in having a sphingolipid rich outer leaflet and unsaturated glycerophospholipid-rich inner leaflet, and thus provide important insights into the relationship between lipid structure and biological membrane organization. Previous studies in supported planar bilayers showing that ordered domains inner and outer leaflets are not always in close register suggested that the formation of ordered domains in both leaflets is not an absolute requirement for ordered domain formation (*140-141*). The experiments in this report show that the thermal stability of SM-rich ordered state domains in the outer leaflet is not adversely affected by interactions with an inner leaflet composed of unsaturated lipids that (by themselves) should tend to form disordered domains, at least in small vesicles. It was also found that the significant increase in the stability of ordered domains in the presence of cholesterol, a crucial cholesterol property observed in symmetric model membrane vesicles, is maintained in asymmetric membranes, and thus should occur in cell membranes. It has been assumed cholesterol stabilizes ordered domains in cells based on detergent-insolubility data, but complications can make it difficult to properly interpret detergent insolubility (*142*). Combined, these biophysical properties indicate that in the sphingolipid and cholesterol rich plasma membrane the sphingolipid-rich outer leaflet is very likely to exist in the Lo state.

Furthermore, there seems to be some degree of ordering of the inner leaflet by an ordered outer leaflet. The effect of the outer leaflet upon the inner leaflet may partly explain why the overall level of membrane order is higher when the ordered state-favoring and disordered state-favoring lipids are asymmetrically disposed than when they are symmetrically disposed. The induction of an ordered state in the inner leaflet by ordered domains in the outer leaflet is consistent with the coupling between ordered formation in inner and outer leaflets in SM vesicles that was detected in an early study (*143*), and with the very recent observations of Kiessling et al (*64*), which were made in planar bilayers insulated from the substrate, and in which it was found that a SM-rich outer leaflet could induce order in an inner leaflet composed of a physiological mixture of mammalian PC, PE and PS. It is also consistent with observations in unsupported planar bilayers and giant unilamellar vesicles indicating that ordered domains in opposite leaflets tend to exist in register with one another, indicating that there is some degree of coupling between ordered domains in opposite leaflets (*18, 104*). However, it is difficult to evaluate the behavior of the inner leaflet with the assays available at present. For

example, some of the order we estimate to exist in the inner leaflet of asymmetric vesicles may reflect a change in the dynamics of inner leaflet DPH molecules when they are trapped in a disordered environment that is only one leaflet wide. It should also be noted that we have not yet determined whether the inner leaflet undergoes segregation into separate ordered and disordered domains under the influence of the ordered domains in the outer leaflet. This will require additional methods for specifically evaluating the domain structure in the inner leaflet at the nano-domain level. In any case, further studies of interleaflet coupling will clearly be an important goal.

The effect of lipid asymmetry upon the orientation of membrane-inserted hydrophobic helices— The observation that transmembrane polypeptides can be incorporated in exchange vesicles without disruption of asymmetry should allow the use of asymmetric vesicles to carry out more detailed studies of protein-lipid interaction than in symmetric vesicles. An important finding of this report in this regard is that lipid asymmetry, in which one membrane leaflet has more anionic lipids than the other, can stabilize the formation of transmembrane topography by hydrophobic helices. This could have important implications for membrane protein topography *in vivo*. A very recent investigation of the behavior of hydrophobic helices during co-translational membrane insertion in natural membranes by Lerch-Bader et al (*144*) has shown that the extent of translocon-dependent formation of a transmembrane state (relative to formation of a non-transmembrane state) can be enhanced by cationic residues flanking the hydrophobic sequence. Our results show this might be explained by an asymmetric distribution of anionic lipid, as is believed to occur in natural membranes. Lipid asymmetry may also be important in controlling the extent of transmembrane insertion in cases of post-translational membrane insertion (*145-147*). Whether this stabilization of transmembrane topography is exclusively electrostatic in origin, or involves other specific lipid-peptide interactions will be investigated in future studies.

Other applications of asymmetric vesicles— Asymmetric vesicles should also be crucial for other applications. One is refining the interpretation and applications of detergent insolubility in cell membranes. Detergent insolubility (especially using Triton X-100) has been widely used to identify the presence of sphingolipid and cholesterol rich domains in cells, and to isolate detergent insoluble sphingolipid and cholesterol rich membranes (*9, 17, 142*). The latter property allows studies of the lipid and protein composition of these membranes, and how composition changes under different physiological conditions (*93, 148-150*)). Nevertheless, there are many cases in which detergent insolubility results are ambiguous (*60, 108, 142, 151-154*), and comparison of

the detergent insolubility properties of asymmetric model membrane vesicles to those of cell membranes should clarify the relationship between detergent insolubility and domain formation, and aid the development of improved detergent insolubility methods for detection of ordered domains in cells.

Finally, asymmetric vesicles may find applications in drug encapsulation. The availability of asymmetric vesicles (especially large vesicles) would allow the design of vesicles in which the lipid composition of the inner leaflet is compatible with the encapsulated drug, while the composition of the outer leaflet is compatible with the surrounding biological milieu.

Table 3.1. Fluorescence anisotropy in ordinary and exchange (asymmetric) vesicles at room temperature.

SAMPLE COMPOSITION	ANISOTROPY (A)		% ORDERED	
	DPH	TMADPH	DPH	TMADPH
SM	**0.309±0.012 (10)**	**0.350±0.013 (7)**	**≡100**	**≡100**
DOPC	**0.115±0.005 (6)**	**0.261±0.010 (3)**	**≡0**	**≡0**
POPC+LW	**0.128±0.005 (4)**	**0.274±0.011 (4)**	**≡0**	**≡0**
POPC	**0.120±0.004 (5)**	**0.272±0.012 (5)**	**≡0**	**≡0**
2:1 POPE:POPS+LW	**0.152±0.002 (4)**	**0.264±0.005 (4)**	**≡0**	**≡0**
2:1 POPE:POPS	**0.143±0.003 (7)**	**0.259±0.009 (4)**	**≡0**	**≡0**
2:1 SM:DOPC	**0.209±0.016 (7)**	**0.293±0.013 (4)**	**49**	**36**
2:1 SM:POPC+LW	**0.212±0.012 (3)**	**0.287±0.005 (3)**	**46**	**17**
2:1 SM:POPC	**0.202±0.011 (3)**	**0.285±0.010 (3)**	**43**	**17**
6:2:1 SM:POPE:POPS+LW	**0.237±0.013 (3)**	**0.292±0.008 (3)**	**54**	**33**
6:2:1 SM:POPE:POPS	**0.233±0.018 (6)**	**0.290±0.015 (6)**	**54**	**34**
Ex SMo/DOPCi	**0.255±0.011 (6)**	**0.350±0.007 (3)**	**72**	**100**
Ex SMo/POPCi+LW	**0.248±0.014 (3)**	**0.337±0.007 (3)**	**66**	**83**
Ex SMo/POPCi	**0.263±0.003 (3)**	**0.349±0.006 (3)**	**76**	**99**
Ex SMo/POPE:POPSi+LW	**0.270±0.011 (3)**	**0.339±0.016 (3)**	**75**	**87**
Ex SMo/POPE:POPSi	**0.271±0.004 (4)**	**0.352±0.013 (3)**	**77**	**102**
3:1 SM:CHOL	**0.320±0.011 (10)**	**0.345±0.015 (8)**	**≡100**	**≡100**
3:1 DOPC:CHOL	**0.140±0.006 (6)**	**0.259±0.009 (4)**	**≡0**	**≡0**
2:1:1 POPE:POPS:CHOL	**0.200±0.011 (4)**	**0.267±0.005 (3)**	**≡0**	**≡0**
2:1:1 SM:DOPC:CHOL	**0.267±0.013 (6)**	**0.310±0.010 (3)**	**71**	**59**
6:2:1:3 SM:POPE:POPS:CHOL	**0.277±0.010 (5)**	**0.314±0.005 (3)**	**64**	**60**
Ex SMo/DOPCi/CHOL	**0.290±0.004 (3)**	**0.352±0.003 (3)**	**83**	**108**
Ex SMo/POPE:POPSi/CHOL	**0.296±0.004 (4)**	**0.346±0.004 (5)**	**80**	**101**

Average anisotropy and standard deviation is shown. Sample number is shown in parentheses. Ordinary vesicles with SM and/or CHOL were formed by ethanol dilution; those without SM and/or CHOL were formed by sonication. Ex=exchange vesicles. Ratios are mol:mol. Samples contained ~50 μM lipid dispersed in PBS, except for POPC-containing samples which had ~100 μM lipid. Fluorescence probe was 0.1mol% of total lipid. The % ordered state bilayer from (DPH A) or outer leaflet (from TMADPH A) was estimated from: % ordered = $(A - A_{100\%Ld})/(A_{100\%\ ordered} - A_{100\%Ld})$. Without CHOL, A is that in a SM/unsaturated lipid mixture, $A_{100\%\ ordered}$ is that in SM, and $A_{100\%\ Ld}$ is that in the appropriate unsaturated lipid. In CHOL-containing samples CHOL was also present. This formula assumes that gel, Lo and Ld domains have A values similar to that in pure gel, Lo and Ld bilayers. Notice that if ordinary POPE:POPS:CHOL vesicles partly form ordered domains at 23°C(*68*), this formula underestimates inner leaflet % ordered in exchange vesicles with these lipids. LW=LW peptide.

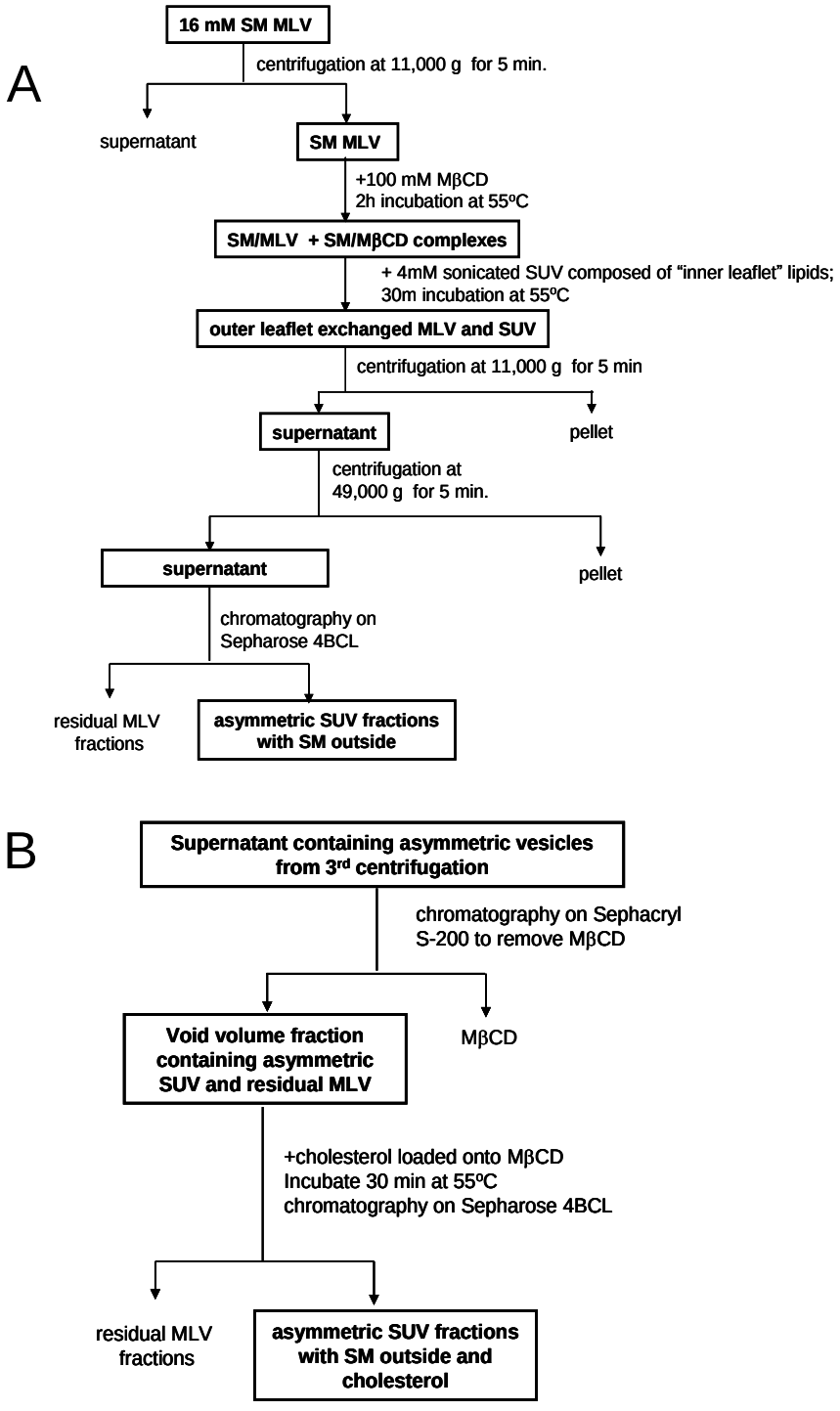

Figure 3.1. Flow chart summary of methods for producing exchange (asymmetric) phospholipid vesicles. Procedures for preparing exchange vesicles without cholesterol (A), and with cholesterol (B).

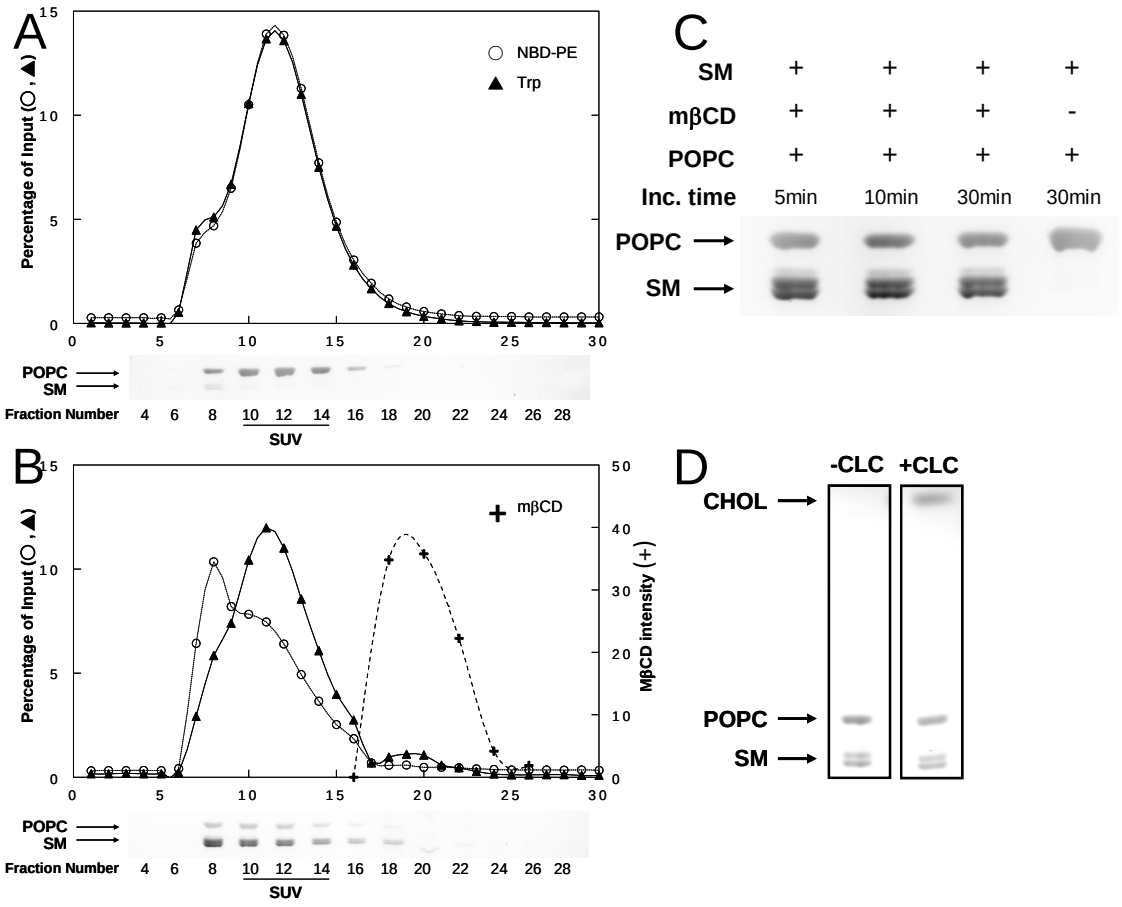

Figure 3.2. Preparation of exchange vesicles. (A) Sepharose CL4B chromatographic profile of control sample without MβCD. (B) Sepharose CL4B chromatographic profile of exchange vesicle preparation. X-axis gives fraction numbers. The % input = % of amount in the sample after exchange (i.e. prior to centrifugation and loading on the column). Symbols: (o) fluorescence of NBD-PE; (Δ) Trp fluorescence of LW peptide; (+) MβCD (intensity of MβCD bands after charring HP-TLC plates). Charred HP-TLC plates containing selected fractions are shown below the column profiles. Upper band: POPC; Lower doublet: SM. [Natural SM migrates as a doublet (*155*).] (C) HP-TLC profile of SUV fractions from Sepharose CL4B chromatography after (from left to right) incubation: of 4 mM POPC SUV for 5 min, 10 min, and 30 min with the resuspended pellet from 16 mM SM MLV (after preincubation at 55 ^{o}C for 2 h with 100 mM MβCD), or for 30 min with the resuspended pellet from 16 mM SM MLV (preincubated at 55 ^{o}C for 2 h with PBS). (D) HP-TLC analysis of Sepharose CL4B SUV fraction from SMo/POPCi exchange vesicles incubated with (left lane) PBS or (right lane) CLC (5 mM MβCD final concentration) [This CLC concentration results in higher cholesterol content (~45mol%) than in the samples used for all of the fluorescence studies (~25mol%).]

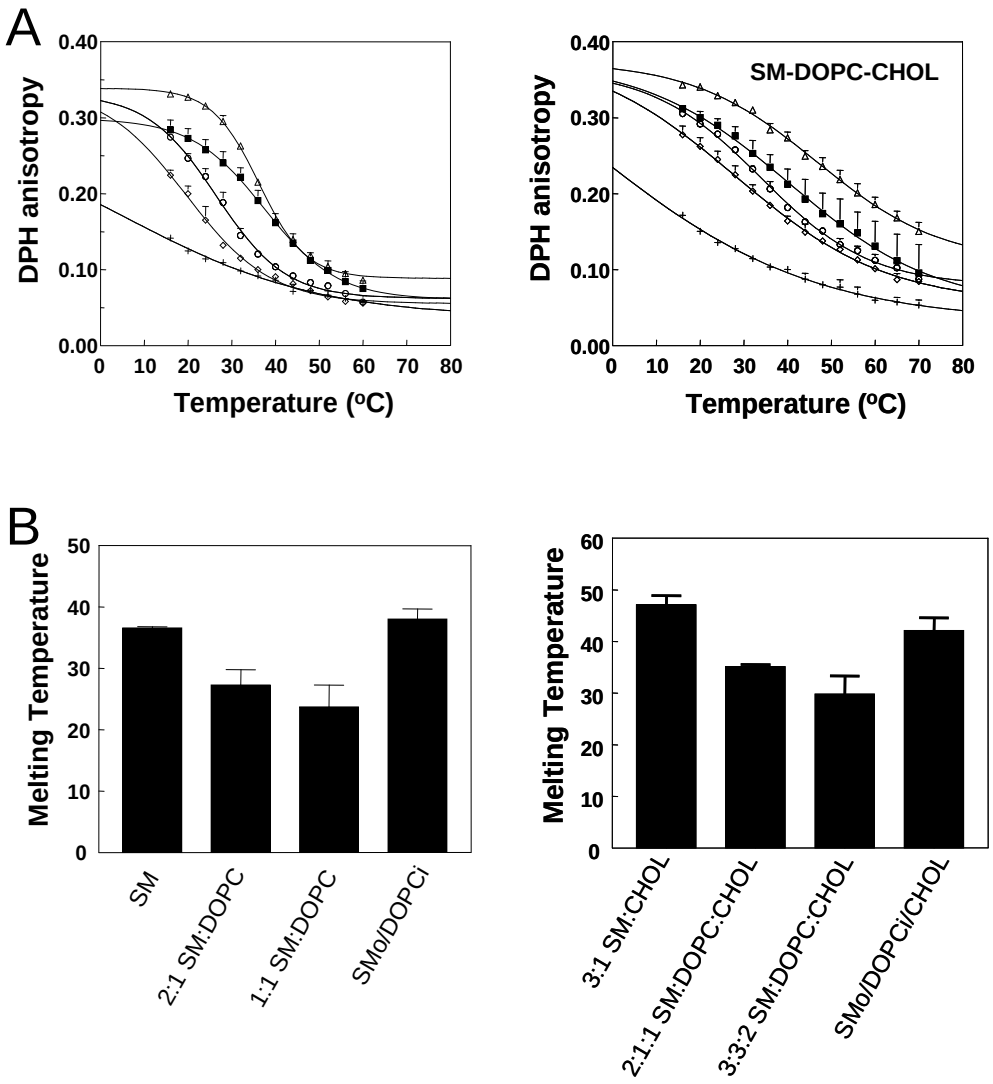

Figure 3.3. Measurement of ordered domain thermal stability. (A) Temperature dependence of DPH anisotropy in ordinary and exchange vesicles. Left panel: (Δ) SM vesicles; (o) ordinary 2:1 mol:mol SM:DOPC vesicles; (◊) ordinary 1:1 SM:DOPC vesicles; (■) SMo/DOPCi vesicles; (+) DOPC vesicles. Right panel: (Δ) 3:1 SM:CHOL vesicles; (o) ordinary 2:1:1 SM:DOPC:CHOL vesicles; (◊) ordinary 3:3:2 SM:DOPC:CHOL vesicles; (■) SMo/DOPCi/CHOL vesicles with about 25mol% CHOL; (+) 3:1 DOPC:CHOL vesicles. PBS-dispersed samples contained ~50 μM total lipid with 0.1% DPH. Lipid ratios given for exchange vesicles are approximate. Average anisotropy values from triplicate experiments and standard deviations are shown. (B) Tm values for curves shown in (A). The average derived from averaging Tm values from different samples and standard deviation in Tm values is shown. X-axis labels give vesicle lipid compositions.

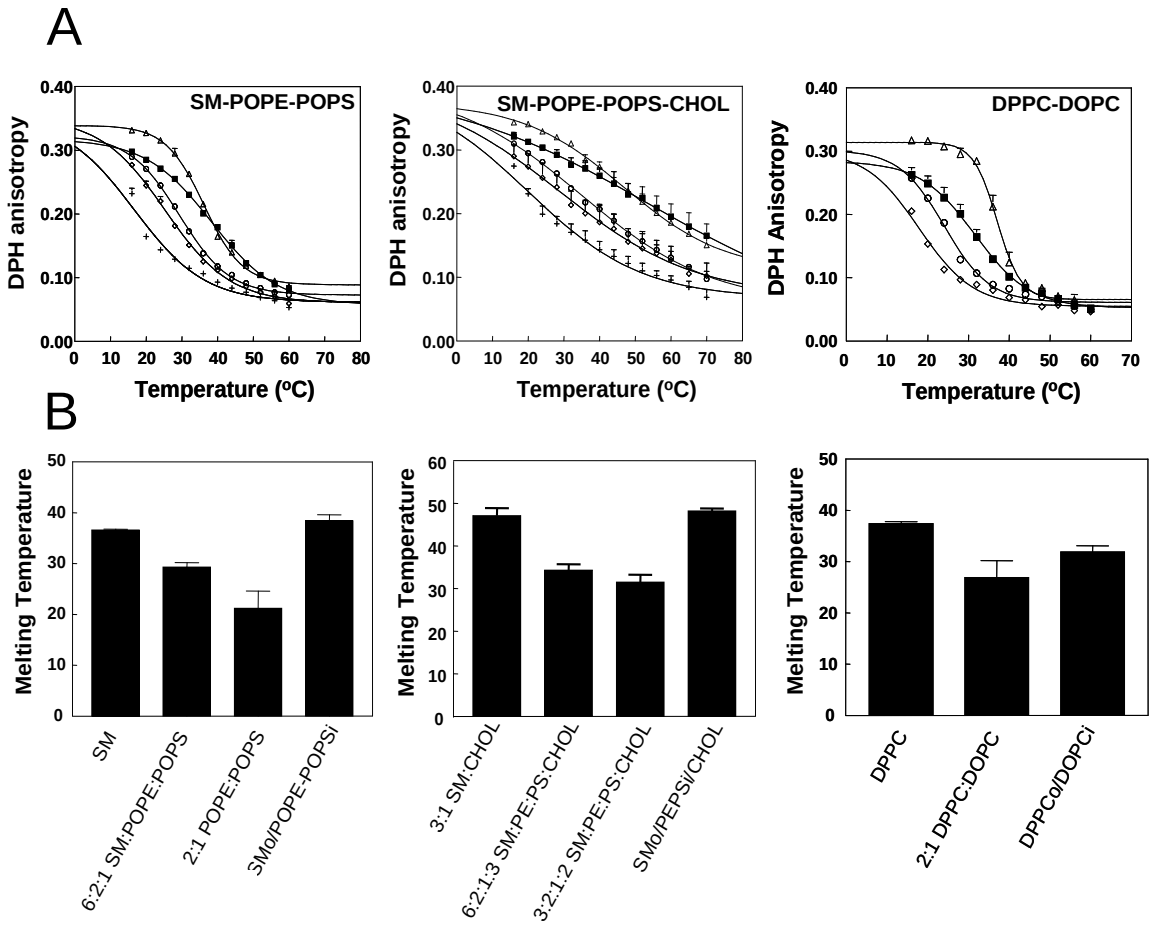

Figure 3.4. Measurement of ordered domain thermal stability in SM-POPE-POPS, SM-POPE-POPS-cholesterol, and DPPC-DOPC vesicles. (A) Temperature dependence of DPH anisotropy in ordinary and exchange vesicles. Left panel: (Δ) SM vesicles; (o) ordinary 6:2:1 SM:POPE:POPS vesicles; (◊) ordinary 3:2:1 SM:POPE:POPS vesicles; (■) SMo/2:1 POPE:POPSi vesicles; (+) 2:1 POPE:POPS vesicles. Middle panel: (Δ) 3:1 SM:CHOL vesicles; (o) ordinary 6:2:1:3 SM:POPE:POPS:CHOL vesicles; (◊) ordinary 3:2:1:2 SM:POPE:POPS:CHOL vesicles; (■) SMo/2:1 POPE:POPSi/CHOL vesicles with ~25 mol% CHOL; (+) 2:1:1 POPE:POPS:CHOL vesicles. Right panel: (Δ) DPPC vesicles; (o) ordinary 2:1 DPPC:DOPC vesicles; (◊) ordinary 1:1 DPPC:DOPC vesicles; (■) DPPCo/DOPCi vesicles. PBS-dispersed samples contained ~50 μM total lipid with 0.1% DPH. Lipid ratios given for exchange vesicles are approximate. Average anisotropy values from triplicate experiments and standard deviations are shown. (B) Tm values for curves shown in (A). The average Tm derived from each sample and the standard deviation in Tm values is shown. X-axis labels give vesicle lipid compositions.

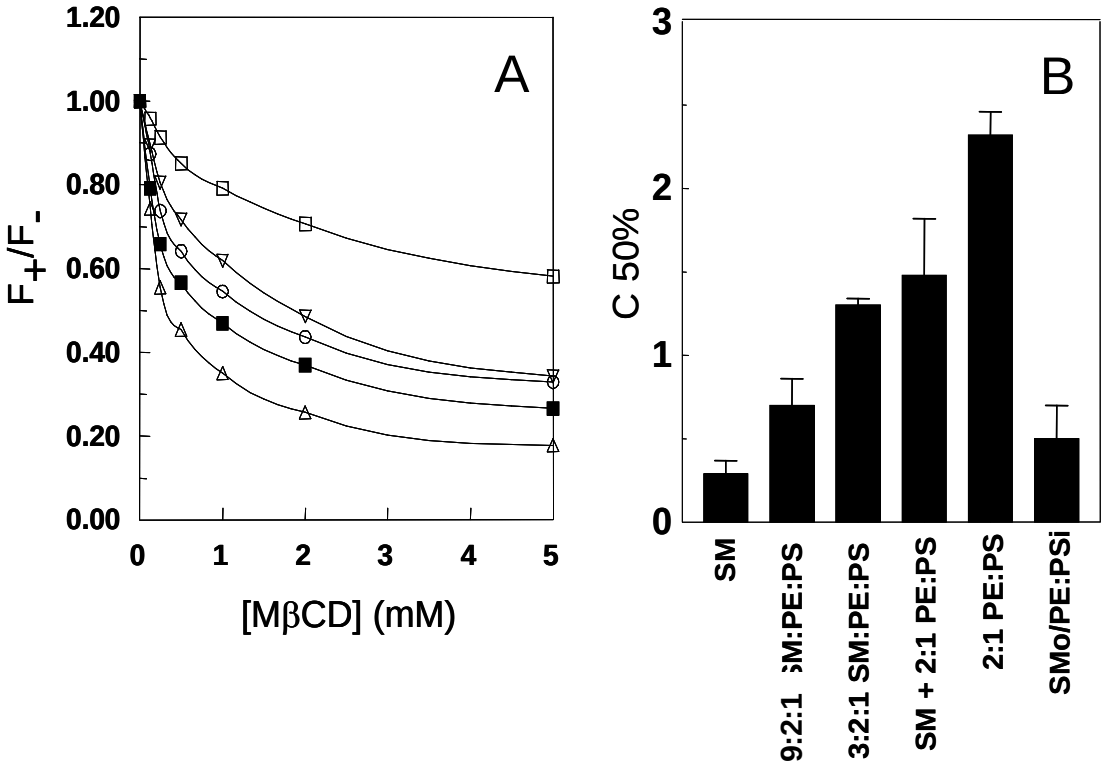

Figure 3.5. MβCD-induced extraction of TMADPH from ordinary and exchange vesicles. (A) Dependence of TMADPH fluorescence upon MβCD concentration for various vesicle compositions. Vesicles composed of: (□) 200 μM 2:1 mol:mol POPE:POPS; (▽)1:1 mixture of 100 μM SM vesicles and 100 μM 2:1 POPE:POPS vesicles; (o) 200 μM 9:2:1 SM:POPE:POPS; (■) ~200 μM SMo/2:1 POPE:POPSi; and (□) 200 μM SM. F+ is TMADPH fluorescence intensity in the presence of MβCD and F- is TMADPH fluorescence intensity in the absence of MβCD. Representative curves for single samples are shown. (B) Comparison of $C_{50\%}$ values for various vesicle compositions shown in Panel (A) plus for ordinary vesicles with a composition of 3:2:1 SM:PE:PS and total lipid concentration 200 μM. $C_{50\%}$ is the concentration of MβCD at which the decrease of F+/F- is half as large as the decrease in F+/F- in the presence of 20 mM MβCD. In the presence of 20mM MβCD, F+/F- of SM vesicles, 9:2:1 SM:POPE:POPS vesicles, 3:2:1 SM:POPE:POPS vesicles, 1:1 mixture of SM vesicles and 2:1 POPE:POPS vesicles, 2:1 POPE:POPS vesicles, and SMo/2:1 POPE:POPSi vesicles are 0.13±0.01, 0.21±0.02, 0.37±0.02, 0.18±0.02, 0.34±0.03, and 0.13±0.02 respectively. Lipid concentrations and composition are as in panel (A). X-axis labels give lipid compositions. The average of triplicate experiments and standard deviations are shown.

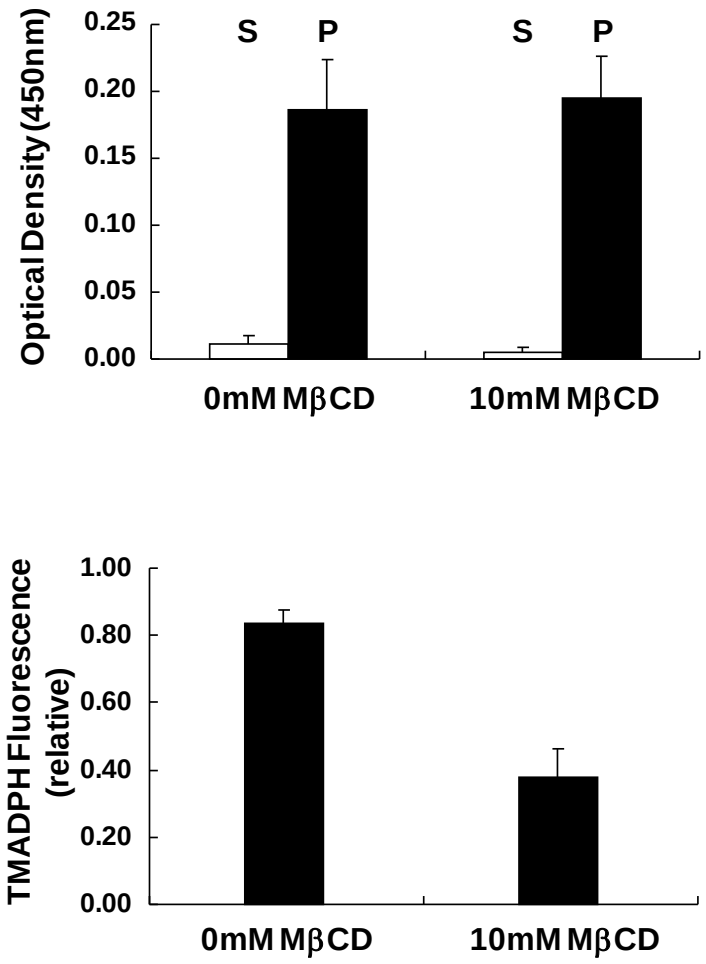

Figure 3.6. MβCD-induced extraction of TMADPH from SM MLV assayed by centrifugation. Upper panel: Optical density at 450nm of supernatant (S) and pellet (P) from 200μM SM MLV treated with or without 10mM MβCD. Lower panel: TMADPH fluorescence of pellet from 200μM SM MLV treated with or without 10mM MβCD. Relative TMADPH fluorescence of pellet or supernatant was normalized to the sum of TMADPH fluorescence from supernatant and pellet in each sample. Notice that due to the decrease in TMADPH fluorescence upon binding to MβCD the fraction of TMADPH bound to MβCD is much higher than the fraction of fluorescence of TMADPH bound to MβCD. In both panels, samples contained 0.05 mol% TMADPH in the outer leaflet of the MLV. Average values from triplicate experiments and standard deviations are shown.

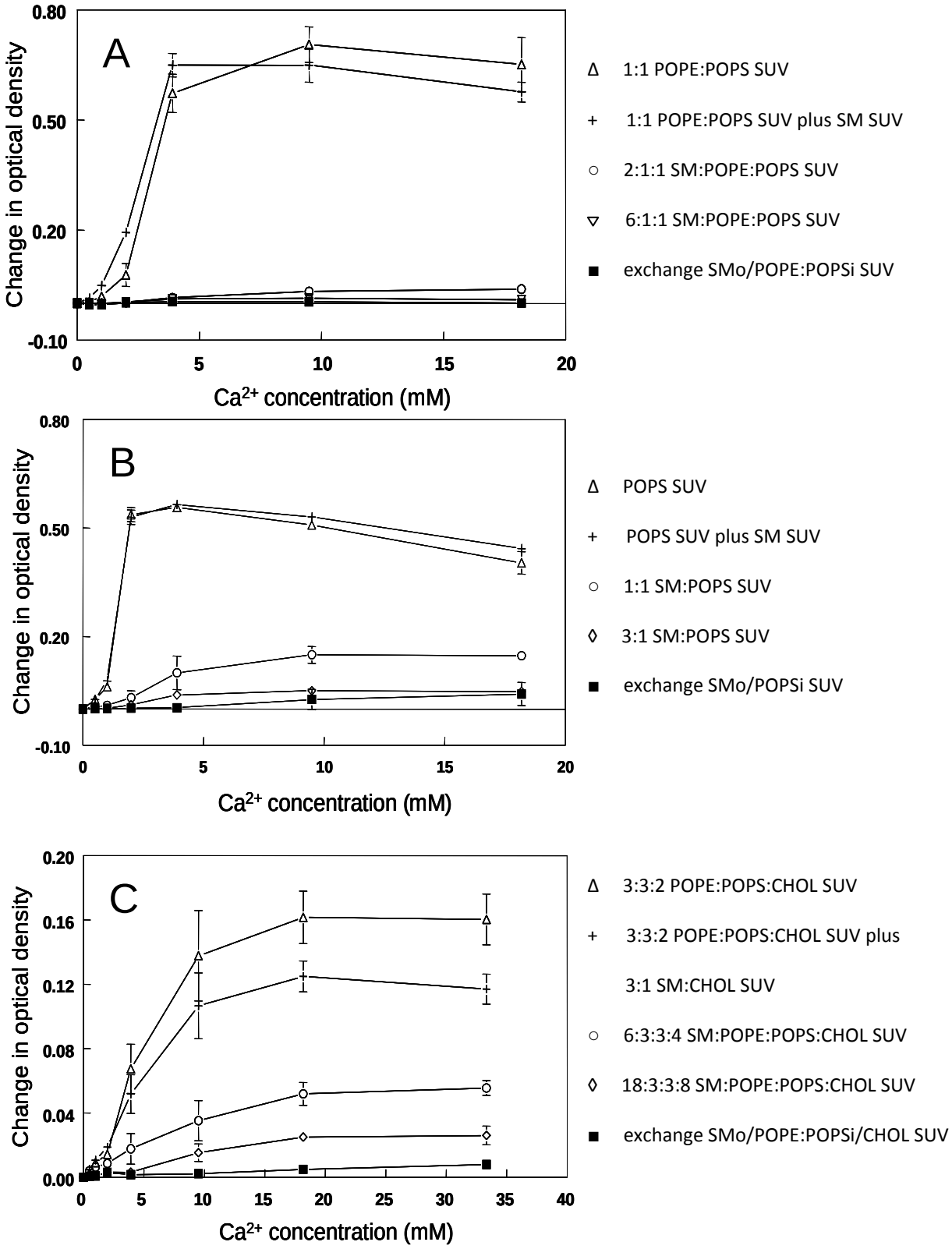
A
Change in optical density
0.80
0.50
0.20
-0.10
0
5
10
15
20
Ca2+ concentration (mM)
Δ 1:1 POPE:POPS SUV
+ 1:1 POPE:POPS SUV plus SM SUV
○ 2:1:1 SM:POPE:POPS SUV
▽ 6:1:1 SM:POPE:POPS SUV
■ exchange SMo/POPE:POPSi SUV
B
Change in optical density
0.80
0.50
0.20
-0.10
0
5
10
15
20
Ca2+ concentration (mM)
Δ POPS SUV
+ POPS SUV plus SM SUV
○ 1:1 SM:POPS SUV
◊ 3:1 SM:POPS SUV
■ exchange SMo/POPSi SUV
C
Change in optical density
0.20
0.16
0.12
0.08
0.04
0.00
0
5
10
15
20
25
30
35
40
Ca2+ concentration (mM)
Δ 3:3:2 POPE:POPS:CHOL SUV
+ 3:3:2 POPE:POPS:CHOL SUV plus
3:1 SM:CHOL SUV
○ 6:3:3:4 SM:POPE:POPS:CHOL SUV
◊ 18:3:3:8 SM:POPE:POPS:CHOL SUV
■ exchange SMo/POPE:POPSi/CHOL SUV

Figure 3.7. Comparison of the sensitivity of ordinary and exchange vesicles to Ca^{2+}-induced aggregation. The effect of aliquots of 200 mM $CaCl_2$ titrated into the samples at room temperature upon optical density at 450 nm was measured for: (A) SM-POPE-POPS vesicles: (Δ) ordinary vesicles composed of 200 µM 1:1 mol:mol POPE:POPS; (+) mixture of ordinary vesicles composed of 200 µM 1:1 mol:mol POPE:POPS plus vesicles composed of 220 µM SM; (o) ordinary vesicles composed of 200 µM 2:1:1 mol:mol SM:POPE:POPS; (▽) ordinary vesicles composed of 200 µM 6:1:1 mol:mol SM:POPE:POPS; (■) exchange vesicles composed of 333 µM SMo/113 µM POPE:130 µM POPSi (average of three preparations). Values shown are the average and standard deviation for 3-4 preparations. (B) SM-POPS vesicles: (Δ) ordinary vesicles composed of 150 µM POPS SUV; (+) mixture of ordinary vesicles composed of 150 µM POPS plus vesicles composed of 200 µM SM; (o) 200 µM ordinary vesicles composed of 1:1 mol:mol SM:POPS; (◊) ordinary vesicles composed of 200 µM 3:1 mol:mol SM:POPS; and (■) exchange vesicles composed of 230 µM SMo/177 µM POPSi (average of two preparations). Values shown are the average and standard deviation for 2-4 preparations. (C) SM-POPE-POPS-CHOL vesicles: (Δ) ordinary vesicles composed of 100 µM 3:3:2 mol:mol POPE:POPS:CHOL; (+) mixture of ordinary vesicles composed of 100 µM 3:3:2 mol:mol POPE:POPS:CHOL plus vesicles composed of 100 µM 3:1 SM:CHOL; (o) ordinary vesicles composed of 200 µM 6:3:3:4 mol:mol SM:POPE:POPS:CHOL; (◊) ordinary vesicles composed of 200 µM 18:3:3:8 mol:mol SM:POPE:POPS:CHOL; (■) exchange vesicles composed of 142 µM SMo/44 µM POPE:60 µM POPSi/56 µM CHOL. Lipid concentrations in the exchange vesicles in these experiments were estimated by HP-TLC. Values shown are the average and range for two to three preparations, except in the case of the exchange vesicles where a single preparation was used. In all cases above vesicles were prepared in 137 mM NaCl/20 mM Tris-Cl buffer pH 7.4 instead of PBS. The addition of $CaCl_2$ to solution by itself has no effect upon optical density.

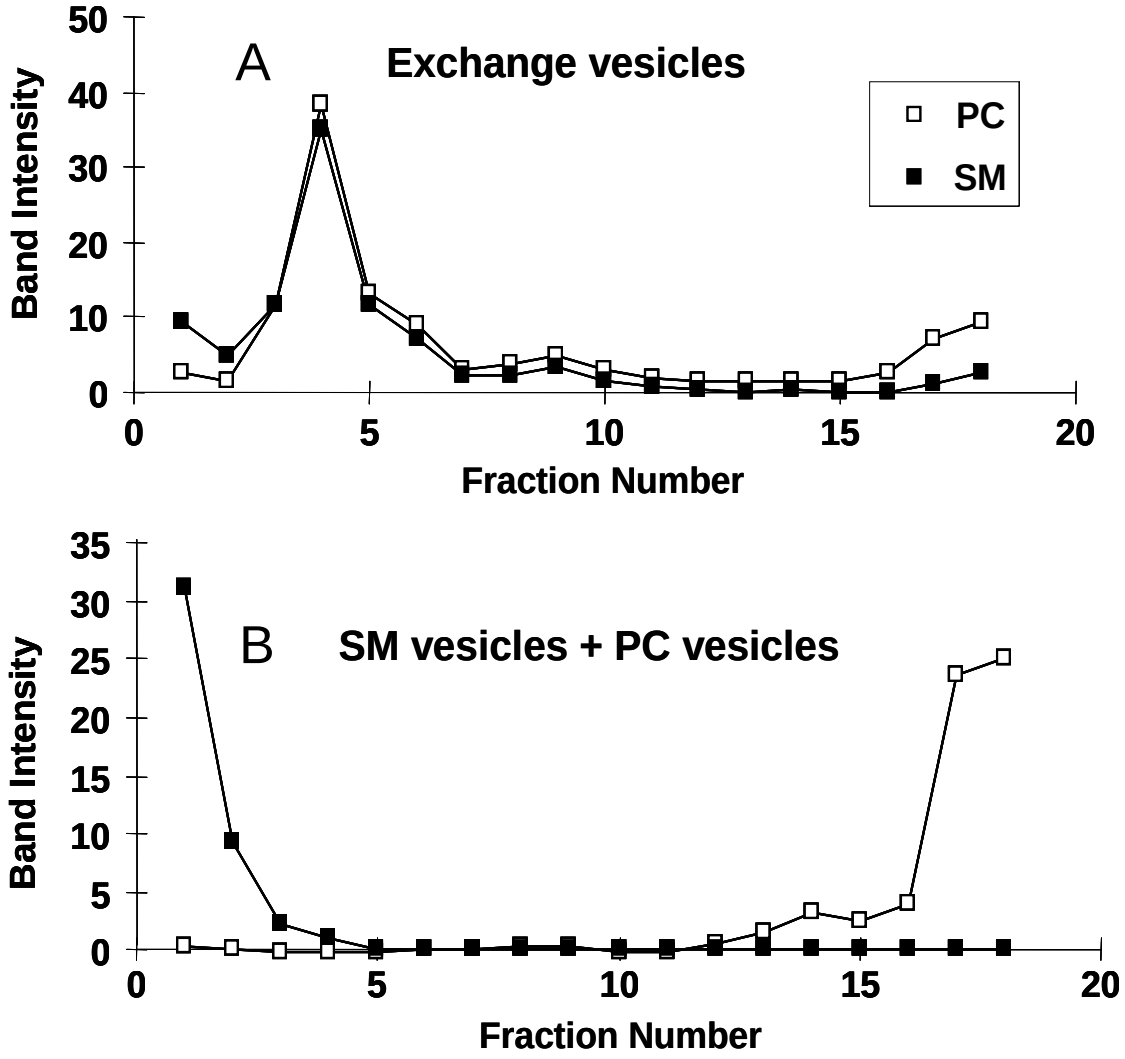

Figure 3.8. Sucrose density gradient centrifugation of SMo/PCi vesicles. (A) Sucrose gradient profile of exchange SUV containing ~200 μM lipid composed of SMo/6:4 (mol:mol) BrPC:DOPCi. (B) Sucrose gradient profile of a mixture of 100 μM SUV composed of SM and 100 μM SUV composed of 6:4 BrPC:DOPC. TLC band intensity is shown for: (■) SM; (□) total PC. Fractions from left to right are from low to high density. Band intensities for SM and PC should not be directly compared because the intensity of charred bands is dependent on lipid type. Sucrose concentrations, estimated from the index of refraction, in fractions with peak lipid concentrations were: fraction 1 (SM) 1%, fraction 4 (exchange SUV) 16%, and fraction 17-18 (PC) 26-28%.

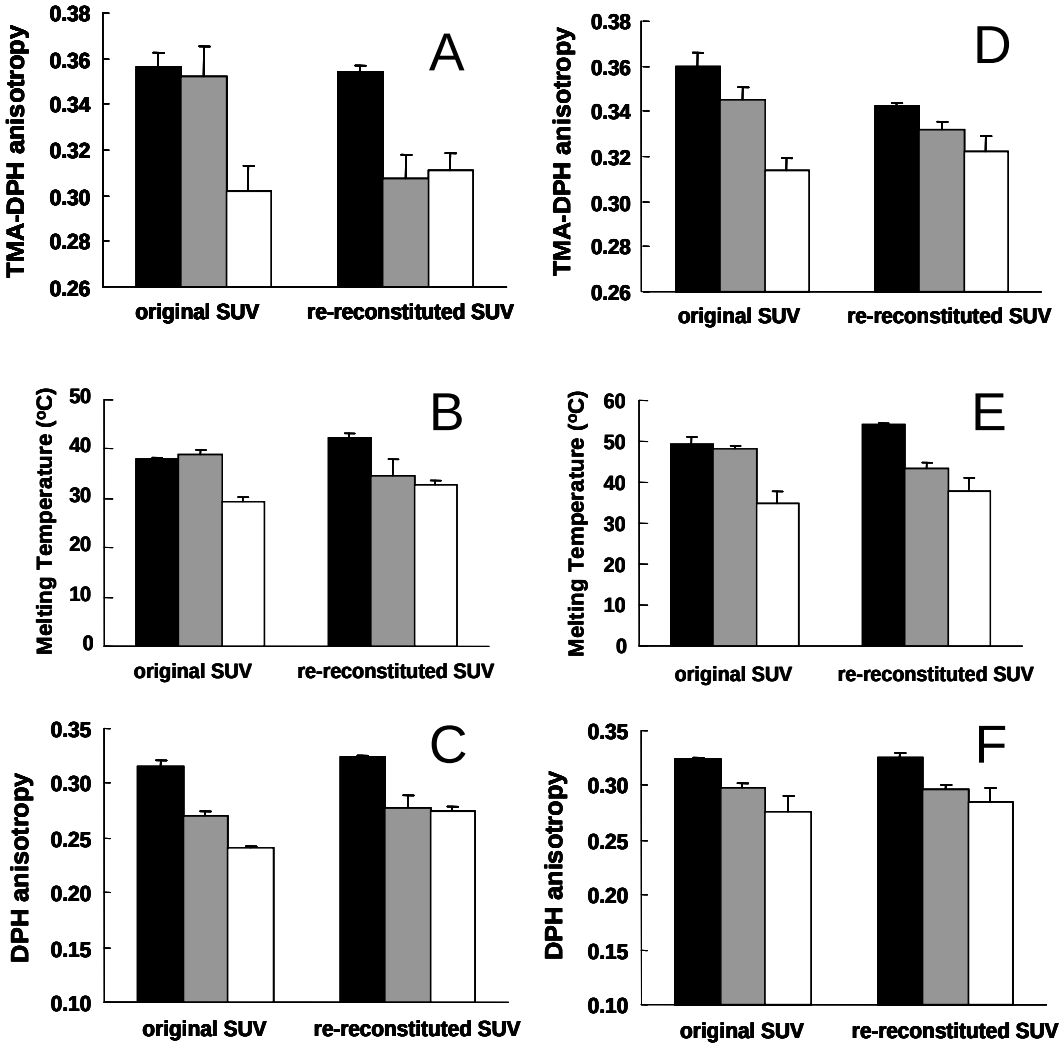

Figure 3.9. Effect of re-reconstitution upon the level and thermal stability of ordered domains. Panels A-C: SM-POPE-POPS vesicles. Panels D-F: SM-POPE-POPS-CHOL vesicles. (A) and (D): TMADPH anisotropy at room temperature. (B) and (E): Ordered domain Tm. (C) and (F): DPH anisotropy at room temperature. Black bars: SM vesicles (panel A-C) or 3:1 SM:CHOL vesicles (panel D-F). Gray bars: Exchange SMo/2:1 POPE:POPSi vesicles (panels A-C) or SMo/2:1 POPE:POPSi vesicles with ~25 mol% cholesterol (panels D-F). Unfilled bars: Ordinary 6:2:1 SM:POPE:POPS vesicles (panels A-C) or ordinary 6:2:1:3 SM:POPE:POPS:CHOL vesicles (panels D-F.) Original SUV= SUV before re-reconstitution. Re-reconstituted SUV = SUV after re-reconstitution. Average values from triplicate experiments and standard deviations are shown.

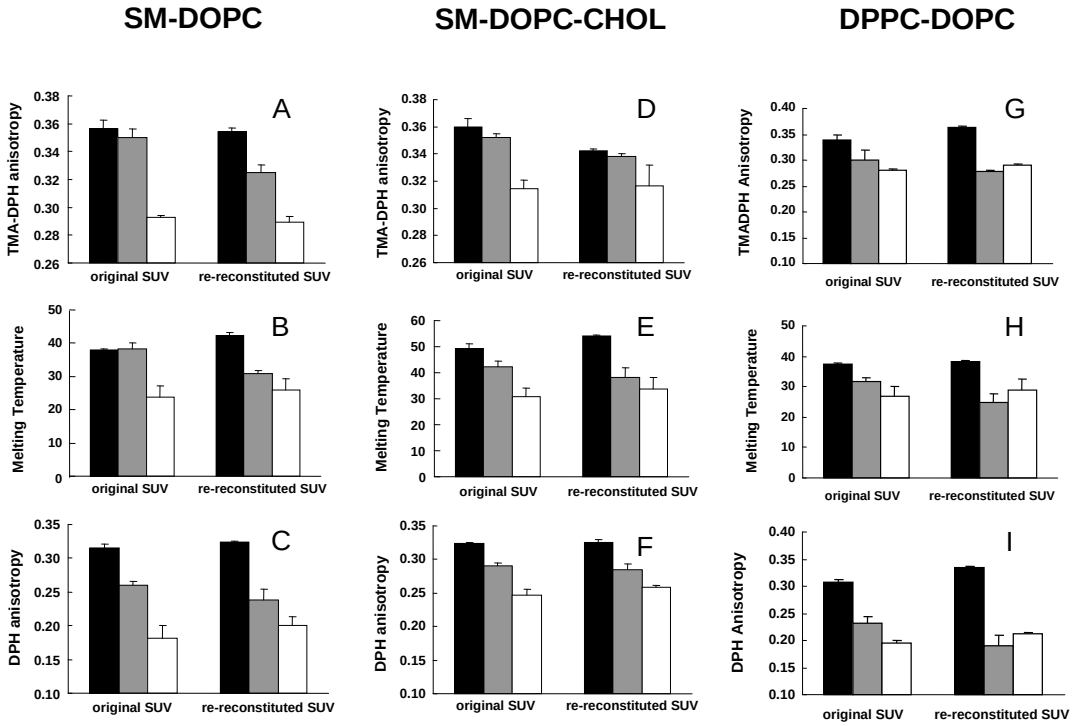

Figure 3.10. Effect of re-reconstitution upon the level and thermal stability of ordered domains in SM-DOPC, SM-DOPC-cholesterol, and DPPC-DOPC vesicles. Panels A-C: SM-DOPC vesicles. Panels D-F: SM-DOPC-CHOL vesicles. Panel G-I: DPPC-DOPC vesicles. (A), (D) and (G): TMADPH anisotropy at room temperature. (B), (E) and (H): Ordered domain Tm. (C), (F) and (I): DPH anisotropy at room temperature. Black bars: SM vesicles (panel A-C), 3:1 SM:CHOL vesicles (panel D-F), or DPPC vesicles (panel G-I). Gray bars: Exchange SMo/DOPCi vesicles (panels A-C), SMo/DOPCi vesicles with ~25 mol% cholesterol (panels D-F), or DPPCo/DOPCi vesicles (panel G-I). Unfilled bars: Ordinary 1:1 SM:DOPC vesicles (panels A-C), ordinary 3:3:2 SM:DOPC:CHOL vesicles (panels D-F), or 2:1 DPPC:DOPC vesicles (panel G-I). Original SUV= SUV before re-reconstitution. Re-reconstituted SUV = SUV after re-reconstitution. Average values from triplicate experiments and standard deviations are shown.

A

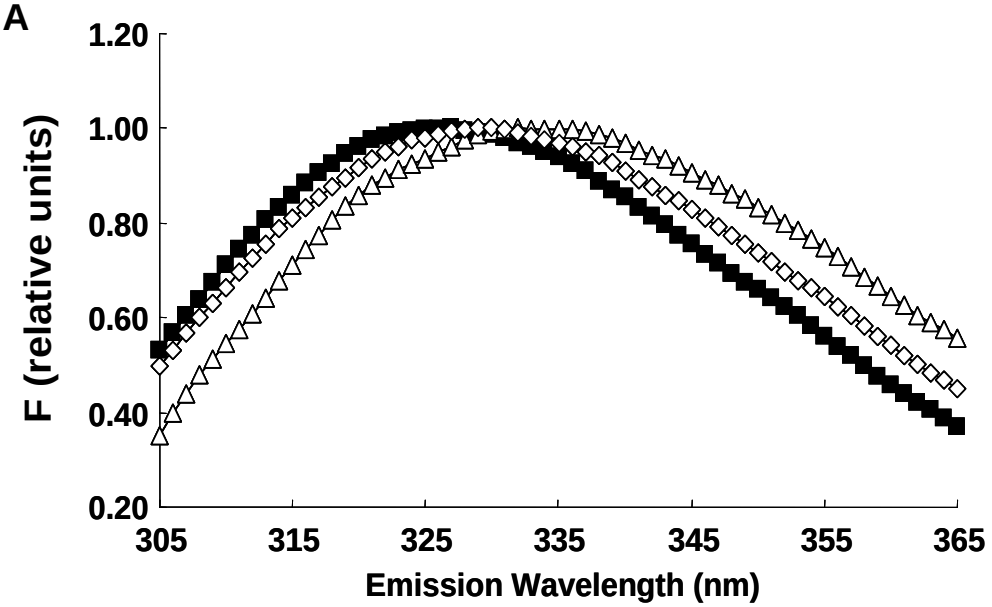

B

SAMPLE COMPOSITION	original vesicles	re-reconstituted vesicles
PBS	359±0	
DOPC[a]	335	
DOPS[a]	325	
3:2 SM:POPC	333±1.4	332±0
1:1 POPE:POPS	329±0.6	327±0
Ex SM:POPCo/POPE:POPSi	326±1.5	331±2.1

Figure 3.11. Effect of lipid asymmetry on the topography of membrane-associating hydrophobic helix pL4A18. (A) Trp fluorescence emission spectra of pL4A18 in (Δ) ordinary 3:2 SM:POPC vesicles; (◊) ordinary 1:1 POPE:POPS vesicles; (■) SM:POPCo/POPE:POPSi vesicles. Fluorescence intensities have been normalized to 1 at λmax. (B) λmax values for pL4A18 peptide in ordinary and exchange vesicles. Original vesicles = before re-reconstitution. Average λmax and standard deviation is shown for duplicate, or in the case of exchange vesicles and the original POPE:POPS vesicles prior to exchange, triplicate, preparations. DOPS = dioleoylphosphatidylserine. [a]Data from reference (*134*).

Chapter 4

Preparation of asymmetric large unilamellar vesicles

Introduction

One characteristic of eukaryotic plasma membranes is an asymmetrical lipid distribution across the bilayer with aminophospholipids (PE and PS) predominating in the inner leaflet and choline-containing phospholipids (PC and sphingolipids) predominating in the outer leaflet (*92*). The different lipid compositions in the inner and outer leaflet of the bilayer may alter bilayer properties. One such property involves lipid packing. Studies from symmetric model membranes have demonstrated that cholesterol molecules can tightly pack with saturated lipids (such as sphingolipids) and form liquid-ordered (Lo) state domains in the bilayer. These domains are resistant to solubilization by some detergents, such as Triton X-100. Sphingolipid/cholesterol-rich Lo domains which co-exist with liquid-disordered (Ld) state domains formed by un-saturated phospholipids are also known as lipid rafts (*25, 156*). Ordered domain formation can be found in symmetric model membranes with lipid mixtures mimicking lipid compositions of the outer leaflet (*11, 19*) but not in membranes with lipid mixtures imitating inner leaflet lipid compositions (*81*). Nevertheless, the recovery of PE (*17*) and inner leaflet-associated proteins (*79-80*) in detergent resistant membranes from cells seems to suggest the presence of lipid rafts in the inner leaflets of plasma membranes. Thus, it is possible that the ordered domains in the outer leaflet can induce the ordered domain formation in the inner leaflet.

Some efforts have been made to prepare asymmetric model membranes (*61, 64, 67, 78, 82-83, 111-117*). In order to understand the inter-leaflet interactions of plasma membranes, Tamm's group has prepared asymmetric planar bilayers mimicking the lipid asymmetry of the plasma membrane and found the formation of ordered domains in one leaflet can induce the occurrence of ordered domains in the other leaflet for some lipid compositions (*64-65, 82*). In our recent work, we prepared plasma membrane mimicking-asymmetric SUVs containing saturated phospholipids (SM or DPPC) in the outer leaflet and un-saturated phospholipids (POPC, POPE, or POPS) in the inner leaflet using a MβCD-induced lipid exchange method (*67*). We found that the formation of ordered domains formed by SM in the outer leaflet was not destabilized by the inner leaflet lipids. We also found that a significant degree of order in the inner leaflet can be induced by the ordered SM domains in the outer leaflet. Furthermore, our data also showed that, like in symmetric membranes, cholesterol can stabilize ordered domain formation in asymmetric membranes based on the observation that higher melting temperature can be found in cholesterol-containing asymmetric SUVs than asymmetric SUVs without cholesterol.

To mimic plasma membrane more closely it would be best to avoid use of SUVs, which have very high curvature. To do this, the MβCD-induced lipid exchange method

was extended to prepare asymmetric LUVs. Similar properties were found in terms of domain-forming behavior in asymmetric LUVs and asymmetric SUVs, indicating that ordered domain formation and leaflet coupling interactions found in asymmetric SUVs do not depend on membrane curvature.

Results

Asymmetric LUVs preparation— The MβCD-induced lipid exchange method (*67*) was modified to prepare asymmetric LUVs with SM in the outer leaflet and 2:1 mol:mol DOPE:POPS in the inner leaflet (designated as SMo/2:1 DOPE:POPSi LUVs). SM MLVs were used as donor vesicles. They were incubated with MβCD first, and then 2:1 mol:mol DOPE:POPS LUVs as acceptor vesicles were added into the mixture. Since LUVs are hard to separate from MLVs by size, we altered the density of DOPE:POPS LUVs by trapping of w/v 25% sucrose inside and separated the two vesicle populations according to their densities. As shown in Fig. 4.1, SM MLVs were too light to a form pellet when samples were overlaid onto a 10% sucrose solution and subjected to ultracentrifugation. This was true both in the presence and absence of MβCD (lane 3 and 4). DOPE:POPS LUVs, on the other hand, could form pellets after centrifugation (lane 5). Comparing samples treated with or without MβCD (lane 1 and 2), SM was only detected when MβCD was present, indicating the lipid exchange was MβCD-dependent. LUV size remained the same after exchange (Fig. 4.2), showing that vesicle-vesicle fusion did not occur during the preparation steps. HP-TLC analysis of the 1 ml final pellet showed this method yielded 291±174 μM (n=8) and 715±190 μM (n=6) lipid in LUVs initially prepared by 100 nm-pore size filters and 200 nm-size pore filters respectively.

Examination of lipid asymmetry by anisotropy— Dynamic light scattering analysis showed an average vesicle size around 120 nm in diameter when LUVs were prepared by 100 nm-size pore filters and around 160 nm in diameter when LUVs were prepared by 200 nm-size pore filters (Fig 4.2). The latter observation implies that most vesicles must be ≤ 200 nm in diameter after freeze/thawing. If assuming a membrane bilayer is 4 nm thick (*157*), the calculated outer leaflet area of LUVs was about 53% in SMo/DOPE:POPSi LUVs when we used actual vesicle sizes obtained from DLS results. HP-TLC analysis found the average SM content in asymmetric LUV samples prepared by 100 nm-pore size filter and 200 nm-pore size filter was 56±3% (n =8) (Fig 4.3), implying nearly all of outer leaflet lipids of the LUVs were composed of SM. A similar result was observed for LUVs prepared using 200 nm-size pore filters (Fig 4.3). To confirm that the

outer leaflets were composed of SM, a pair of steady state fluorescence anisotropy probes was used. DPH is a small hydrophobic fluorescence probe that distributes throughout the bilayer. TMADPH contains a charged quaternary amino group so it is restricted to the outer leaflet if added to preformed vesicles. Low anisotropy indicates the bilayer is in the Ld state, while high anisotropy is observed when a membrane bilayer is in the gel or Lo states (referred to as ordered states in this chapter). Intermediate values can be found if both ordered states and Ld state co-exist in the bilayer. As shown in Table 4.1, pure SM LUVs, which exist in the gel phase at room temperature gave higher DPH and TMADPH anisotropy value than other symmetric vesicles containing DOPE and POPS (unsaturated lipids) which are in the Ld state at room temperature. It has to be noted that TMADPH has higher intrinsic anisotropy than DPH due to the restriction of its motional range by its anchoring to the membrane surface. Table 4.1 also shows that the outer leaflet TMADPH anisotropy in asymmetric LUVs was as high as that in pure SM vesicles, indicating that the outer leaflet of SMo/2:1 DOPE:POPSi LUVs was in the ordered state and probably mainly composed of SM. In contrast, DPH reported a value significantly lower than pure SM in the asymmetric vesicles, suggesting that the inner leaflet is less ordered than the outer leaflet. The difference between inner and outer leaflet indicates an asymmetrical lipid distribution across the membrane bilayer of SMo/2:1 DOPE:POPSi LUVs. This anisotropy difference is not observed in symmetric vesicles with a nearly identical lipid composition. Moreover, the DPH anisotropy of SMo/2:1 DOPE:POPSi LUVs was higher than that of the corresponding symmetric vesicles, indicating that the overall level of order is higher in asymmetric vesicles than symmetric vesicles of the same composition. Assuming DPH anisotropy reflects both leaflets and TMADPH reflects the outer leaflet order, the percentage of order in the inner leaflet can be calculated. Correcting for the fact that, in LUVs, about 53% of total lipids are in the outer leaflet, 38% of the inner leaflet lipid in asymmetric LUVs appears to be in an ordered state as calculated by the following equation:

overall % order in bilayer = outer leaflet % ordered*0.53 + inner leaflet % ordered*0.47

Where overall % order in bilayer was derived from the DPH anisotropy value and outer leaflet % ordered was derived from TMADPH anisotropy (see Table 4.1). After rearrangement, we get this equation.

inner leaflet order = (overall % order in bilayer – outer leaflet % ordered*0.53) / 0.47

Properties of ordered domains in asymmetric LUVs— The thermal stability of ordered domains in asymmetric SMo/2:1 DOPE:POPSi LUVs was determined by melting transition, as measured by DPH anisotropy versus temperature. As mentioned above,

DPH anisotropy measures the order/fluidity of the bilayer. Thus, as temperature is increased, a decrease in DPH anisotropy should be found corresponding to the melting of ordered domains. The melting temperature (Tm) can be defined as the midpoint of the large change in anisotropy and used as an indicator of thermal stability. The higher Tm represents more stable ordered domains. As shown in Fig. 4.4*A*, at low temperature, asymmetric SMo/2:1 DOPE:POPSi LUVs had an intermediate DPH anisotropy falling between the fully ordered (SM LUVs) and fully disordered (2:1 DOPE:POPS LUVs) states. This suggests that part of the bilayer (most likely the outer leaflet) is in an ordered state and part of the bilayer (most likely the inner leaflet) is in a disordered state. However, it can also be seen in Fig. 4.4 that asymmetric SMo/2:1 DOPE:POPSi LUVs had a Tm as high as pure SM LUVs, indicating that ordered domains in the asymmetric LUVs were as thermally stable as in pure SM and the existence of unsaturated DOPE:POPS inner leaflet did not decrease to the stability of ordered domains formed in the outer leaflet by SM. Additionally, the ordered domains in asymmetric SMo/2:1 DOPE:POPSi LUVs were stable for at least 3 days based on their Tm value, which decreases when asymmetry is lost (data not shown).

Confirmation of the formation of asymmetric LUVs by alamethicin— It has been reported that the peptide alamethicin can induce transverse movements of lipid molecules in the bilayer (*158*). We thus used alamethicin to examine the asymmetry of the SMo/2:1 DOPE:POPSi LUV. As mentioned above and shown in Fig. 4.5, outer leaflet TMADPH anisotropy and Tm in asymmetric SMo/2:1 DOPE:POPSi LUVs were similar to pure SM and significantly higher than those in symmetric 3:2:1 SM:DOPE:POPS LUV which have a lipid composition nearly identical to that of the asymmetric vesicles. However, when alamethicin was added to samples, the DPH anisotropy, TMADPH anisotropy and melting temperature in asymmetric vesicles dropped and became close to those in the symmetric 3:2:1 SM:DOPE:POPS LUV, indicating the disappearance of asymmetry. This result rules out the hypothesis that the difference between the properties found in the symmetric and asymmetric LUVs were due to a small difference in lipid composition rather than the asymmetrical lipid distribution in asymmetric LUVs. A similar change in properties of the asymmetric vesicles was observed when asymmetric LUVs were dried, destroyed by solubilization in ethanol, and re-reconstituted to form symmetric LUVs in aqueous solution (data not shown).

In addition, similar vesicle sizes were found by DLS in the presence or absence of alamethicin, indicating that alamethicin did not cause vesicle disruption or fusion. This result eliminates the possibility that the unique physical properties we found in asymmetric SMo/2:1 DOPE:POPSi LUV preparation was actually due to the co-existence of SM LUVs and 2:1 DOPE:POPS LUVs which fuse when alamethicin is added to them.

Verification of lipid asymmetry by peptide topography— It has been found that 20 to 30% anionic lipids can strongly stabilize the formation of transmembrane (TM) topography of the peptides containing positive charged residues flanking the hydrophobic sequence (*90*). By taking advantage of this finding, we further assayed the extent of lipid asymmetry of asymmetric LUVs using the Lys flanked peptide called pL4A18 (acetyl-$K_2LA_9LWLA_9LK_2$-amide). The pL4A18 peptide contains a Trp residue in the middle of its sequence so its configuration can be monitored by its Trp fluorescence emission (the wavelength of maximum emission, λmax). In the TM state, λmax is more blue shifted (i.e. to a lower wavelength) than in the non-TM state. As shown in Fig. 4.6*A*, in agreement with previous findings the λmax of pL4A18 peptide gave most blue shifted fluorescence when about 20% or more POPS was present. Although at least 14% of POPS was found in asymmetric SMo/2:1 DOPE:POPSi LUV samples by HP-TLC, the λmax of asymmetric vesicles (346±6 nm, Fig. 4.6*B*) fell between pure SM LUVs (350±2 nm) and 5% POPS-containing LUVs (342±5 nm) in the outer leaflet (Fig 4.6*A*). This result indicates only small amounts of POPS remained in the outer leaflet after exchange and thus further confirms the asymmetry of lipid distribution in the asymmetric LUVs. In the presence of alamethicin, the λmax of the sample initially containing asymmetric vesicles was significantly blue shifted to 326±4 nm (Fig. 4.6*B*), showing more POPS became exposed to the outer leaflet as expected. Control experiments showed a smaller blue shift in λmax for symmetric LUV samples with similar lipid composition in the presence of alamethicin (Fig. 4.6*B*). Control experiments also showed that a mixture contains co-existing SM LUVs and 2:1 DOPE:POPS LUVs behaved differently from asymmetric SMo/2:1 DOPE:POPSi LUVs (Fig. 4.6*B*). This further rules out the possibility that the asymmetric preparations are mixtures of SM vesicles and DOPE:POPS vesicles.

Discussion

Preparation of asymmetric LUVs— The successful preparation of asymmetric SUVs by MβCD-induced lipid exchange method could have important applications in membrane biology. However, the high membrane curvature of SUVs is a drawback. Here, we extended the method to the preparation of asymmetric LUVs. Asymmetric SMo/2:1 DOPE:POPSi LUVs were successful prepared. We found asymmetric LUVs with SM outside and 2:1 POPE:POPS inside can also be prepared by this method (data not shown). Asymmetric SMo/2:1 DOPE:POPSi LUVs prepared from 2:1 DOPE:POPS LUVs which made by passing through a 200 nm-pore size filter yielded a higher amount of asymmetric LUVs than when a 100 nm filter was used. This high yield helps overcome

limitations due to preparation of only a small amount of LUV. In addition, preliminary results show that, with a 2nd exchange step, cholesterol-containing asymmetric LUVs can also be prepared (Fig. 4.7).

Comparison of domain formation in asymmetric SUVs and LUVs— Some degree of ordering was found both in asymmetric SUVs and LUVs with SM in the outer leaflet. This can be an explanation for the higher DPH anisotropy found in asymmetric vesicles with SM outside and un-saturated phospholipids inside than that in symmetric vesicles having similar lipid composition. This result that the domain formation in the outer leaflet induced the domain formation in the inner leaflet agrees with the domain coupling behavior found by other groups using asymmetric planar bilayer (*64-65, 82-83*). Furthermore, analogous results were found in asymmetric SUVs and LUVs, indicating that membrane curvature probably does not play a big role in domain formation in asymmetric membranes.

Applications of asymmetric LUVs— Since asymmetric LUVs mimic plasma membrane compositions, they should find applications in studying the effects of proteins on lipid raft formation and other lipid raft-related topics, such as the interpretation and applications of detergent insolubility in cell membranes. Additionally, several kinds of enzymes that regulate the asymmetry of plasma membrane have been found. However, not all of their substrates and properties are understood. If the MβCD-induced lipid exchange method can be extended to prepare asymmetric vesicles with diverse types of lipids and these enzymes can be incorporated into the vesicles, they might be a tool to analyze their enzymatic function.

Table 4.1. Fluorescence anisotropy in symmetric and asymmetric LUVs.

Sample composition	Anisotropy (A)		Percent ordered	
	DPH	TMADPH	DPH	TMADPH
SM	0.322±0.010 (5)	0.327±0.025 (5)	≡ 100	≡ 100
3:2:1 SM:DOPE:POPS	0.189±0.011 (5)	0.265±0.017 (5)	38	34
2:1 DOPE:POPS	0.107±0.005 (8)	0.234±0.009 (5)	≡ 0	≡ 0
SMo/2:1 DOPE:POPSi	0.259±0.009 (7)	0.331±0.014 (7)	71	104

Average anisotropy and S.D. from 5 to 8 preparations (shown in parentheses) of LUVs prepared from 100 nm-pore size membrane are shown. DPH or TMADPH (0.1 μM) was added into samples containing symmetric LUVs (100 μM) or asymmetric SMo/2:1 DOPE:POPSi LUVs (50 μM to 135 μM). Anisotropy was measured at room temperature. The percent ordered state bilayer (from DPH anisotropy) or ordered state outer leaflet (from TMADPH anisotropy) was estimated from anisotropy (A) by the following equation: Percent ordered = $(A_{sample} - A_{100\% Ld})/(A_{100\% ordered} - A_{100\% Ld})$. $A_{100\% ordered}$ is that in SM LUVs and $A_{100\% Ld}$ is that in 2:1 DOPE:POPS LUVs.

A

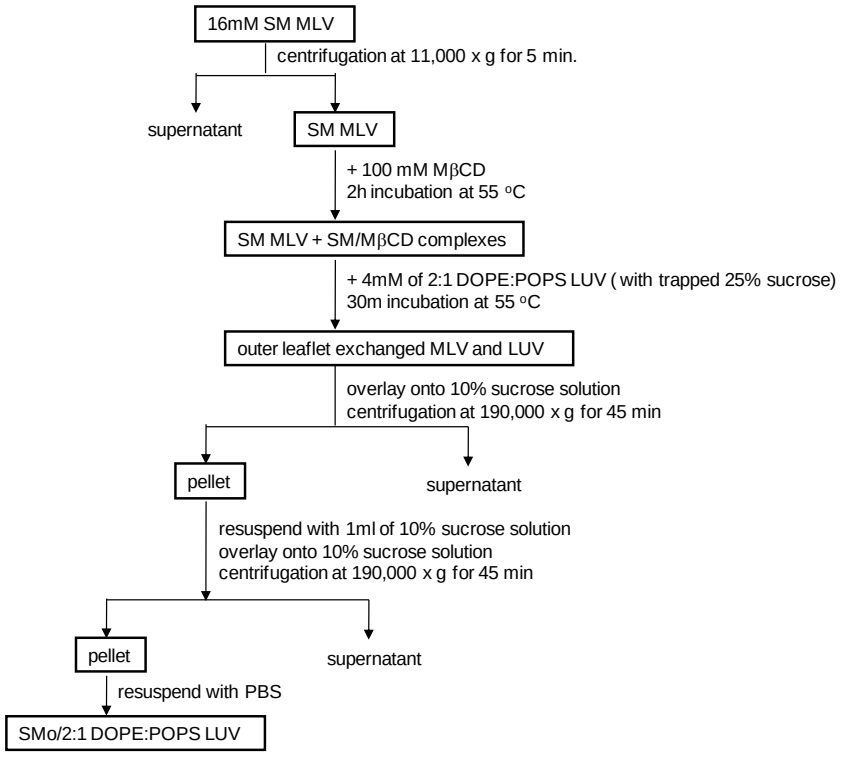

B

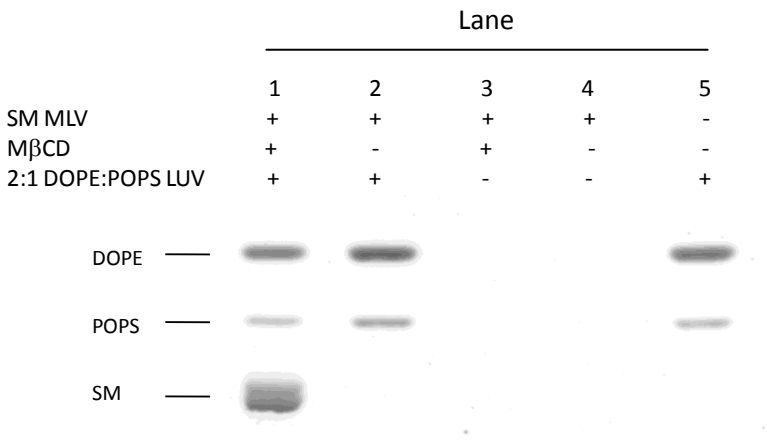

Figure 4.1 Preparation of asymmetric LUVs. (A) Flow chart of method for preparation of asymmetric SMo/2:1 DOPE:POPSi LUVs. (B) TLC analysis of final pellet from asymmetric LUV protocol. SM MLVs (lane 1 to 4) or PBS (lane 5) were incubated with (lane 1 and 3) or without (lane 2, 4, and 5) MβCD for 2h and 2:1 DOPE:POPS LUV (lane 1, 2, and 5) or PBS (lane 3 and 4) were then added and incubated for 30 min following by centrifugation steps. HP-TLC analysis of resuspended pellets from asymmetric LUV preparation was performed as described in Materials and Methods.

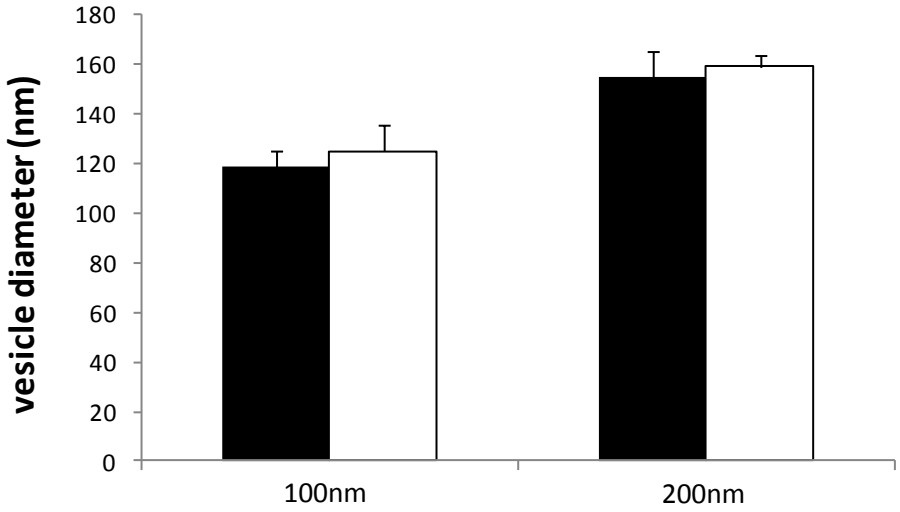

Figure 4.2. Comparison of vesicle sizes before and after MβCD-induced lipid exchange. 2:1 DOPE:POPS LUV were prepared by extrusion through either a 100 nm-pore size or a 200 nm-pore size polycarbonate filter. LUV vesicle sizes before (black bar: 2:1 DOPE:POPS LUV) and after (white bar: SMo/2:1 DOPE:POPSi LUV) exchange were determined by dynamic light scattering. Average vesicle diameter and S.D. (represented by error bars) were obtained from 5 different preparations in samples prepared by 100 nm-pore size filter (labeled as 100 nm in the figure) and from 3 different preparations in samples prepared by 200 nm-pore size filter (labeled as 200 nm in the figure).

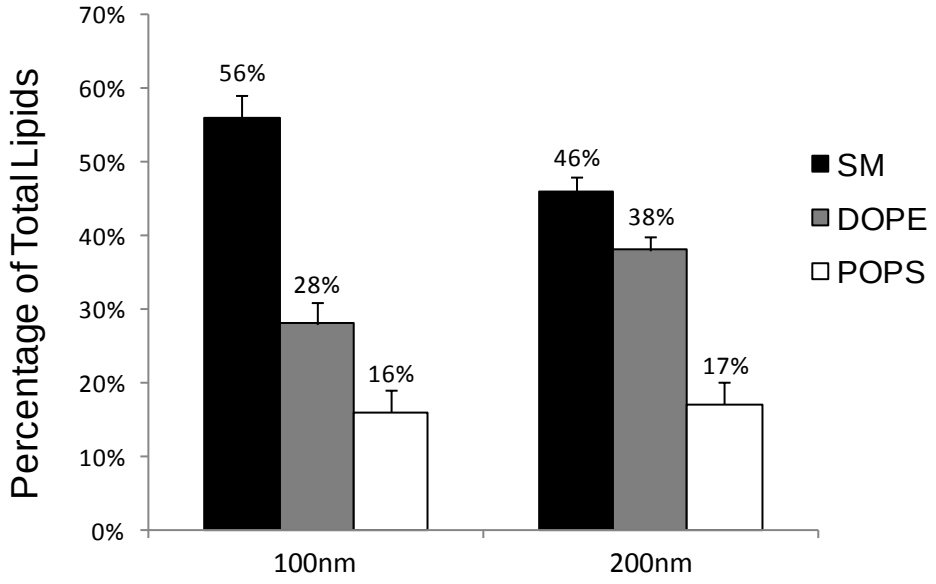

Figure 4.3. Lipid composition of asymmetric SMo/2:1 DOPE:POPSi LUVs. Lipid composition of asymmetric SMo/2:1 DOPE:POPSi LUVs were analyzed by HP-TLC. Average values and S.D. from 8 different preparations in samples prepared by 100 nm-pore size filter (labeled as 100 nm in the figure) and from 3 different preparations in samples prepared by 200 nm-pore size filter (labeled as 200 nm in the figure) are shown.

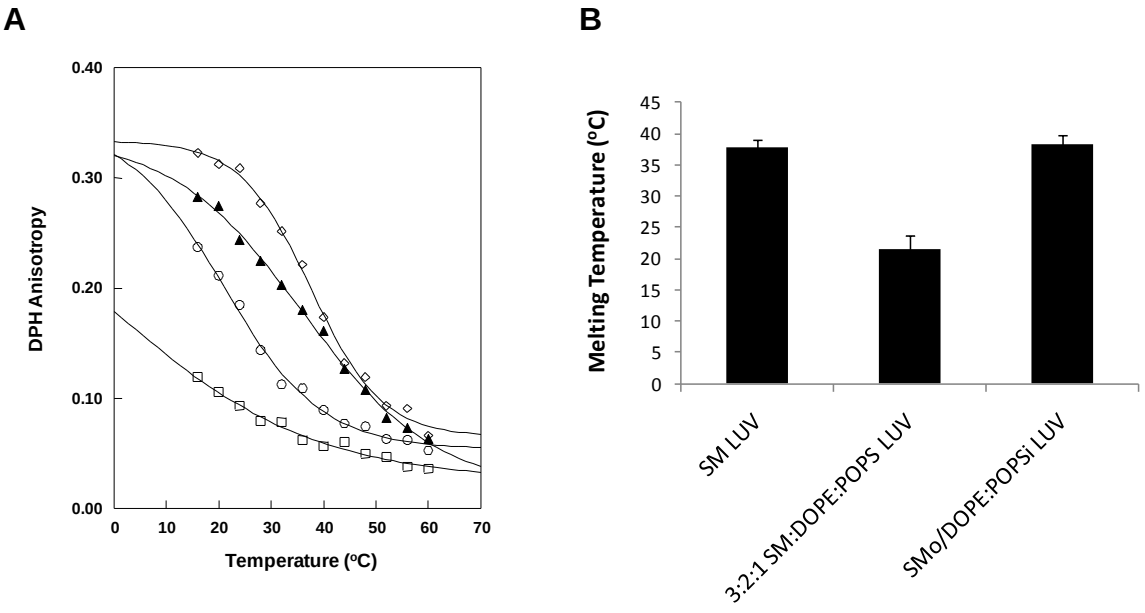

Figure 4.4. Thermal stability of ordered domains in symmetric and asymmetric LUVs prepared using 100 nm-pore size filters. (A) Temperature dependence of DPH anisotropy in symmetric and asymmetric LUVs. Symbols: ▲: SMo/2:1 DOPE:POPSi LUV, ◊: SM LUVs, ○: 3:2:1 SM:DOPE:POPS LUVs, and □: 2:1 DOPE:POPS LUVs. A representative result from n≥4 experiments is shown. (B) Average Tm values and S.D. derived from n≥4 experiments are shown.

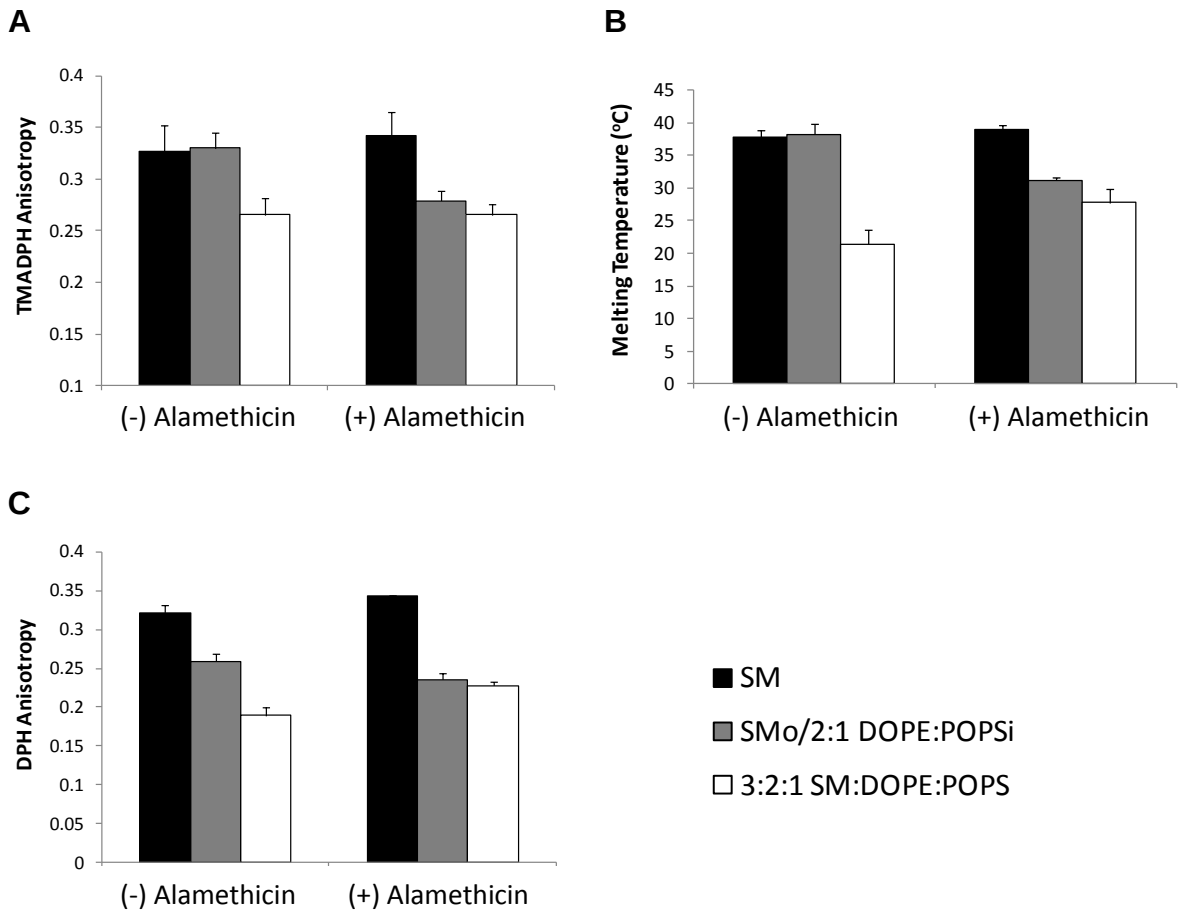

Figure 4.5. Effect of alamethicin on the level and thermal stability of ordered domains in symmetric and asymmetric LUVs. (A) TMADPH anisotropy at room temperature; (B) Tm of ordered domains; (C) DPH anisotropy at room temperature were measured in the absence or presence of 0.5 μM alamethicin. Black bars, SM LUVs. Gray bars, asymmetric SMo/2:1 DOPE:POPSi LUVs. Unfilled bars, 3:2:1 SM:DOPE:POPS LUVs. (-) Alamethicin, no alamethicin was added to samples. (+) Alamethicin, 0.5 μM of alamethicin was added to each sample. LUVs were prepared using 100 nm-pore size filters. Average results from 4 to 7 samples and S.D. are shown.

A

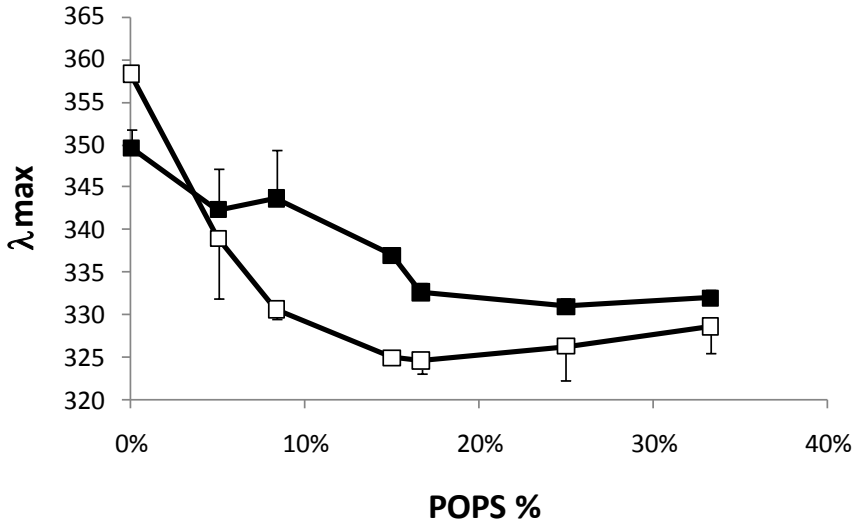

B

Lipid Composition	(-) Alamethicin	(+) Alamethicin
	λmax	λmax
PBS	358 ± 0.6	358 ± 0.6
SM LUV	350 ± 2.1	358 ± 0.6
2:1 DOPE:POPS LUV	332 ± 1.0	329 ± 3.1
SM LUV & 2:1 DOPE:POPS LUV mix	333 ± 2.1	333 ± 2.1
SMo/DOPE:POPSi LUV	346 ± 6.4	326 ± 4.0

Figure 4.6. Verification of lipid asymmetry of asymmetric SMo/2:1 DOPE:POPSi LUV by measurement of pL4A18 peptide binding to anionic lipid. (A) Standard curve of λmax of pL4A18 versus percentage of POPS in symmetric LUVs composed of SM:DOPE:POPS. DOPE:POPS molar ratio was always 2:1. Filled squares indicate λmax of symmetric LUV samples in the absence of alamethicin. Open squares indicate λmax of symmetric LUV samples in the presence of 0.5 μM alamethicin. (B) λmax of pL4A18 in symmetric and asymmetric vesicles. Average λmax values and S.D. were obtained from 3 different preparations except the sample containing SM LUV & 2:1 DOPE:POPS LUV mix which show range from 2 different preparations. The LUVs used in this experiment were prepared using 100 nm-pore size filters. Peptides (pL4A18) were added after vesicles formed.

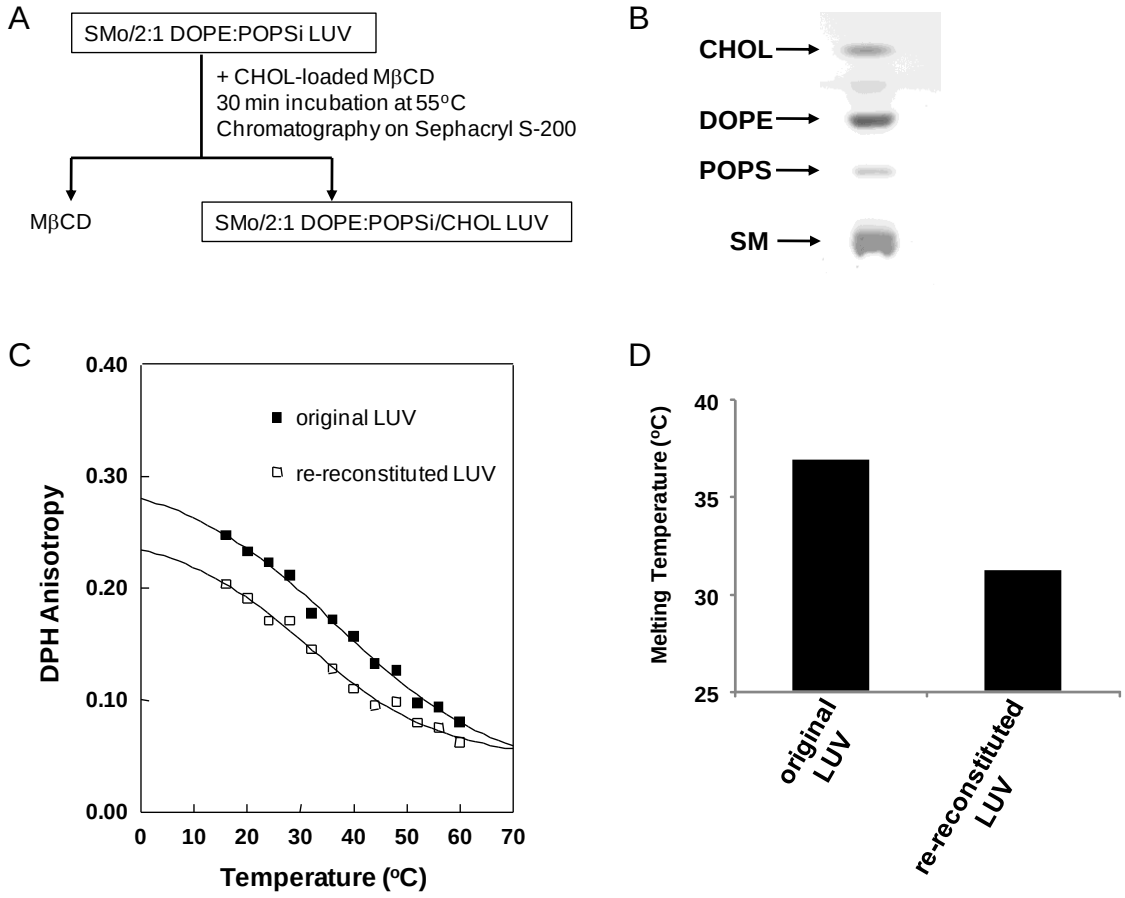

Figure 4.7. Preparation of SMo/2:1 DOPE:POPSi/CHOL LUVs. (A) Flow chart of method for preparation of asymmetric SMo/2:1 DOPE:POPSi/CHOL LUVs. (B) HP-TLC analysis of combined LUV-containing fractions. In this preparation, total lipid concentration was 282μM in 2 ml volume. The molar ratio of CHOL:DOPE:POPS:SM was 19:34:15:32. (C) Temperature dependence of DPH anisotropy in original and re-reconstituted LUVs. Symbols: ■: original LUVs, □: re-reconstituted LUVs. (D) Melting temperature of original and re-reconstituted LUVs.

Chapter 5

Summary and future directions

Summary

In this report we used a MβCD-induced lipid exchange method to prepare asymmetric SUVs and LUVs with different lipid compositions in the inner and outer leaflets. Several different types of asymmetric vesicles, including SMo/DOPCi SUVs; SMo/POPCi SUVs; SMo/POPSi SUVs; SMo/POPE:POPSi SUVs, SM:POPCo/POPE:POPSi SUVs, DPPCo/DOPCi SUVs, SMo/POPE:POPSi LUVs, and SMo/DOPE:POPSi LUVs have been successfully made. Additionally, about 25 mol% of cholesterol can also be introduced into SMo/DOPCi and SMo/POPE:POPSi SUVs without destroying asymmetry.

We tried to understand domain formation behaviors in plasma membranes by characterizing the physical properties of these biological membrane-like vesicles. Several important conclusions were made. First, outer leaflet ordered domain formation was not affected by the presence of inner unsaturated phospholipids. This was true in every kind of asymmetric vesicles we prepared. Second, as has been observed previously in symmetric membranes, cholesterol stabilized ordered domains in asymmetric membranes. Third, the ordered domains in the outer leaflet can induce a certain amount of ordered domain formation in the inner leaflet (about 16%, 31%, and 38% ordered bilayer formation in the inner leaflet of SMo/DOPCi SUVs, SMo/2:1 POPE-POPSi SUVs, and SMo/2:1 DOPE:POPSi LUVs, respectively, and in the presence of cholesterol, 49% and 40% ordered bilayer was found in the inner leaflet of SMo/DOPCi/CHOL and SMo/POPE:POPSi/CHOL SUVs, respectively). Last, the thermal stability of ordered domains in asymmetric vesicles (with or without cholesterol) was as stable as that of pure SM symmetric vesicles (with or without cholesterol), which indicates that (1) the inner leaflet unsaturated phospholipids do not destabilize the stability of ordered domains in the outer leaflet of asymmetric vesicles and (2) an asymmetric lipid distribution like that in eukaryotic plasma membranes can be conducive to ordered domain (raft) formation. Furthermore, it seems that membrane curvature is not important for ordered domain formation and leaflet coupling interaction in asymmetric membranes, since similar properties were found in asymmetric SUVs and LUVs.

Future directions

Preparing asymmetric LUVs with natural lipids— The goal of preparing asymmetric membranes is to establish a study model for biological membranes. Thus, the next step to further imitate plasma membrane is to use natural extracted lipids (not synthetic lipids) and prepare 1:1 brain SM: brain PC outside/ 1:1:1 brain PC: brain PE:

brain PS inside LUVs with 25-40% cholesterol. This composition would be very close to that of mammalian plasma membranes (*1*). The domain forming ability of such vesicles should reveal the capability of lipid molecules to form ordered domains in plasma membranes.

Studying the effect of membrane proteins on lipid domain formation— Membrane proteins may also have an influence upon lipid domain formation (*159-160*), thus it is important to incorporate membrane proteins to asymmetric membranes and study their effects on domain formation. In this report, without destroying asymmetry, we have successfully incorporated transmembrane peptides into asymmetric vesicles by co-mixing peptides with lipids when prepared initial symmetric vesicles, so it should be possible for us to explore the interaction between protein and lipids without breaking asymmetry.

Investigating the possible mechanism of membrane protein positive-inside rule— The positive-inside rule states that the cytofacial end of a transmembrane segment contains more positive charges than its exofacial end (*161*). The existence of negative charged lipids in the inner leaflet of plasma membranes provides a possible explanation for this rule. However, whether lipid charge asymmetry can influence transmembrane helix orientation has never been studied. The ability to prepare asymmetric vesicles with negative lipids inside should help to elucidate if the negative charge lipids contribute to the determination of the orientation of a transmembrane peptide or protein. Several kinds of peptides can be designed and used to answer this question. Peptides containing positive charges at one or both ends, with negative charges at one and both end, with positive charge at one end and negative charge at another, or peptides with charges that can be controlled by pH could all be studied. The results would be especially convincing if we can prepare reverse asymmetric vesicles, in which the lipids in the inner and outer leaflet are reversed, and opposite peptide orientations are observed. Thus, development of methods to prepare vesicles with inner and outer leaflet lipid compositions would be another important goal.

Clarifying the meaning of detergent resistance— Another important question that can be addressed by asymmetric membranes is that if the asymmetric lipid distribution affects the membrane insolubility upon detergent treatment. It is known that DRMs from cell membranes can only be found at low temperature (*17*), nonetheless, it is not the case in symmetric model membranes in which detergent resistance persists at elevated temperatures (*11, 24, 162*). Therefore, to test if lipid asymmetry plays a role in this

disagreement is a reasonable idea. It has shown in this report and by other groups (*158*) that alamethicin can break lipid asymmetry, so in addition to compare DRM results from asymmetric vesicles and symmetric vesicles, one can compare the results from asymmetric vesicles with or without the presence of alamethicin.

Preparing asymmetric GUVs— In this report, we used fluorescence spectroscopic analysis to examine and characterize domain formation in asymmetric SUVs and LUVs. However, there was no direct image information to prove domain formation/separation in these vesicles due to their small sizes. Thus, to prepare asymmetric GUVs which are microns in size and are visible by fluorescence microscopy seems to be another important step. Combined with fluorescent probes, it should be possible to directly observe domain formation/separation in both inner and outer leaflets of asymmetric membranes, as has been the case in symmetric GUVs (*163-164*). The successful preparation of asymmetric GUVs will also provide us a powerful tool to visualize the co-localization of lipid rafts and raft-binding proteins in asymmetric membranes. Furthermore, this system should also allow us to test if raft-binding proteins induce larger domain formation in asymmetric membranes and allow us to examine if transmembrane proteins aid domain formation in the inner and outer leaflet of asymmetric membranes.

Applications of asymmetric vesicles in drug delivery— Another possible application for asymmetric LUVs is in drug encapsulation. The inner leaflet negative charged lipids may prevent a leak of charged molecules by interacting with cationic molecules or by repelling anionic molecules from the membrane. This will become more important when the substance trapped inside of the vesicle is toxic. The outer leaflet could then be designed to have a different lipid composition that might be more compatible with delivery to cells or prolonged circulation in the blood.

The finding that asymmetric SM:POPCo/POPE:POPSi SUVs have the ability to stabilize the transmembrane topography of a cationic peptide better than symmetric SUVs with 50% POPS provides the possibility of using asymmetric vesicles to deliver positive charged peptides to cells with better efficiency. This idea will be valuable if a non-water soluble peptide does not associate well with symmetric vesicles but can bind to asymmetric vesicles.

References

1. van Meer, G., Voelker, D. R., and Feigenson, G. W. (2008) Membrane lipids: where they are and how they behave, *Nat Rev Mol Cell Biol 9*, 112-124.
2. Alberts, B. (2002) *Molecular biology of the cell*, 4th ed., Garland Science, New York.
3. Ali, M. R., Cheng, K. H., and Huang, J. (2006) Ceramide drives cholesterol out of the ordered lipid bilayer phase into the crystal phase in 1-palmitoyl-2-oleoyl-sn-glycero-3-phosphocholine/cholesterol/ceramide ternary mixtures, *Biochemistry 45*, 12629-12638.
4. Huang, J., and Feigenson, G. W. (1999) A microscopic interaction model of maximum solubility of cholesterol in lipid bilayers, *Biophys J 76*, 2142-2157.
5. Tannert, A., Pohl, A., Pomorski, T., and Herrmann, A. (2003) Protein-mediated transbilayer movement of lipids in eukaryotes and prokaryotes: the relevance of ABC transporters, *Int J Antimicrob Agents 22*, 177-187.
6. Huijbregts, R. P., de Kroon, A. I., and de Kruijff, B. (2000) Topology and transport of membrane lipids in bacteria, *Biochim Biophys Acta 1469*, 43-61.
7. Mishra, N. N., Yang, S. J., Sawa, A., Rubio, A., Nast, C. C., Yeaman, M. R., and Bayer, A. S. (2009) Analysis of cell membrane characteristics of in vitro-selected daptomycin-resistant strains of methicillin-resistant Staphylococcus aureus, *Antimicrob Agents Chemother 53*, 2312-2318.
8. Op den Kamp, J. A. (1979) Lipid asymmetry in membranes, *Annu Rev Biochem 48*, 47-71.
9. Brown, D. A., and London, E. (2000) Structure and function of sphingolipid- and cholesterol-rich membrane rafts, *J Biol Chem 275*, 17221-17224.
10. Thompson, T. E., and Tillack, T. W. (1985) Organization of glycosphingolipids in bilayers and plasma membranes of mammalian cells, *Annual review of biophysics and biophysical chemistry 14*, 361-386.
11. Ahmed, S. N., Brown, D. A., and London, E. (1997) On the origin of sphingolipid/cholesterol-rich detergent-insoluble cell membranes: physiological concentrations of cholesterol and sphingolipid induce formation of a detergent-insoluble, liquid-ordered lipid phase in model membranes, *Biochemistry 36*, 10944-10953.
12. Ipsen, J. H., Karlstrom, G., Mouritsen, O. G., Wennerstrom, H., and Zuckermann, M. J. (1987) Phase equilibria in the phosphatidylcholine-cholesterol system, *Biochimica et biophysica acta 905*, 162-172.
13. Silvius, J. R., del Giudice, D., and Lafleur, M. (1996) Cholesterol at different bilayer concentrations can promote or antagonize lateral segregation of phospholipids of differing acyl chain length, *Biochemistry 35*, 15198-15208.
14. Simons, K., and van Meer, G. (1988) Lipid sorting in epithelial cells, *Biochemistry 27*, 6197-6202.
15. van Meer, G., and Simons, K. (1988) Lipid polarity and sorting in epithelial cells, *Journal of cellular biochemistry 36*, 51-58.
16. van Meer, G., Stelzer, E. H., Wijnaendts-van-Resandt, R. W., and Simons, K. (1987) Sorting of sphingolipids in epithelial (Madin-Darby canine kidney) cells, *J Cell Biol 105*, 1623-1635.
17. Brown, D. A., and Rose, J. K. (1992) Sorting of GPI-anchored proteins to glycolipid-enriched membrane subdomains during transport to the apical cell surface, *Cell 68*, 533-544.
18. Korlach, J., Schwille, P., Webb, W. W., and Feigenson, G. W. (1999) Characterization of lipid bilayer phases by confocal microscopy and fluorescence correlation spectroscopy, *Proc Natl Acad Sci U S A 96*, 8461-8466.

19. Schroeder, R. J., Ahmed, S. N., Zhu, Y., London, E., and Brown, D. A. (1998) Cholesterol and sphingolipid enhance the Triton X-100 insolubility of glycosylphosphatidylinositol-anchored proteins by promoting the formation of detergent-insoluble ordered membrane domains, *J Biol Chem 273*, 1150-1157.
20. Schroeder, R., London, E., and Brown, D. (1994) Interactions between saturated acyl chains confer detergent resistance on lipids and glycosylphosphatidylinositol (GPI)-anchored proteins: GPI-anchored proteins in liposomes and cells show similar behavior, *Proc Natl Acad Sci U S A 91*, 12130-12134.
21. Simons, K., and Ikonen, E. (1997) Functional rafts in cell membranes, *Nature 387*, 569-572.
22. Coskun, U., and Simons, K. (2010) Membrane rafting: from apical sorting to phase segregation, *FEBS Lett 584*, 1685-1693.
23. Campbell, S. M., Crowe, S. M., and Mak, J. (2001) Lipid rafts and HIV-1: from viral entry to assembly of progeny virions, *J Clin Virol 22*, 217-227.
24. Scheiffele, P., Rietveld, A., Wilk, T., and Simons, K. (1999) Influenza viruses select ordered lipid domains during budding from the plasma membrane, *J Biol Chem 274*, 2038-2044.
25. Brown, D. A., and London, E. (1998) Functions of lipid rafts in biological membranes, *Annu Rev Cell Dev Biol 14*, 111-136.
26. Ikonen, E. (2001) Roles of lipid rafts in membrane transport, *Curr Opin Cell Biol 13*, 470-477.
27. van der Goot, F. G., and Harder, T. (2001) Raft membrane domains: from a liquid-ordered membrane phase to a site of pathogen attack, *Semin Immunol 13*, 89-97.
28. Kusumi, A., Nakada, C., Ritchie, K., Murase, K., Suzuki, K., Murakoshi, H., Kasai, R. S., Kondo, J., and Fujiwara, T. (2005) Paradigm shift of the plasma membrane concept from the two-dimensional continuum fluid to the partitioned fluid: high-speed single-molecule tracking of membrane molecules, *Annu Rev Biophys Biomol Struct 34*, 351-378.
29. Lagerholm, B. C., Weinreb, G. E., Jacobson, K., and Thompson, N. L. (2005) Detecting microdomains in intact cell membranes, *Annu Rev Phys Chem 56*, 309-336.
30. Feigenson, G. W., and Buboltz, J. T. (2001) Ternary phase diagram of dipalmitoyl-PC/dilauroyl-PC/cholesterol: nanoscopic domain formation driven by cholesterol, *Biophys J 80*, 2775-2788.
31. Edidin, M. (2001) Shrinking patches and slippery rafts: scales of domains in the plasma membrane, *Trends Cell Biol 11*, 492-496.
32. Pike, L. J. (2006) Rafts defined: a report on the Keystone Symposium on Lipid Rafts and Cell Function, *J Lipid Res 47*, 1597-1598.
33. Fadeel, B., and Xue, D. (2009) The ins and outs of phospholipid asymmetry in the plasma membrane: roles in health and disease, *Crit Rev Biochem Mol Biol 44*, 264-277.
34. Malinverni, J. C., and Silhavy, T. J. (2009) An ABC transport system that maintains lipid asymmetry in the gram-negative outer membrane, *Proc Natl Acad Sci U S A 106*, 8009-8014.
35. Mukhopadhyay, K., Whitmire, W., Xiong, Y. Q., Molden, J., Jones, T., Peschel, A., Staubitz, P., Adler-Moore, J., McNamara, P. J., Proctor, R. A., Yeaman, M. R., and Bayer, A. S. (2007) In vitro susceptibility of Staphylococcus aureus to thrombin-induced platelet microbicidal protein-1 (tPMP-1) is influenced by cell membrane phospholipid composition and asymmetry, *Microbiology 153*, 1187-1197.
36. Devaux, P. F., and Morris, R. (2004) Transmembrane asymmetry and lateral domains in biological membranes, *Traffic 5*, 241-246.
37. Kornberg, R. D., and McConnell, H. M. (1971) Inside-outside transitions of phospholipids in vesicle membranes, *Biochemistry 10*, 1111-1120.

38. Sprong, H., van der Sluijs, P., and van Meer, G. (2001) How proteins move lipids and lipids move proteins, *Nat Rev Mol Cell Biol 2*, 504-513.
39. De Kruijff, B., and Van Zoelen, E. J. (1978) Effect of the phase transition on the transbilayer movement of dimyristoyl phosphatidylcholine in unilamellar vesicles, *Biochim Biophys Acta 511*, 105-115.
40. John, K., Schreiber, S., Kubelt, J., Herrmann, A., and Muller, P. (2002) Transbilayer movement of phospholipids at the main phase transition of lipid membranes: implications for rapid flip-flop in biological membranes, *Biophys J 83*, 3315-3323.
41. Kol, M. A., de Kroon, A. I., Killian, J. A., and de Kruijff, B. (2004) Transbilayer movement of phospholipids in biogenic membranes, *Biochemistry 43*, 2673-2681.
42. Pomorski, T., Holthuis, J. C., Herrmann, A., and van Meer, G. (2004) Tracking down lipid flippases and their biological functions, *J Cell Sci 117*, 805-813.
43. Seigneuret, M., and Devaux, P. F. (1984) ATP-dependent asymmetric distribution of spin-labeled phospholipids in the erythrocyte membrane: relation to shape changes, *Proc Natl Acad Sci U S A 81*, 3751-3755.
44. Zwaal, R. F., and Schroit, A. J. (1997) Pathophysiologic implications of membrane phospholipid asymmetry in blood cells, *Blood 89*, 1121-1132.
45. Daleke, D. L. (2007) Phospholipid flippases, *J Biol Chem 282*, 821-825.
46. Balasubramanian, K., and Schroit, A. J. (2003) Aminophospholipid asymmetry: A matter of life and death, *Annu Rev Physiol 65*, 701-734.
47. Bevers, E. M., and Williamson, P. L. (2010) Phospholipid scramblase: an update, *FEBS Lett 584*, 2724-2730.
48. Roux, M., Perly, B., and Djedaini-Pilard, F. (2007) Self-assemblies of amphiphilic cyclodextrins, *Eur Biophys J 36*, 861-867.
49. Uekama, K., Hirayama, F., and Irie, T. (1998) Cyclodextrin Drug Carrier Systems, *Chem Rev 98*, 2045-2076.
50. Zidovetzki, R., and Levitan, I. (2007) Use of cyclodextrins to manipulate plasma membrane cholesterol content: evidence, misconceptions and control strategies, *Biochim Biophys Acta 1768*, 1311-1324.
51. Keller, P., and Simons, K. (1998) Cholesterol is required for surface transport of influenza virus hemagglutinin, *J Cell Biol 140*, 1357-1367.
52. Lange, Y., Ye, J., Rigney, M., and Steck, T. L. (1999) Regulation of endoplasmic reticulum cholesterol by plasma membrane cholesterol, *J Lipid Res 40*, 2264-2270.
53. Gaus, K., Rodriguez, M., Ruberu, K. R., Gelissen, I., Sloane, T. M., Kritharides, L., and Jessup, W. (2005) Domain-specific lipid distribution in macrophage plasma membranes, *J Lipid Res 46*, 1526-1538.
54. Ottico, E., Prinetti, A., Prioni, S., Giannotta, C., Basso, L., Chigorno, V., and Sonnino, S. (2003) Dynamics of membrane lipid domains in neuronal cells differentiated in culture, *J Lipid Res 44*, 2142-2151.
55. Rouquette-Jazdanian, A. K., Pelassy, C., Breittmayer, J. P., and Aussel, C. (2006) Revaluation of the role of cholesterol in stabilizing rafts implicated in T cell receptor signaling, *Cell Signal 18*, 105-122.
56. Anderson, T. G., Tan, A., Ganz, P., and Seelig, J. (2004) Calorimetric measurement of phospholipid interaction with methyl-beta-cyclodextrin, *Biochemistry 43*, 2251-2261.
57. Giocondi, M. C., Milhiet, P. E., Dosset, P., and Le Grimellec, C. (2004) Use of cyclodextrin for AFM monitoring of model raft formation, *Biophys J 86*, 861-869.
58. Leventis, R., and Silvius, J. R. (2001) Use of cyclodextrins to monitor transbilayer movement and differential lipid affinities of cholesterol, *Biophys J 81*, 2257-2267.

59. Niu, S. L., Mitchell, D. C., and Litman, B. J. (2002) Manipulation of cholesterol levels in rod disk membranes by methyl-beta-cyclodextrin: effects on receptor activation, *J Biol Chem 277*, 20139-20145.
60. London, E. (2005) How principles of domain formation in model membranes may explain ambiguities concerning lipid raft formation in cells, *Biochim Biophys Acta 1746*, 203-220.
61. Tanhuanpaa, K., and Somerharju, P. (1999) gamma-cyclodextrins greatly enhance translocation of hydrophobic fluorescent phospholipids from vesicles to cells in culture. Importance of molecular hydrophobicity in phospholipid trafficking studies, *J Biol Chem 274*, 35359-35366.
62. Zasadzinski, J. A., Viswanathan, R., Madsen, L., Garnaes, J., and Schwartz, D. K. (1994) Langmuir-Blodgett films, *Science 263*, 1726-1733.
63. Peetla, C., Stine, A., and Labhasetwar, V. (2009) Biophysical interactions with model lipid membranes: applications in drug discovery and drug delivery, *Mol Pharm 6*, 1264-1276.
64. Kiessling, V., Crane, J. M., and Tamm, L. K. (2006) Transbilayer effects of raft-like lipid domains in asymmetric planar bilayers measured by single molecule tracking, *Biophysical journal 91*, 3313-3326.
65. Kiessling, V., Wan, C., and Tamm, L. K. (2009) Domain coupling in asymmetric lipid bilayers, *Biochim Biophys Acta 1788*, 64-71.
66. Mimms, L. T., Zampighi, G., Nozaki, Y., Tanford, C., and Reynolds, J. A. (1981) Phospholipid vesicle formation and transmembrane protein incorporation using octyl glucoside, *Biochemistry 20*, 833-840.
67. Cheng, H. T., Megha, and London, E. (2009) Preparation and properties of asymmetric vesicles that mimic cell membranes: effect upon lipid raft formation and transmembrane helix orientation, *J Biol Chem 284*, 6079-6092.
68. Bakht, O., Pathak, P., and London, E. (2007) Effect of the structure of lipids favoring disordered domain formation on the stability of cholesterol-containing ordered domains (lipid rafts): identification of multiple raft-stabilization mechanisms, *Biophys J 93*, 4307-4318.
69. Bakht, O., Delgado, J., Amat-Guerri, F., Acuna, A. U., and London, E. (2007) The phenyltetraene lysophospholipid analog PTE-ET-18-OMe as a fluorescent anisotropy probe of liquid ordered membrane domains (lipid rafts) and ceramide-rich membrane domains, *Biochim Biophys Acta 1768*, 2213-2221.
70. Wang, J., Megha, and London, E. (2004) Relationship between sterol/steroid structure and participation in ordered lipid domains (lipid rafts): implications for lipid raft structure and function, *Biochemistry 43*, 1010-1018.
71. Megha, and London, E. (2004) Ceramide selectively displaces cholesterol from ordered lipid domains (rafts): implications for lipid raft structure and function, *J Biol Chem 279*, 9997-10004.
72. Xu, X., and London, E. (2000) The effect of sterol structure on membrane lipid domains reveals how cholesterol can induce lipid domain formation, *Biochemistry 39*, 843-849.
73. Veatch, S. L., and Keller, S. L. (2003) Separation of liquid phases in giant vesicles of ternary mixtures of phospholipids and cholesterol, *Biophys J 85*, 3074-3083.
74. Zhao, J., Wu, J., Heberle, F. A., Mills, T. T., Klawitter, P., Huang, G., Costanza, G., and Feigenson, G. W. (2007) Phase studies of model biomembranes: complex behavior of DSPC/DOPC/cholesterol, *Biochim Biophys Acta 1768*, 2764-2776.
75. Kahya, N., Scherfeld, D., Bacia, K., Poolman, B., and Schwille, P. (2003) Probing lipid mobility of raft-exhibiting model membranes by fluorescence correlation spectroscopy, *J Biol Chem 278*, 28109-28115.

76. Walde, P., Cosentino, K., Engel, H., and Stano, P. (2010) Giant vesicles: preparations and applications, *Chembiochem 11*, 848-865.
77. Abraham, S. A., Waterhouse, D. N., Mayer, L. D., Cullis, P. R., Madden, T. D., and Bally, M. B. (2005) The liposomal formulation of doxorubicin, *Methods Enzymol 391*, 71-97.
78. Pautot, S., Frisken, B. J., and Weitz, D. A. (2003) Engineering asymmetric vesicles, *Proc Natl Acad Sci U S A 100*, 10718-10721.
79. Simons, K., and Toomre, D. (2000) Lipid rafts and signal transduction, *Nature reviews 1*, 31-39.
80. Rodgers, W., Crise, B., and Rose, J. K. (1994) Signals determining protein tyrosine kinase and glycosyl-phosphatidylinositol-anchored protein targeting to a glycolipid-enriched membrane fraction, *Molecular and cellular biology 14*, 5384-5391.
81. Wang, T. Y., and Silvius, J. R. (2001) Cholesterol does not induce segregation of liquid-ordered domains in bilayers modeling the inner leaflet of the plasma membrane, *Biophys J 81*, 2762-2773.
82. Wan, C., Kiessling, V., and Tamm, L. K. (2008) Coupling of cholesterol-rich lipid phases in asymmetric bilayers, *Biochemistry 47*, 2190-2198.
83. Collins, M. D., and Keller, S. L. (2008) Tuning lipid mixtures to induce or suppress domain formation across leaflets of unsupported asymmetric bilayers, *Proc Natl Acad Sci U S A 105*, 124-128.
84. Pohl, A., Devaux, P. F., and Herrmann, A. (2005) Function of prokaryotic and eukaryotic ABC proteins in lipid transport, *Biochim Biophys Acta 1733*, 29-52.
85. Du, H., Fuh, R. C. A., Li, J. Z., Corkan, L. A., and Lindsey, J. S. (1998) PhotochemCAD: A computer-aided design and research tool in photochemistry, *Photochem. Photobiol. 68*, 141-142.
86. Bakht, O., London, E. . (2007) Detection of Ordered Domain Formation (Lipid Rafts) in Model Membranes Using Tempo In *Lipid Rafts*, Humana Press, Totowa, NJ.
87. Megha, Bakht, O., and London, E. (2006) Cholesterol precursors stabilize ordinary and ceramide-rich ordered lipid domains (lipid rafts) to different degrees. Implications for the Bloch hypothesis and sterol biosynthesis disorders, *J Biol Chem 281*, 21903-21913.
88. Lacowicz, J. (1999) Priniciples of Fluorescence Spectroscopy, 2nd edition ed., pp 298-299, Klewer Academic/Plenum Publishers, New York
89. London, E., and Feligenson, G. W. (1978) A convenient and sensitive fluorescence assay for phospholipid vesicles using diphenylhexatriene, *Anal Biochem 88*, 203-211.
90. Shahidullah, K., and London, E. (2008) Effect of lipid composition on the topography of membrane-associated hydrophobic helices: stabilization of transmembrane topography by anionic lipids, *J Mol Biol 379*, 704-718.
91. Savitsky, A., M.J.E. Golay. (1964) Smoothing and differentiation of data by simplified least squares procedures., *Anal. Chem. 36*, 1627-1639.
92. Verkleij, A. J., Zwaal, R. F., Roelofsen, B., Comfurius, P., Kastelijn, D., and van Deenen, L. L. (1973) The asymmetric distribution of phospholipids in the human red cell membrane. A combined study using phospholipases and freeze-etch electron microscopy, *Biochim Biophys Acta 323*, 178-193.
93. Brown, D. A., and London, E. (1998) Functions of lipid rafts in biological membranes, *Annual Review of Cell & Developmental Biology 14*, 111-136.
94. Ayuyan, A. G., and Cohen, F. S. (2008) Raft composition at physiological temperature and pH in the absence of detergents, *Biophys J 94*, 2654-2666.
95. Bjorkqvist, Y. J., Nyholm, T. K., Slotte, J. P., and Ramstedt, B. (2005) Domain formation and stability in complex lipid bilayers as reported by cholestatrienol, *Biophys J 88*, 4054-4063.

96. Chiantia, S., Kahya, N., Ries, J., and Schwille, P. (2006) Effects of ceramide on liquid-ordered domains investigated by simultaneous AFM and FCS, *Biophys J 90*, 4500-4508.
97. Chiantia, S., Ries, J., Kahya, N., and Schwille, P. (2006) Combined AFM and two-focus SFCS study of raft-exhibiting model membranes, *Chemphyschem 7*, 2409-2418.
98. Dietrich, C., Bagatolli, L. A., Volovyk, Z. N., Thompson, N. L., Levi, M., Jacobson, K., and Gratton, E. (2001) Lipid rafts reconstituted in model membranes, *Biophys J 80*, 1417-1428.
99. Fidorra, M., Duelund, L., Leidy, C., Simonsen, A. C., and Bagatolli, L. A. (2006) Absence of fluid-ordered/fluid-disordered phase coexistence in ceramide/POPC mixtures containing cholesterol, *Biophys J 90*, 4437-4451.
100. Ira, and Johnston, L. J. (2008) Sphingomyelinase generation of ceramide promotes clustering of nanoscale domains in supported bilayer membranes, *Biochim Biophys Acta 1778*, 185-197.
101. Kahya, N., and Schwille, P. (2006) Fluorescence correlation studies of lipid domains in model membranes, *Mol Membr Biol 23*, 29-39.
102. Nybond, S., Bjorkqvist, Y. J., Ramstedt, B., and Slotte, J. P. (2005) Acyl chain length affects ceramide action on sterol/sphingomyelin-rich domains, *Biochim Biophys Acta 1718*, 61-66.
103. Ramstedt, B., and Slotte, J. P. (2006) Sphingolipids and the formation of sterol-enriched ordered membrane domains, *Biochim Biophys Acta*.
104. Samsonov, A. V., Mihalyov, I., and Cohen, F. S. (2001) Characterization of cholesterol-sphingomyelin domains and their dynamics in bilayer membranes, *Biophysical journal 81*, 1486-1500.
105. Sot, J., Bagatolli, L. A., Goni, F. M., and Alonso, A. (2006) Detergent-resistant, ceramide-enriched domains in sphingomyelin/ceramide bilayers, *Biophys J 90*, 903-914.
106. Veatch, S. L., Gawrisch, K., and Keller, S. L. (2006) Closed-loop miscibility gap and quantitative tie-lines in ternary membranes containing diphytanoyl PC, *Biophys J 90*, 4428-4436.
107. Veatch, S. L., Soubias, O., Keller, S. L., and Gawrisch, K. (2007) Critical fluctuations in domain-forming lipid mixtures, *Proc Natl Acad Sci U S A 104*, 17650-17655.
108. Wang, T. Y., Leventis, R., and Silvius, J. R. (2000) Fluorescence-based evaluation of the partitioning of lipids and lipidated peptides into liquid-ordered lipid microdomains: a model for molecular partitioning into "lipid rafts", *Biophys J 79*, 919-933.
109. Wang, T. Y., Leventis, R., and Silvius, J. R. (2001) Partitioning of lipidated peptide sequences into liquid-ordered lipid domains in model and biological membranes, *Biochemistry 40*, 13031-13040.
110. Xu, X., Bittman, R., Duportail, G., Heissler, D., Vilcheze, C., and London, E. (2001) Effect of the structure of natural sterols and sphingolipids on the formation of ordered sphingolipid/sterol domains (rafts). Comparison of cholesterol to plant, fungal, and disease-associated sterols and comparison of sphingomyelin, cerebrosides, and ceramide, *J Biol Chem 276*, 33540-33546.
111. Crane, J. M., Kiessling, V., and Tamm, L. K. (2005) Measuring lipid asymmetry in planar supported bilayers by fluorescence interference contrast microscopy, *Langmuir 21*, 1377-1388.
112. Malewicz, B., Valiyaveettil, J. T., Jacob, K., Byun, H. S., Mattjus, P., Baumann, W. J., Bittman, R., and Brown, R. E. (2005) The 3-hydroxy group and 4,5-trans double bond of sphingomyelin are essential for modulation of galactosylceramide transmembrane asymmetry, *Biophys J 88*, 2670-2680.
113. Barsukov, L. I., Victorov, A. V., Vasilenko, I. A., Evstigneeva, R. P., and Bergelson, L. D. (1980) Investigation of the inside-outside distribution, intermembrane exchange and

transbilayer movement of phospholipids in sonicated vesicles by shift reagent NMR, *Biochim Biophys Acta 598*, 153-168.
114. Eastman, S. J., Hope, M. J., and Cullis, P. R. (1991) Transbilayer transport of phosphatidic acid in response to transmembrane pH gradients, *Biochemistry 30*, 1740-1745.
115. Hope, M. J., Redelmeier, T. E., Wong, K. F., Rodrigueza, W., and Cullis, P. R. (1989) Phospholipid asymmetry in large unilamellar vesicles induced by transmembrane pH gradients, *Biochemistry 28*, 4181-4187.
116. Bloj, B., and Zilversmit, D. B. (1981) Lipid transfer proteins in the study of artificial and natural membranes, *Mol Cell Biochem 40*, 163-172.
117. Everett, J., Zlotnick, A., Tennyson, J., and Holloway, P. W. (1986) Fluorescence quenching of cytochrome b5 in vesicles with an asymmetric transbilayer distribution of brominated phosphatidylcholine, *J Biol Chem 261*, 6725-6729.
118. Huang, C. (1969) Studies on phosphatidylcholine vesicles. Formation and physical characteristics, *Biochemistry 8*, 344-352.
119. Prendergast, F. G., Haugland, R. P., and Callahan, P. J. (1981) 1-[4-(Trimethylamino)phenyl]-6-phenylhexa-1,3,5-triene: synthesis, fluorescence properties, and use as a fluorescence probe of lipid bilayers, *Biochemistry 20*, 7333-7338.
120. Kaiser, R. D., and London, E. (1998) Location of diphenylhexatriene (DPH) and its derivatives within membranes: comparison of different fluorescence quenching analyses of membrane depth, *Biochemistry 37*, 8180-8190.
121. Koynova, R., and Caffrey, M. (1994) Phases and phase transitions of the hydrated phosphatidylethanolamines, *Chem Phys Lipids 69*, 1-34.
122. Koynova, R., and Caffrey, M. (1998) Phases and phase transitions of the phosphatidylcholines, *Biochim Biophys Acta 1376*, 91-145.
123. Shaikh, S. R., Dumaual, A. C., Castillo, A., LoCascio, D., Siddiqui, R. A., Stillwell, W., and Wassall, S. R. (2004) Oleic and docosahexaenoic acid differentially phase separate from lipid raft molecules: a comparative NMR, DSC, AFM, and detergent extraction study, *Biophysical journal 87*, 1752-1766.
124. Untrach, S. H., and Shipley, G. G. (1977) Molecular interactions between lecithin and sphingomyelin. Temperature- and composition-dependent phase separation, *J Biol Chem 252*, 4449-4457.
125. Lentz, B. R., Barenholz, Y., and Thompson, T. E. (1976) Fluorescence depolarization studies of phase transitions and fluidity in phospholipid bilayers. 1. Single component phosphatidylcholine liposomes, *Biochemistry 15*, 4521-4528.
126. London, E., and Feigenson, G. W. (1981) Fluorescence Quenching in Model Membranes: An Analysis of the Local Phospholipid Environments of Diphenylhexatriene and Gramicidin A', *Biochim Biophys Acta 649*, 89-97.
127. Beck, A., Heissler, D., and Duportail, G. (1993) Influence of the length of the spacer on the partitioning properties of amphiphilic fluorescent membrane probes, *Chem Phys Lipids 66*, 135-142.
128. Huang, C., and Mason, J. T. (1978) Geometric packing constraints in egg phosphatidylcholine vesicles, *Proc Natl Acad Sci U S A 75*, 308-310.
129. Wenz, J. J., and Barrantes, F. J. (2003) Steroid structural requirements for stabilizing or disrupting lipid domains, *Biochemistry 42*, 14267-14276.
130. Koynova, R., and Caffrey, M. (1995) Phases and phase transitions of the sphingolipids, *Biochim Biophys Acta 1255*, 213-236.
131. Sripada, P. K., Maulik, P. R., Hamilton, J. A., and Shipley, G. G. (1987) Partial synthesis and properties of a series of N-acyl sphingomyelins, *J Lipid Res 28*, 710-718.

132. Portis, A., Newton, C., Pangborn, W., and Papahadjopoulos, D. (1979) Studies on the mechanism of membrane fusion: evidence for an intermembrane Ca2+-phospholipid complex, synergism with Mg2+, and inhibition by spectrin, *Biochemistry 18*, 780-790.
133. Dawidowicz, E. A., and Rothman, J. E. (1976) Fusion and protein-mediated phospholipid exchange studied with single bilayer phosphatidylcholine vesicles of different density, *Biochim Biophys Acta 455*, 621-630.
134. Shahidullah, K., and London, E. (2008) Effect of lipid composition on the topography of membrane-associated hydrophobic helices: stabilization of transmembrane topography by anionic lipids, *J. Mol. Biol. 379*, 704-718.
135. Caputo, G. A., and London, E. (2003) Cumulative effects of amino acid substitutions and hydrophobic mismatch upon the transmembrane stability and conformation of hydrophobic alpha-helices, *Biochemistry 42*, 3275-3285.
136. Krishnakumar, S. S., and London, E. (2007) The control of transmembrane helix transverse position in membranes by hydrophilic residues, *J Mol Biol 374*, 1251-1269.
137. Krishnakumar, S. S., and London, E. (2007) Effect of sequence hydrophobicity and bilayer width upon the minimum length required for the formation of transmembrane helices in membranes, *J Mol Biol 374*, 671-687.
138. Fastenberg, M. E., Shogomori, H., Xu, X., Brown, D. A., and London, E. (2003) Exclusion of a transmembrane-type peptide from ordered-lipid domains (rafts) detected by fluorescence quenching: extension of quenching analysis to account for the effects of domain size and domain boundaries, *Biochemistry 42*, 12376-12390.
139. Ren, J., Lew, S., Wang, Z., and London, E. (1997) Transmembrane orientation of hydrophobic alpha-helices is regulated both by the relationship of helix length to bilayer thickness and by the cholesterol concentration, *Biochemistry 36*, 10213-10220.
140. Rinia, H. A., Snel, M. M., van der Eerden, J. P., and de Kruijff, B. (2001) Visualizing detergent resistant domains in model membranes with atomic force microscopy, *FEBS Lett 501*, 92-96.
141. Crane, J. M., and Tamm, L. K. (2004) Role of cholesterol in the formation and nature of lipid rafts in planar and spherical model membranes, *Biophysical journal 86*, 2965-2979.
142. London, E., and Brown, D. A. (2000) Insolubility of lipids in triton X-100: physical origin and relationship to sphingolipid/cholesterol membrane domains (rafts), *Biochim Biophys Acta 1508*, 182-195.
143. Schmidt, C. F., Barenholz, Y., Huang, C., and Thompson, T. E. (1978) Monolayer coupling in sphingomyelin bilayer systems, *Nature 271*, 775-777.
144. Lerch-Bader, M., Lundin, C., Kim, H., Nilsson, I., and von Heijne, G. (2008) Contribution of positively charged flanking residues to the insertion of transmembrane helices into the endoplasmic reticulum, *Proc Natl Acad Sci U S A 105*, 4127-4132.
145. Antignani, A., and Youle, R. J. (2006) How do Bax and Bak lead to permeabilization of the outer mitochondrial membrane?, *Curr Opin Cell Biol 18*, 685-689.
146. Fujita, K., Krishnakumar, S. S., Franco, D., Paul, A. V., London, E., and Wimmer, E. (2007) Membrane topography of the hydrophobic anchor sequence of poliovirus 3A and 3AB proteins and the functional effect of 3A/3AB membrane association upon RNA replication, *Biochemistry 46*, 5185-5199.
147. Shepard, L. A., Heuck, A. P., Hamman, B. D., Rossjohn, J., Parker, M. W., Ryan, K. R., Johnson, A. E., and Tweten, R. K. (1998) Identification of a membrane-spanning domain of the thiol-activated pore-forming toxin Clostridium perfringens perfringolysin O: an alpha-helical to beta-sheet transition identified by fluorescence spectroscopy, *Biochemistry 37*, 14563-14574.

148. Young, R. M., Holowka, D., and Baird, B. (2003) A lipid raft environment enhances Lyn kinase activity by protecting the active site tyrosine from dephosphorylation, *J Biol Chem 278*, 20746-20752.
149. Sohn, H. W., Tolar, P., Jin, T., and Pierce, S. K. (2006) Fluorescence resonance energy transfer in living cells reveals dynamic membrane changes in the initiation of B cell signaling, *Proc Natl Acad Sci U S A 103*, 8143-8148.
150. Sohn, H. W., Pierce, S. K., and Tzeng, S. J. (2008) Live Cell Imaging Reveals that the Inhibitory Fc{gamma}RIIB Destabilizes B Cell Receptor Membrane-Lipid Interactions and Blocks Immune Synapse Formation, *J Immunol 180*, 793-799.
151. Shogomori, H., and Brown, D. A. (2003) Use of detergents to study membrane rafts: the good, the bad, and the ugly, *Biol Chem 384*, 1259-1263.
152. Heerklotz, H. (2002) Triton promotes domain formation in lipid raft mixtures, *Biophysical journal 83*, 2693-2701.
153. Heerklotz, H., Szadkowska, H., Anderson, T., and Seelig, J. (2003) The sensitivity of lipid domains to small perturbations demonstrated by the effect of Triton, *J Mol Biol 329*, 793-799.
154. Lichtenberg, D., Goni, F. M., and Heerklotz, H. (2005) Detergent-resistant membranes should not be identified with membrane rafts, *Trends Biochem Sci 30*, 430-436.
155. Ramstedt, B., Leppimaki, P., Axberg, M., and Slotte, J. P. (1999) Analysis of natural and synthetic sphingomyelins using high-performance thin-layer chromatography, *Eur J Biochem 266*, 997-1002.
156. Brown, D. A., and London, E. (1997) Structure of detergent-resistant membrane domains: does phase separation occur in biological membranes?, *Biochemical & Biophysical Research Communications 240*, 1-7.
157. Nagle, J. F., and Tristram-Nagle, S. (2000) Structure of lipid bilayers, *Biochim Biophys Acta 1469*, 159-195.
158. Wimley, W. C., and White, S. H. (2000) Determining the membrane topology of peptides by fluorescence quenching, *Biochemistry 39*, 161-170.
159. Babiychuk, E. B., and Draeger, A. (2006) Regulation of ecto-5'-nucleotidase activity via Ca2+-dependent, annexin 2-mediated membrane rearrangement?, *Biochem Soc Trans 34*, 374-376.
160. Abrami, L., Fivaz, M., Kobayashi, T., Kinoshita, T., Parton, R. G., and van der Goot, F. G. (2001) Cross-talk between caveolae and glycosylphosphatidylinositol-rich domains, *J Biol Chem 276*, 30729-30736.
161. Heijne, G. (1986) The distribution of positively charged residues in bacterial inner membrane proteins correlates with the trans-membrane topology, *EMBO J 5*, 3021-3027.
162. Scherfeld, D., Kahya, N., and Schwille, P. (2003) Lipid dynamics and domain formation in model membranes composed of ternary mixtures of unsaturated and saturated phosphatidylcholines and cholesterol, *Biophys J 85*, 3758-3768.
163. Hess, S. T., Gudheti, M. V., Mlodzianoski, M., and Baumgart, T. (2007) Shape analysis of giant vesicles with fluid phase coexistence by laser scanning microscopy to determine curvature, bending elasticity, and line tension, *Methods Mol Biol 400*, 367-387.
164. Kahya, N. (2006) Targeting membrane proteins to liquid-ordered phases: molecular self-organization explored by fluorescence correlation spectroscopy, *Chem Phys Lipids 141*, 158-168.